QUANTIFYING GLOBAL POSITION SYSTEM SIGNAL ATTENUATION AS A FUNCTION OF THREE-DIMENSIONAL FOREST CANOPY STRUCTURE

By

WILLIAM C. WRIGHT

A THESIS PRESENTED TO THE GRADUATE SCHOOL
OF THE UNIVERSITY OF FLORIDA IN PARTIAL FULFILLMENT
OF THE REQUIREMENTS FOR THE DEGREE OF
MASTER OF SCIENCE

UNIVERSITY OF FLORIDA

2008

To my wife and parents.

ACKNOWLEDGMENTS

I thank my professors William Carter, Ramesh Shrestha and Clint Slatton for their support and encouragement. PhD Clint Slatton provided much needed insight and guidance. Direction provided by PhD William Carter during the editing portion of this study was quintessential. I also express my gratitude to Sidney Schofield for setting up the GPS data capture devices. Most significantly I would like to thank Pang-Wei Liu for his assistance on this project during our Remote Sensing project. His work with the Airborne Laser Swath Mapping data was nothing short of fantastic.

TABLE OF CONTENTS

page

LIST OF TABLES

LIST OF FIGURES

LIST OF ABBREVIATIONS

3D	Three dimensional
ALSM	Airborne laser swath mapping
DBH	Diameter at breast height
DEM	Digital elevation model
ALSM	Airborne laser swath mapping
EM	Electromagnetic radiation
GPS	Global positioning system
GSE	Geosensing systems engineering
IMPAC	Intensive management practice assessment center used interchangeably with managed forest.
IMU	Inertial measuring unit
LiDAR	Light detecting and ranging
LOSV	Line of sight visibility
NMEA	National marine electronic association
SNR	Signal to noise ratio. When used as a numerical figure this indicates the average signal to noise value not considering measurements of zero. All units of SNR are in db:1Hz.
SNR(0)	Average signal to noise ratio counting zero values. All units of SNR are in db:1Hz.
STD	Standard deviation
SV	Satellite vehicle
VS	Versus

Abstract of Thesis Presented to the Graduate School
of the University of Florida in Partial Fulfillment of the
Requirements for the Degree of Master of Sciences

QUANTIFYING GLOBAL POSITION SYSTEM SIGNAL ATTENUATION AS A FUNCTION OF THREE-DIMENSIONAL FOREST CANOPY STRUCTURE

By

William C. Wright

May 2008

Chair: Ramesh Shrestha
Cochair: Clint Slatton
Major: Civil Engineering

The NAVSTAR Global Positioning System (GPS) has in recent years become a critical tool in fields ranging from military applications, to scientific earth measurement. GPS satellites transmit signals at 1575.42 MHz on the L1 band and 1227.60 MHz on the L2 band, with a wavelength of approximately 19.0 cm and 24.4 cm respectively. At these frequencies, the signals are attenuated by vegetation, making it problematical to anticipate if GPS will work at all, and if so, how the positioning may be degraded by various types and densities of forest canopies. At the same time, precisely measuring the degree to which the GPS signal is affected by a forest canopy may provide useful information about signal degradation.

The Civil and Coastal Engineering Department and the Electrical Engineering Department at the University of Florida are interested in developing a method to predict GPS signal attenuation caused by forest canopy by relating field measurements of GPS signals in forested terrain to three dimensional forest structure as determined from Airborne Laser Swath Mapping (ALSM) data collected by the Geo-Sensing program. This study investigates the impact of GPS signal to noise ratio levels under different vegetation types. Results of the GPS data such as

signal reception, position accuracy are compared with ALSM data in order to determine any relationships among these variables.

To compare GPS data to ALSM data for the modeling of signal attenuation, GPS data were collected in areas around the University of Florida where recent ALSM data is currently on hand. These locations include the Intensive Management Practice Assessment Center (IMPAC), a managed forest north of the Airport Gainesville Regional, a natural forest in Hogtown, and a base station on the Gainesville campus. Data collection devices include two identical Ashtech Z-Surveyor GPS receivers, two antennas, cables, and computers for data capture. A total of eleven forest locations, six points located in IMPAC and five located in the Hogtown natural forest, were measured with GPS data capture covering in excess of twenty minutes at each location.

Upon analysis of the data I found that 3D positional accuracy is inversely proportional to point cloud density of the ALSM data and it is directly proportional to the signal to noise measurements taken at the site. I was also able to verify that as a satellite approaches the horizon with respect to the GPS receiver the signal to noise measurements decrease exponentially. With the above findings further work on developing a method to predict positional accuracy was conducted. The prediction of position accuracy under complex forested terrain is of significant interest to the Army research center. Given ALSM data the model developed attempts to predict the level of position accuracy a user can obtain over a period of time.

CHAPTER 1
INTRODUCTION

1.1 Problem Background

Worldwide reliance on the NAVSTAR Global Positioning System (GPS) has grown to the point where today it is the primary source people use for position determination. While it was originally developed by the United States Department of Defense for military applications, GPS is now more predominately used by civilian users than military and is used throughout the world not just in the United States (Andrade, 2001). Uses of GPS range from recreation, fleet management, surveying, vessel navigation, to car navigation systems. As the use and users of GPS grow, an understanding of how GPS accuracy is affected by different environmental conditions continues to be a topic of interest. GPS has significant capabilities that allow for experiments and measurements of signals from its space based platforms and the effects on those signals caused by tree canopy. This signal attenuation detection analysis has a myriad of significant applications. Some examples include: forest parameter estimation, timber volume estimation, wireless communication, and predicting position accuracy under canopy, which is useful in the study of seismology, tectonics, glacial rebound, and even animal behavior (GPS collars), and a variety of military operations including search-and-rescue operations.

In addition to the explosion of GPS users, Light Detection and Ranging (LiDAR) technology has also grown in capability and in the number of systems in operation. LiDAR can provide a wealth of information on a large scale about the terrain being analyzed. The Division of Geosensing Systems Engineering (GSE) at the University of Florida in Gainesville owns and operates a LiDAR System. They refer to their LiDAR system as an Airborne Laser Swath Mapper or ALSM. This system can provide information on a forest canopy to include tree canopy height, ground Digital Elevation Model (DEM), and canopy under story data.

1.2 Purpose

The purpose of this research is to analyze GPS signal behavior and the effect of three dimensional forest terrain on the signals. Researchers in the Civil and Coastal Engineering and with the Electrical Engineering Departments, at the University of Florida, are interested in developing methods to predict GPS signal attenuation caused by forest canopies by relating field measurements of GPS signals in forested terrain to 3D forest structure as determined from Airborne Laser Swath Mapping (ALSM) data collected by the Geosensing program. The first step in this process is the development of a methodology that allows for the collection, processing, and analysis of GPS measurements and comparing these measurements to different canopy coverage in order to determine if this methodology effectively captures signal attenuation data for further analysis and model development.

In order to determine if ALSM data can accurately predict "position accuracy" under a tree canopy I will attempt to determine the correlations between several different aspects of the problem as listed below:

- The angle of a GPS satellite above the horizon and the effect on its signal to noise ratio (SNR)
- Position accuracies compared to overall SNR
- ALSM point density to SNR
- Digital photography of canopy density compared to SNR

Given these relationships the next step will be model development to predict GPS position accuracy given ALSM data.

1.3 Experiment Design

The experiment design for this research is as follows; data collection devices include two identical GPS receivers, two antennas, cables, and computers for data capture. At the base station, I used the already installed antenna that is mounted to the roof of Reed Lab, a building

located next to Weil Hall on the University of Florida campus. In order to establish a good basis for comparison of data captured from both receivers and to verify the data captured by the receivers are similar, initial measurements consisted of data captured in the same environment. Then five data points were collected in Hogtown natural forest and six points from the IMPAC site near Gainesville Regional Airport with twenty minutes of data collection at each point. Data collection included three National Marine Electronics Association (NMEA) messages collected at a rate of 1 Hz. In addition, six points were collected in October 2007 in Hogtown forest in order to ensure enough data is on hand for analysis.

Upon completion of the data collection effort, the text files with the captured NMEA messages were converted into single line data strings with three NMEA messages on a single line representing a particular second of data capture information. This information was combined with the base station data to provide a relative data comparison to an open field of view. Further information of the experiment setup and data processing is detailed in Chapter 5.

1.4 Report Structure

This thesis project covers information on two significant technologies, GPS and LIDAR, and as such Chapter 2 provides a base level explanation of GPS theory with a more in depth look at GPS error sources and, Chapter 3 provides a discussion on LiDAR technology and the basics of how the system works and operates. Chapter 4 provides an insight of previous work on the subject and simply highlights the literary review on the subject matter. Chapter 5 describes in detail the experimental setup and data processing for this research. Chapter 6 provides the experimental results. Finally, Chapter 7 provides the conclusions and recommendations for further avenues of research on this topic.

CHAPTER 2
NAVSTAR GLOBAL POSITIONING SYSTEM

2.1 Introduction

The NAVSTAR Global Positioning System is an integral system used for the determination of position on the earth's surface out to lower orbit satellites. This system uses a constellation of satellites transmitting signals from known locations in orbit around the earth and providing a receiver with the necessary information to calculate its position. Since the development of GPS, it has become a primary tool in surveying, fleet management, scientific measurement, world wide navigation, and as ground control points for different map making techniques in addition to its intended design, military applications. To explain how GPS works and is operated it is commonly broken down into three segments; Space, Control, and User.

2.2 Space Segment

The space segment of GPS consists of at least 24 satellites with 3 operational spares in orbit around the earth. These satellite vehicles (SVs) are distributed in six difference orbital planes, which have inclinations of 55-degree, relative to the equator (Logston, 1995). The SVs are at a nominal altitude of 20,200 kilometers altitude and there are at least four satellites in each orbital plane. The number of SVs has changed over the years, and as of September 2007 there were actually 31 Block II SVs in orbit (Larson, 2006). The additional SVs provide better precision by providing better geometry and redundant measurements to the receivers. See figure 2-1 for an image of the orbital array of satellites.

The system is financed by the United States Department of Defense but provides continuous coverage to anyone who purchases a GPS receiver. Each satellite makes two orbits each sidereal day with a small amount of drift. The drifts are caused by differing speeds along orbit, due to changes in the masses of the SVs as fuel is expended, and other effects such as

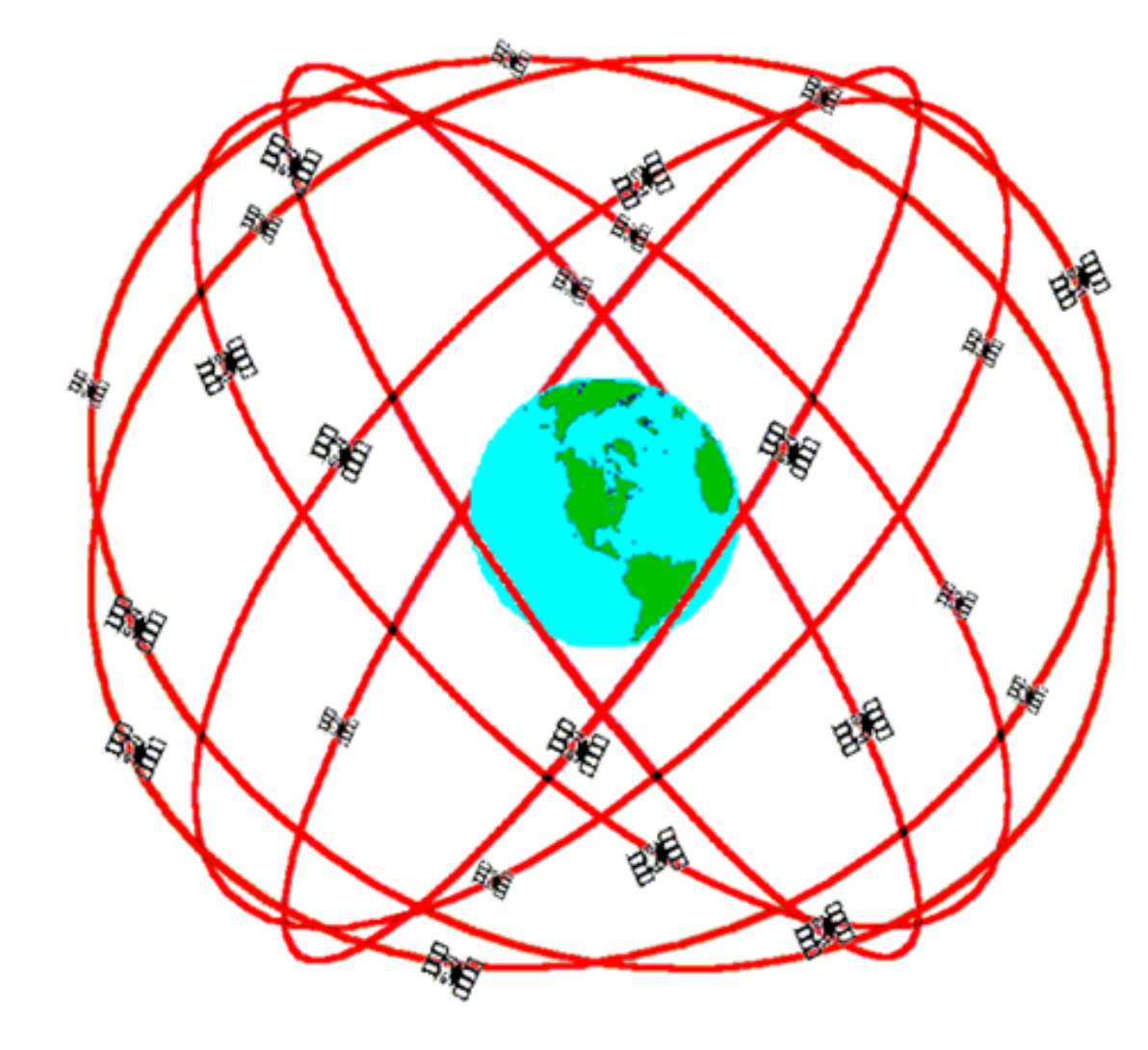

Figure 2-1. Constellation diagram. Reprinted with permission from Dana, Peter H. 2008. University of Colorado at Boulder, Department of Geography.

variations in solar radiation pressure as the SVs go into and out of the Earth's shadow. The spacing between SVs requires constant monitoring of position and frequent thruster burns to reposition SVs (Andrews and Weill, 2007). This is achieved by the control segment and will be discussed further later. In order to determine the location of a receiver, GPS uses trilateration or measuring distance from known positions in this case the GPS satellites.

Each GPS SV transmits time tagged signals from which a receiver can derive the satellite's signal travel time (Markel, 2002). The distance the signal travels is calculated by the

time that it travels multiplied by the speed of light. With this information the receiver needs four satellites in order to calculate the receiver's three-dimensional position. This is shown in figure 2-2 below where the spheres of each satellite's radio signal intersects with another; it takes four signals to refine the position of intersection to one point. Two signals gives an intersection of a circle, three gives an intersection of two points (one of the points can normally be thrown out by determining which of the two points fit on the reference ellipsoid), and four signals consolidate the intersection onto one point. Each additional satellite gives an addition degree of freedom in the measurement of position.

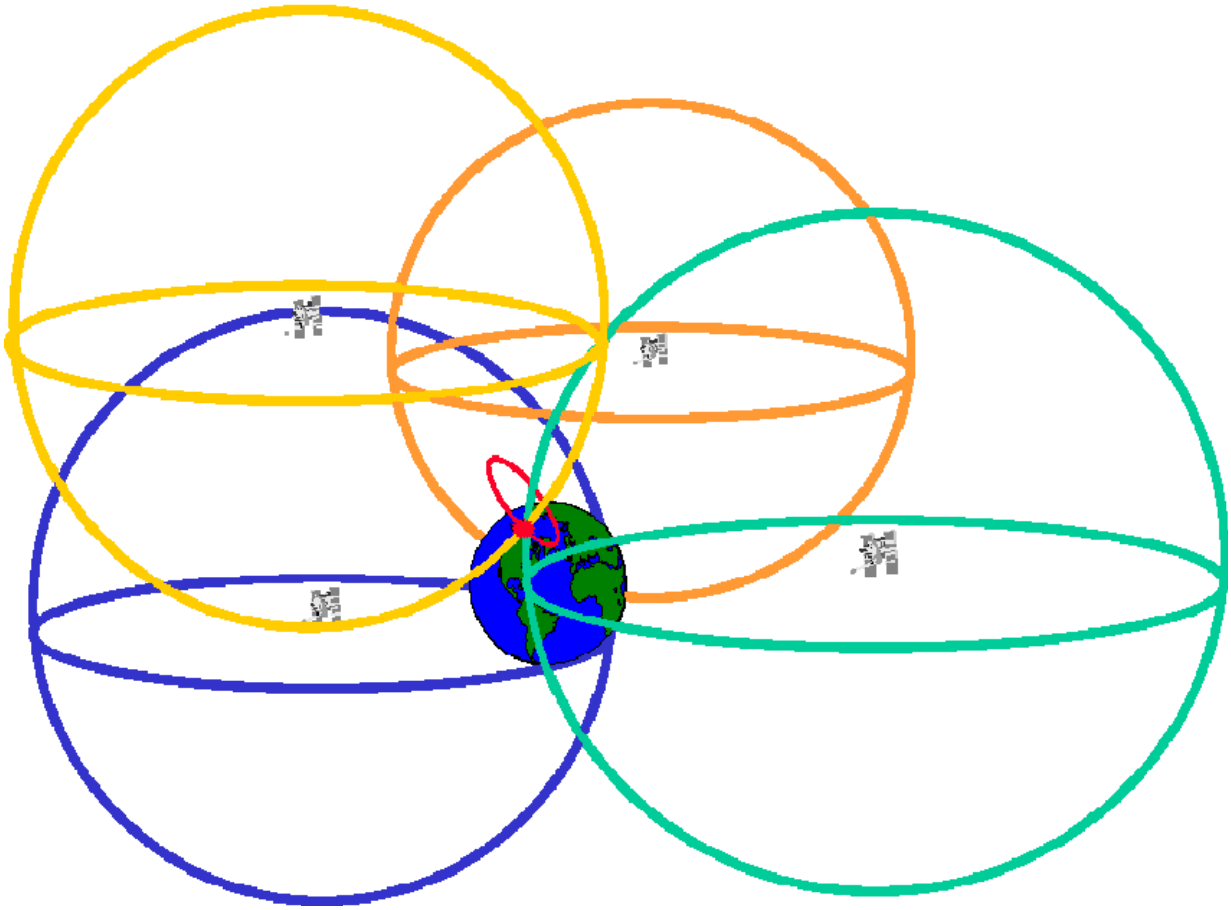

Figure 2-2. Signal intersection diagram. Reprinted with permission from Oxendine, Christopher, 2007. West Point Instructor, EV 380 Surveying

Determining the position using a satellite in space requires significant technology and the math involved in calculating position is not as simple as one might expect upon first thought.

One important component for the derivation of position is time and more specifically how GPS utilizes this information. Since we know the speed of light, we can calculate that an error as small as one billionth of a second equals the distance of approximately 30 cm (one foot). Therefore, precise time is demanded in order to maintain a precise measurement of the position of a GPS receiver. Each of the block II GPS satellites has four atomic clocks, two clocks are cesium and two are rubidium based. The most significant factor that must be taken into account with the onboard clocks is the relativistic effects on the atomic clocks. Because the gravitational field is weaker at the position of the SV's the clocks run faster than they would on the earth's surface. However, the SV's are in orbit around the earth thereby slowing their clocks measure of time by their orbital velocity. If not accounted for, relativistic effects would cause errors in the navigation solution of kilometers within hours (Carter et. al., 2007). The control segment of the system updates the clock of each satellite once a day from the ground (Logsdon, 1995). The signals received from the SVs also provide updates to the position information of the SVs. This position information is crucial in the development of the equations for determining the receiver's position. Below is a diagram that depicts the formulas used to calculate the spatial information of the receiver and satellites using what is known as the code pseudo-range technique.

$$P_1 = \sqrt{(x_1\text{-}X)^2 + (y_1\text{-}Y)^2 + (z_1\text{-}Z)^2} + C_b$$

$$P_2 = \sqrt{(x_2\text{-}X)^2 + (y_2\text{-}Y)^2 + (z1\text{-}Z)^2} + C_b$$

$$P_3 = \sqrt{(x_3\text{-}X)^2 + (y_3\text{-}Y^2)^2 + (z_3\text{-}Z)^2} + C_b$$

$$P_4 = \sqrt{(x_4\text{-}X)^2 + (y_4\text{-}Y^2)^2 + (z_4\text{-}Z)^2} + C_b$$

Figure 2-3. Pseudo range equations

Where
Cb = Clock bias
x,y,z = satellite position coordinates
X,Y,Z = receiver position coordinates
P = Pseudo-range of satellite to receiver

We end up with four unknowns and at least four equations (more equations with more satellites). The unknowns are the (X,Y,Z) positions of the receiver, and the clock bias in the receiver (Logsdon, 1995). Probably the most significant portion of this is the ability to remove the clock bias. This ability removes the need to spend substantial amounts of money for highly accurate clocks in every receiver. As a result, GPS receivers on the market today are affordable and can be purchased by just about anyone with an interest in GPS.

To determine the travel time of the signal from the SV, the signal that a GPS satellite transmits is composed of a timed binary pulse along with a set of ephemeris constants that define the orbit of the satellite. Each satellite transmits a code on the same two frequencies (L-band) and the receiver can determine which satellite it is by using a division process on the code. There are two codes, the P-code or precision code which is transmitted on each frequency and the C/A code or Coarse Acquisition code in which is only transmitted on the L1 band frequency. The precision code during the initial development of the system was encrypted and could only used by the US Department of Defense. This however has since been removed and can be used by receivers that have the capability to read the P-code. The differences between the two codes are the chipping rates and how often each pattern repeats itself. The C/A code has a chipping rate of about 1 bit per second and repeats itself after $1/1000^{th}$ of a second. The P-code, on the other hand, has a rate of 10 million per second and repeats after one week. Each satellite transmits the signals on the two bands L1 and L2 at frequencies of 1575.42 MHz and 1227.60 MHz (Hurn, 1993). Each satellite transmits a precisely timed unique binary code in which the

receiver knows when it was received. The receiver can then derive when the signal left by the difference in time between the signal patterns and thereby derive the travel time. See the description below in figure 2-4 (Oxendine, 2006).

Another technique of position determination is called carrier phase pseudo ranging, which goes further into the calculation of position. In the carrier phase derivation of position all the calculations are the same as in the code phase but an additional wavelength portion is calculated (Andrews and Weill, 2007). This additional portion of a wavelength is simply the remainder of a wavelength and deriving this information provides the user an order of magnitude better resolution on position. See figure 2-5 for a diagram. The most important and most difficult portion of carrier phase pseudo ranging is to ensure the number of wavelengths is calculated correctly. With the wrong integer of wavelengths calculated, a significant error is induced into the system and the signal interruption called cycle slip requires a recalculation (Oxendine, 2006).

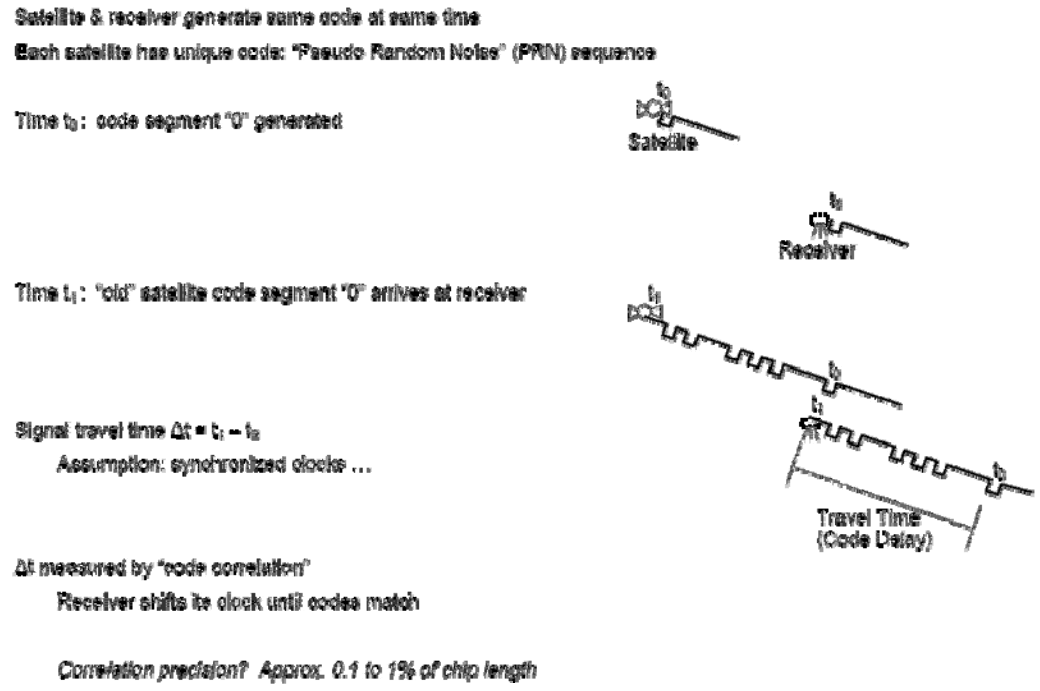

Figure 2-4. Signal travel time diagram. Reprinted with permission from Oxendine, Christopher, 2007. West Point Instructor, EV 380 Surveying

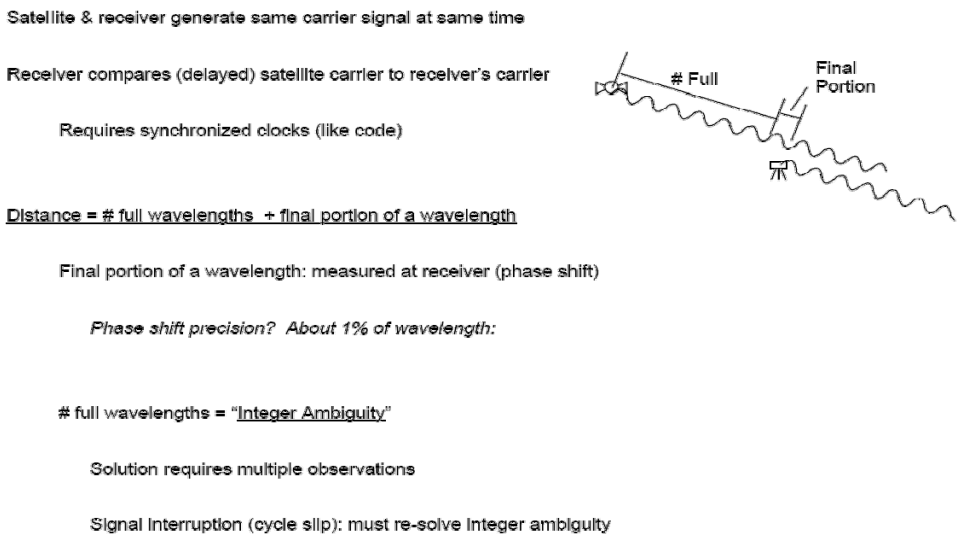

Figure 2-5. Carrier phase GPS diagram. Reprinted with permission from Oxendine, Christopher, 2007. West Point Instructor, EV 380 Surveying

2.3 Control Segment

The control segment is designed to provide updates to the constellation of satellites by correcting the clock bias errors of each satellite, and correcting the ephemeris constants that each SV transmits. This ephemeris data includes information on clock time, SV health, and location (Andrews and Weill, 2007). In order to update this information, each satellite's position is calculated by the control segment using the inverted navigation solution. This is done by establishing four monitoring stations (of known locations) scattered across the earth; these stations track the satellite and are able to take range measurements from these four positions to correct for satellite location and timing errors. This adjustment takes place at the master control station where it takes into account hundreds to thousands of measurements from each monitoring station and uses a least squares adjustment to calculate the adjustment value. A message is then sent to each SV daily from different ground antennas to adjust each satellite location and time (Logston, 1995). Figure 2-6 shows the positions of the different portions of the control segment (Oxendine, 2006).

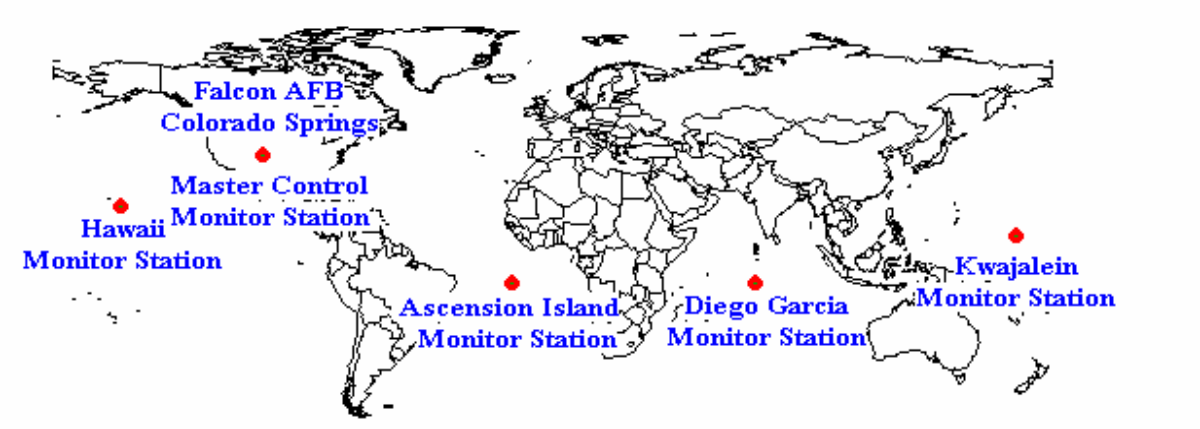

Figure 2-6. Control segment map. Reprinted with permission from Dana, Peter H. 2008. University of Colorado at Boulder, Department of Geography.

2.4 User Segment

The User segment consists of those people or systems in possession of GPS receivers. Today the civilian users outnumber military users and the range of uses includes the applications of aviation, recreation, surveying, vehicle tracking, emergency services, mapping, and a myriad of other applications. The typical GPS receiver consists of a display screen for the display of position, speed, and other desired data, a crystal oscillator clock, a data processor to perform the calculations, and an antenna. A common discriminator on the receiver is the number of channels they have which correlates to the number of SVs the receiver can simultaneously track and use in the position determination.

2.5 Selective Availability, Errors, and Differential GPS

Because the Global Positioning System was developed by the Department of Defense (DoD) and due to the needs of National Security, the DoD created a technique to reduce or limit access to the highly precise measurements that GPS can provide. This technique is through what is called Selective Availability (SA), and during the initial years of the GPS system SA was always in operation. This component of the system actually induced error into the system to reduce the accuracy of the system to plus or minus 100 meters (NAVSTAR, 2006). This was

accomplished by manipulating the message data and clock frequency. While SA is in operation, the Y-code or encrypted P-code is used in place of the P-code and can only be read by military and Department of Defense authorized users. The Y-code is generated by multiplying the P-code by what is called the W-code (Andrews and Weill, 2007). A way to get around this is through differential GPS, which will be discussed later. However, during President Clinton's term, he signed an executive order on 1 May 2000 directing SA be turned off and only be turned back on during a time of national emergency (Andrews and Weill, 2007).

There are other sources of significant error in the formulation of a position using GPS. These sources of error are: ionospheric propagation, tropospheric propagation, multi-path, ephemeris data, onboard clock and receiver clock (Andrews and Weill, 2007). Ionosphere error is caused by the differing effects of the sun on the gas molecules in the ionosphere releasing electrons. This changes the path length caused by the index of refraction due to the number of free electrons per meter squared the signal must travel through (Wells et al, 1986). Normally, the ionosphere has a greater effect on SVs located closer to the horizon. One can reduce this effect by using L1/L2 frequency corrections because the ionospheric effect is dependant upon frequency (Wells et. al., 1986).

Tropospheric propagation delays are caused by gases and water vapor in the troposphere at altitudes up to 80 km and is the result of refraction due to the gases found there. This causes a delay of the signal as a function of the refractive index of the gases along the path of propagation (Wells et. al., 1986). This source of error is not a function of frequency or wavelength and therefore L1/L2 pseudo-range measurement comparisons will not suffice as a technique to remove the error. The effect of this error hinges on the water vapor content, temperature, and angle of the SV from the horizon, and range measurement errors can reach up to 5 meters. The

best technique to reduce this error is the use of DGPS but even DGPS can have significant error if there is a sizable difference in temperature, humidity or pressure between the base station receiver and the user receiver (Andrews and Weill, 2007).

Multi-path error is caused by one or more secondary paths of the signal, between a satellite and the receiver antenna. One example of multi-path would be the reflection of the signal from the surfaces of buildings or even the ground, before they reach the receiver antenna. The result of multi-path is a superimposed signal that distorts the phase and amplitude of the direct path signal. This cannot be corrected by DGPS or L1/L2 pseudo-range measurement comparisons (Andrews and Weill, 1986). The best technique is the use of an antenna beam shaping to limit the ability to detect multi-path signals, such as antennas that employ choke rings (Wells et. al., 2007). However, even this is not a perfect solution and in different environments has different effects. If the receiver is on the ground near a building for example the likelihood and significance of multi-path remains relatively high.

The ephemeris data, SV on-board clock errors, and receiver clock errors can cause errors in the amount of roughly one meter. Improvements of satellite tracking can reduce the error in the messages updating the SV information and will therefore reduce this error. Also the on-board clocks are not perfect, as no clocks that humans can currently produce are completely perfect. In addition to this, the effects of placing atomic clocks in an orbit kilometers above the earth places the clocks in a weaker gravitation field causing the clocks time kept to be slower, but with a velocity that in essence increases the time (Carter et. al., 2007). In addition to this, the earth's gravitational field is not the same throughout the entire orbit of each SV making the adjustments for relativistic effects imperfect. Therefore, there is a certain amount of error with the SV on board clocks and they are updated daily. The receiver clock error is also significant. While it is

less important to have a highly accurate receiver clock, and more expensive to the user, it is an important portion of the position solution; however, as discussed earlier in the paper there are equations that reduce and correct for this error (Andrews and Weill, 2007).

Differential GPS requires two receivers. One is with the user collecting data, often referred to as the rover, at the point of interest. The other receiver, commonly called the base station, is positioned at a known point collecting position information at real time. The important aspect of this technique is that the known point receiver must be within a reasonable distance to the collection receiver in order to ensure the same conditions and constellation is being observed by both receivers. The result is a set of data from the known point that varies due to the different types of errors discussed earlier. This information can then be taken to derive the difference in the known point coordinates. This data can then be subtracted from the user receiver data to adjust the coordinates and thereby removing the error. This technique is capable of removing significant amounts of errors associated with SV clock, ionosphere, troposphere, and selective availability (Hurn 22). This can be done in real time where the base station broadcasts the correction information to the rover or the corrections can be post-processed where the user downloads the rover data into a computer along with the base station data and allows the computer to run the corrections. An example of a real time correction system is the Wide Area Augmentation System (WAAS). This system consists of base stations established throughout North America. WAAS stations send the correction information to geostationary satellites which then in turn broadcasts the correction to the user (Trimble, 2006).

GPS has changed the way people navigate the world. While the system has many expensive and complex algorithms to operate, the beauty of this system is its ability to provide the user an inexpensive receiver. These inexpensive receivers provide the capability to be

available to everyone on earth. Not even ten years ago a road atlas was a must in every car; however, today even rental cars have navigation systems available.

CHAPTER 3
INTRODUCTION TO AIRBORNE LASER SWATH MAPPING

3.1 Principles of ALSM

Airborne Laser Swath Mapping (ALSM) is a particular technique of using LiDAR or Light Detection and Ranging. LiDAR is an active form of remote sensing similar to RADAR but transmits light as opposed to radio signals. The basic principle behind LiDAR is the timing of the transmission of a photon packet from a laser directed towards an object and calculating the time of flight of that photon packet to the object and back to the sensor. ALSM is a form of LiDAR that mounts the LiDAR system in an airborne platform and directs the laser towards the earth in order to generate a three dimensional depiction of the earth's surface. ALSM is rapidly becoming one of the most accurate forms of conducting topographic surveys providing accuracies to .2 meters or better on the horizontal and vertical components (Luzum et. al., 2004). The purpose of this chapter is to provide a basic understanding of how ALSM works, the data that can be obtained by such a system and the attributes of the ALSM system used in this study.

A typical ALSM system consists of a laser, scanner, sensor, cooling system, GPS, and an inertial measuring unit (IMU). ALSM mounts the system in an airborne platform, normally an airplane but not always, and directs laser pulses towards the ground. These pulses of light interact with the ground and many of the transmitted photons are reflected off the surfaces of trees, sidewalks, buildings and other objects on the earth's surface. When a photon returns to the sensor the ALSM system is able to calculate the total travel time and thereby determine the distance the photon traveled using the following basic equation: $D = \left(\frac{c * t}{2} \right)$. In this equation D is distance, c is the speed of light through the medium of propagation, and t is travel time (OPTECH, 2007). For each pulse of light transmitted by the laser there is the possibility for

many return pulses, depending on nature of the reflecting surfaces or surfaces encountered in the fight of each laser pulse. Most systems only record a certain number of returns. The early systems normally recorded only the first and last return pulses, but as the technology developed many systems are starting to record multiple stops such as the new system at the University of Florida, which records up to four returns per shot.

In order to generate a map using ALSM we must have good three dimensional position information of the points we are mapping. In the case of ALSM that starts with the necessity of highly accurate information about the position and orientation of sensor on-board. The aircraft has a GPS receiver on board and the ALSM sensor head contains an IMU, which has three solid state accelerometers and 3 fiber optic or ring laser gyroscopes. This combination of GPS, IMU, and some ground based GPS control points operating in conjunction with each other provides the capability of providing not only highly accurate position information, but will also provide attitude information (roll, pitch, and yaw) of the sensor head.

Attitude information is obtained using the IMU. An IMU consists of three accelerometers and three gyroscopes mounted in its own three dimensional coordinate system. This allows for the system to measure acceleration, velocity, and changes in attitude (Rogers, 2003). Attitude information is important because as the attitude changes the direction the laser is pointing changes as well. This is important because the system needs to know where the laser and detector are located, where or in what direction the laser is pointed, and the distance to the measured point on the ground in order to get a quality position for the registered photon returns. This also includes the scan angle of the laser at each pulse instant. Figure 3-1 depicts the different components of position and attitude determination that are necessary for the determination of position of the laser point returns.

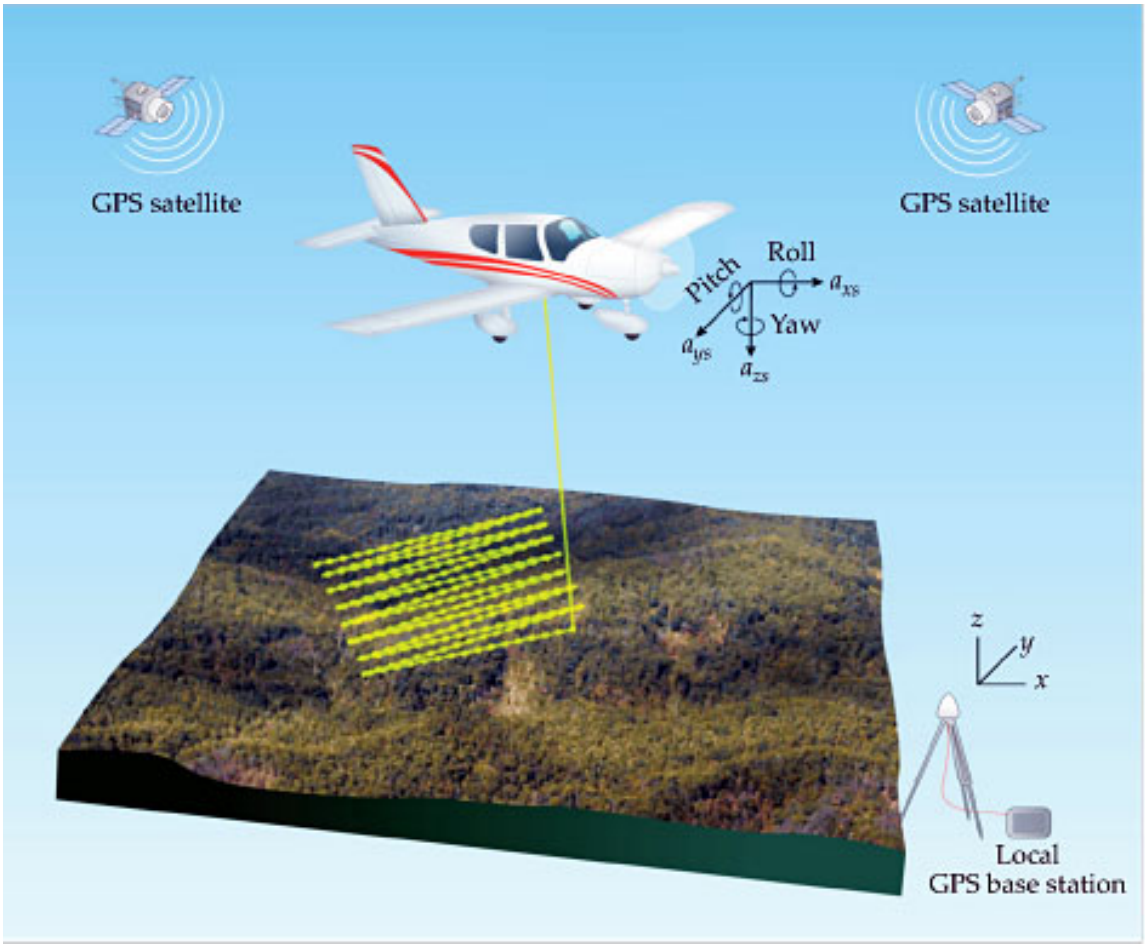

Figure 3-1. Diagram of ALSM. Reprinted with permission from Carter, W.E., R.L. Shrestha, and K.C. Slatton, 2007. Geodetic Laser Scanning, *Physics Today*, (December): 41-47.

Determining the coordinates of the ALSM data points require a transformation of data into a mapping frame of reference. In order to make this transformation many different reference frames must be considered. These frames of reference include: mapping frame, navigation frame, body frame, sensor frame, and the image frame. A brief description on how the transformation matrix from mapping frame to image frame is given below for more information on this subject see *Applied Mathematics in Integrated Navigation Systems* by R. Rogers.

$$C_m^i = C_c^i \times C_b^c \times C_n^b \times C_m^n$$

Where

$$C_m^n = \begin{bmatrix} 0 & 1 & 0 \\ 1 & 0 & 0 \\ 0 & 0 & -1 \end{bmatrix}$$

$$C_n^b = C_b^{n^{-1}} = \begin{bmatrix} \cos\theta y \cos\theta p & \cos\theta y \sin\theta p \sin\theta r - \sin\theta y \cos\theta r & \cos\theta y \sin\theta p \cos\theta r + \sin\theta y \sin\theta r \\ \sin\theta y \cos\theta p & \sin\theta y \sin\theta p \sin\theta r + \cos\theta y \cos\theta r & \sin\theta y \sin\theta p \cos\theta r - \cos\theta y \sin\theta r \\ -\sin\theta p & \cos\theta p \sin\theta r & \cos\theta p \cos\theta r \end{bmatrix}'$$

$$C_b^c = C_c^{b^{-1}} = \begin{bmatrix} \cos\theta ym \cos\theta pm & \cos\theta ym \sin\theta pm \sin\theta rm - \sin\theta ym \cos\theta rm & \cos\theta ym \sin\theta pm \cos\theta rm + \sin\theta ym \sin\theta rm \\ \sin\theta ym \cos\theta pm & \sin\theta ym \sin\theta pm \sin\theta rm + \cos\theta ym \cos\theta rm & \sin\theta ym \sin\theta pm \cos\theta rm - \cos\theta ym \sin\theta rm \\ -\sin\theta pm & \cos\theta pm \sin\theta rm & \cos\theta pm \cos\theta rm \end{bmatrix}'$$

$$C_c^i = C_m^{n^{-1}} = \begin{bmatrix} 0 & 1 & 0 \\ 1 & 0 & 0 \\ 0 & 0 & -1 \end{bmatrix}^{-1}$$

Rotation from image to mapping frame by:

$$C_i^m = C_m^{i^{-1}}$$

To obtain the image coordinates use the following equation:

$$\begin{bmatrix} Xi - Xs \\ Yi - Ys \\ Zi - Zs \end{bmatrix} = \lambda (C_i^m) \begin{bmatrix} xi \\ yi \\ zi \end{bmatrix}$$

Where

Xi,Yi and Zi = Coordinates in the mapping frame

Xs, Ys, Zs = Sensor position coordinates in mapping frame of sensor position

λ = scale factor

xi,yi = image pixel coordinates

zi = -f(focal length)

C_i^m = rotation matrix for coordinate transformation from image to mapping frame

(Singhania, 2007 and Rogers, 2003)

Once the data are collected and processed, the data can be used in many different ways. Unlike many remote sensing techniques, ALSM provides three dimensional information about the surface of the earth not only providing X,Y, Z of the earth's surface but also about objects on the earth's surface. The ALSM data can provide a user with a simple elevation model of the earth's surface, but it can also show the height of a forest canopy as well. Figure 3-2 shows how using one ALSM data set, collected for the forestry commission consisting of multiple flights with a pulse rate between 20,000 and 50, 000 pulses per second, can reveal both the bare earth Digital Elevation Model (DEM) and information about the tree canopy height as well. The figures below (Forestry Commission, 2006) were used for archaeological prospecting in woodland environments using LiDAR.

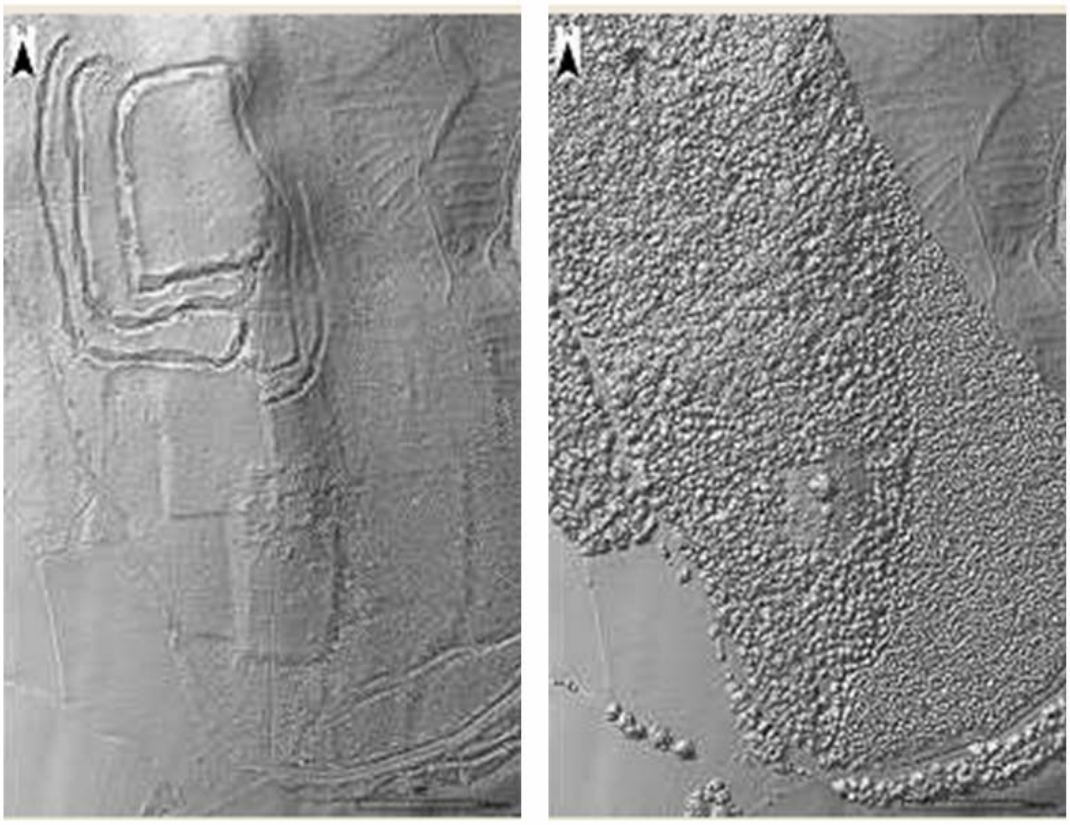

A B

Figure 3-2. Images showing both bare earth and tree canopy from ALSM data. (A) Image of the bare earth surface. (B) Image showing the canopy.

In addition to these kinds of images, you can take ALSM data and plot the returns in MATLAB and obtain a 3 dimensional image. Figure 3-3 was generated using Matlab software using the Hogtown ALSM data collected in Feb 2006 by GSE. Represented in the figure is a 20 meter by 20 meter area in the X, Y directions with ground points removed. The image shows that in a small forested area you can clearly see a diverse array of point returns in the under story of a forest canopy.

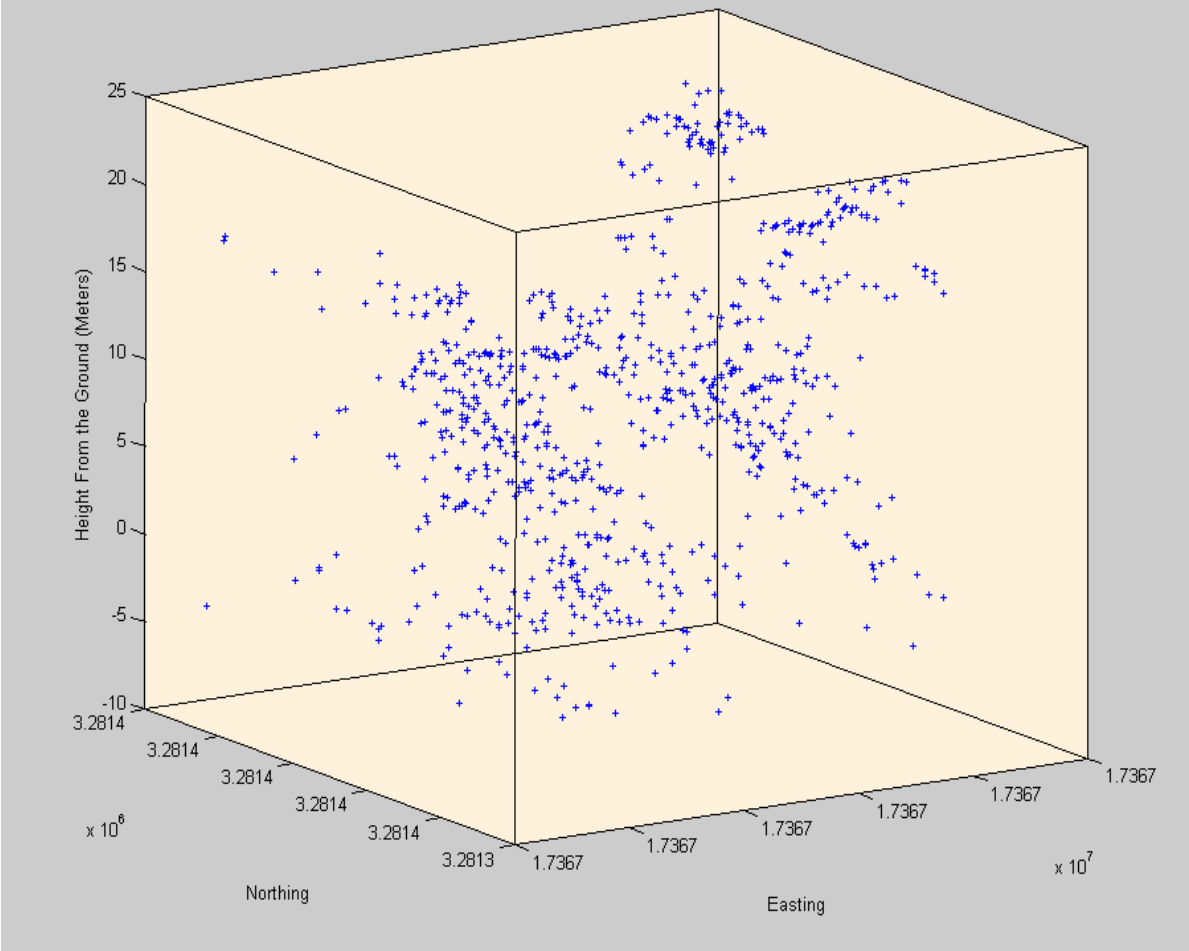

Figure 3-3. Point returns inside a 20x20 meter box

3.2 Attributes

The University of Florida has operated two ALSM systems. The first system they operated up to 2007, when it was replaced with a newer and more robust system. During the course of

this project data were collected by the older two return system, and the primary specifications of that system are given in table 3-1 (Singhania, 2007).

Table 3-1. System attributes used for this study

Attribute	*ALTM 1233*
Wavelength	1.064 µm
Pulse Rate	5,000 to 33,000pps
Range Accuracy	2 to 15 cm (single-shot).
Scan Angle	0 to 30 degrees
Scan Rate	0 to 50 Hz.
Scan Design	Oscillating mirror, Nutating mirror, Compound
Operating Altitudes	Mission specific
Data storage	8 mm tape, CD-ROM, hard disk
Stops	(2) First and Last

3.3 Advantages and Accuracy

The use of ALSM remote sensing has several distinct advantages over other technologies. One of the most significant advantages is the level of resolution that is obtainable from ALSM. The use of a laser allows the system to direct the photon packet to a small footprint, typically no more than a few decimeters in diameter, on the ground. This is different from other distance ranging techniques such as RADAR, which illuminates a wide area, 100s to thousands of meters in diameter on the ground. Photogrammetry is also capable of making range estimates by the use of stereoscopic measurements or using overlapping images taken from a flight line. Clearly in this case the advantage is that LiDAR makes the range measurement directly and without the distortion inherent in aerial photography (NCALM, 2007).

ALSM does have some significant drawbacks. The most significant drawback is similar to that of photogrammetry in the sense that under certain conditions the sensor will not work well. Some of these conditions include hazy, smoggy, foggy, or even cloudy conditions in which the laser will not transmit though the medium well. In this sense, RADAR has the advantage

because the radio waves are not obstructed by these conditions and therefore the system will maintain its effectiveness (NCALM, 2007).

CHAPTER 4
LITERATURE REVIEW

The NAVSTAR Global Positioning System (GPS) has in recent years become a critical tool in fields ranging from military applications, to scientific earth measurement. Precisely measuring the degree to which GPS signals are affected by forest canopy provides useful information about signal degradation. With the advancement in LiDAR technology, in particular ALSM, we can obtain detailed information on the estimation of forest vegetation and canopy structure. In this research both GPS as well as ALSM data are used in order to precisely measure the degree to which GPS signals from individual Satellite Vehicles (SVs) are affected by forest canopy, as measured by ALSM, and measure the signal degradation

By the nature of the NAVSTAR Global Positioning System (GPS), early researchers had a need for significant improvements in positional accuracy. One of the first techniques used to improve positional accuracy to include removing the effects of SA was the use of Differential GPS (DGPS). Initial researchers studied the accuracy and precision of GPS under different environmental conditions. Some of the findings and lessons from their research include expected positional accuracies under different environmental conditions, experiment set up techniques, different NMEA message formats useful for analysis, and initial findings.

Previous work on the study of the propagation of signal through the canopy of a forest, or other medium, show there is an effect on the signal as it moves through both the canopy as well as the atmosphere. The way the L-band reacts as it propagates can be initially described by Beer's Law, or the Beer-Lambert Law. Beer's Law associates the effect of electromagnetic radiation (EM) and the transmittance of the radiation through a substance. This law states that there is an exponential relationship between the density of a substance through which the EM must pass and the transmittance of the EM. This law applies as radiation passes through the

atmosphere but would also directly apply in this study to the passage of a GPS signal through vegetation or tree canopy. As the distance the signal must propagate through tree foliage increases as well as the density of the foliage increases, the absorption of the signal should increase in an exponential pattern. Figure 4-1 illustrates how the distance through the tree foliage changes based on the position of the signal from the receiver and how the signal strength is affected by the density of the foliage through which the signal must propagate.

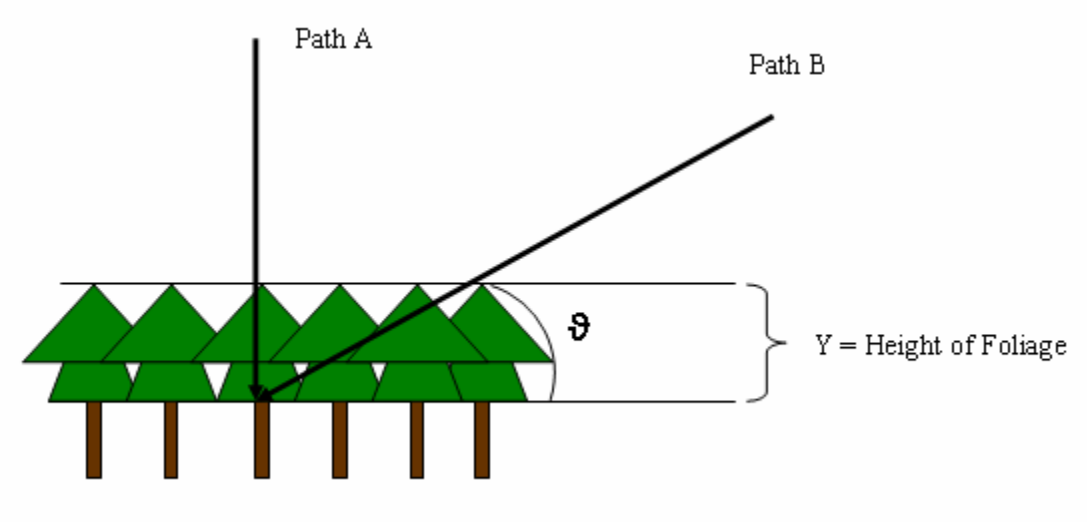

Figure 4-1. Distance of the signal propagation through tree foliage based on the angle of transmission source with respect to the horizon. In this case the path of propagation through the medium for the two different incident angles are Path A = Y and Path B = Y/SIN θ.

In 2001, a group of researchers in Ireland used skyward looking photography in conjunction with GPS data in an attempt to develop a quantitative method of classifying forest canopy and relating this classification to the degradation of carrier phase differential GPS performance. In the article the use of the skyward looking photography included converting the image into an eight bit grayscale image to classify canopy closure and obstruction. This technique led to a definite correlation between canopy obstruction and DGPS performance with a R^2 value reaching up to .74 when fitting a trend line to their findings (Holden et. al., 2001). A

particular interest in this article is the use of standard deviation of fix values from the GPS as the measure of precision for the experiment. This is useful as the forests in which the ALSM data I used in this study do not have easy access to survey in GPS points, and we do not have access to nor the expertise with the needed equipment to accurately survey in each of the GPS points.

In 1999 a paper entitled "Impacts of Forest Canopy on Quality and Accuracy of GPS Measurements" found that with 300 GPS fixes, PDOP or Position Dilution of Precision "is not as good an indicator for positional accuracy under forest canopy as is universally acclaimed (Sigrist and Hermy, 1999)." The study focused on quantitative analysis of GPS accuracy on different forest canopy types and how PDOP affects positional accuracies as well as how foliage relates to signal blockage. In this particular study the researchers used skyward looking photos to classify the forest and converted the images into 2-bit black and white images for the analysis. In the 2-bit image, black represents foliage and white represents an unobstructed view of the sky. The most significant contents of this paper were that as canopy density increased the signal attenuation increased, PDOP is not a good indicator of position precision, and the use of skyward photography techniques as a measure of canopy closure. This paper also refers to a paper by Yang and Breck from 1996 that supports their findings showing that PDOP is not a good predictor of position precision in forested terrain.

Axelrad and Behre submitted a paper to the Proceedings of the IEEE, where they demonstrated that NMEA messages in the GPS receivers included individual SV signal to noise ratios and are capable of showing significant signal attenuation based on the angle of the SV from the zenith. This particular research was measuring this signal attenuation from space based platforms so the attenuation was mainly attributed to the atmosphere (Axelrad and Behre, 1998). It therefore is rational to think that the addition of forest canopy between the SV and antenna

should attenuate the signal further. The technique of signal to noise ratios from each SV can provide us the information from each SV and the SV location relative to the antenna as to the effect of forest canopy density and the effect of the propagation of the signal as caused by the forest.

Up to this point different techniques have been used to measure canopy properties. Some forest experts use instruments that measure how much light passes through the canopy, other researchers actually take measurements of the trees themselves such as Diameter at Breast Height (DBH) and use forest indexes to determine a canopy density; however, in November of 2000 a paper on laser altimetry demonstrated the potential of using lasers to characterize forest parameters and showed that they can provide reproducible and accurate results (Harding et. al., 2001). This technology can now be exploited for this study as a substitute or supplement of skyward looking photography or other measurements of forest canopy density and closure.

The ability to obtain forest canopy information from ALSM technology is significant because it will allow for the gain of detailed three dimensional information of the forest at any given point where the data coverage applies without a physical presence at that location being necessary. As explained so far, all the canopy measurements require physical measurements of some sort to be taken at the actual location of interest. The ability to gain the needed data to make these measurements with a simple single flight on an airplane with an ALSM device could possibly remove this necessity. Clearly, such a capability would have significant benefits for military applications in hostile environments, time savings when research requires taking hundreds of measurements of forest parameters into account—and the data would consist of digital information that could easily be manipulated by computer models.

Previous research shows that topography and land cover (i.e. foliage) are two of the most important factors governing detection and communication in natural terrain. ALSM systems are capable of mapping topography with sub-meter-scale resolution and, in particular, provide three-dimensional canopy structures in the forest. Since GPS signal transmissions are employed in three-dimension space, ALSM data is suitable for analyzing attenuation measurement in these conditions.

ALSM studies have proven to be capable of providing the user information about forest structure. In 2004, researchers simulated the LOSV (Line of Sight Visibility) for trail detection in forests by using ALSM data. In the study candidate foliage voids are seeded on the ground surface and then visibility vectors between seeds are estimated using cylindrical scope functions for identifying optical lines of sight over the terrain (Lee et. al. 2004). In addition, the study went on to develop a model to estimate the sunlight flux by analyzing the directional foliage density from high-resolution ALSM data. The foliage points are first extracted by using an adaptive multi-scale filter to remove the ground point data. Then, cylindrical and conical scope functions are used for computing the foliage density. By using this approach an estimate, of the sunlight flux at any location in the test site can be predicted (Lee et al., 2005). This study provided a preliminary concept about the use of space scope functions for determining the direction of radiation propagation using LiDAR data.

In particular interest to this study was the development of a weighted conical scope function for estimating the intercepted solar radiation (*IPAR*) by using ALSM data in the forest. Instead of a simple scope function and just counting the number of points in the scope, a weighted scope function is developed considering the distance between LiDAR points and the observer, as well as, the angular divergence from the central vector of the cone (Lee et. al., 2007).

Although these applications are proposed for estimating different radiation transmissions, they still provide two critical viewpoints. First, by analyzing 3D ALSM data in forested terrain the radiation transmission can be accurately modeled and estimated. Secondly, the scope function with weighted algorithm is useful for analyzing a limited path in which the signal is propagated.

CHAPTER 5
EXPERIMENTAL SETUP AND DATA PROCESSING

5.1 Data

ALSM data used for this research was collected by the GeoSensing Engineering and Mapping (GEM) Research Center at the University of Florida. The center flew both forest areas of interest and post processed the data collected in February and March of 2006. The data set was collected by a commercial Optech system mounted in a Cessna 337 aircraft flying at an average 600 meter height. The system works at a 1064 nm wavelength and records first and last returns per laser pulse. The system shoots 33333 pulses per second and has a variable scan angle ranging from 0 to 20 degrees at a maximum of 50 Hz scan frequency. According to flying parameters, between 1 and 2 returns per square meter can be obtained. This system belongs to the small-footprint (diameter around 15cm) system which is capable of sensing the structure over meter or even sub-meter-scale extent, and thus, is suitable for our forest analysis (Bortolot and Wynne, 2005). The spatial resolution of the data points provided by the ALSM system allows us to determine ground DEM information as well as the three dimensional point cloud information inside the forest. This allows us to determine the height of the canopy and a normalized point density inside the cone through which the GPS signals are propagating.

5.2 Equipment and Setup

GPS data collection efforts were taken on multiple occasions and in two different forests using: two Ashtech mapping grade receivers (one as a base station on top of a building and one as the rover), two antennas, cables, and computers for data capture. The antennas used for both the base station and the rover are model AT 1671-1 see figure 5-1 and table 5-1 for more information on this antenna.

Figure 5-1. Image of AT1675-1

Table 5-1. Antenna attributes for AT1675-1

AT1675-1	
Frequency	1575 +/- 10MHz(L1)+ Glonass
Polarization	Right Hand Circular
Axial Ratio	3 db max
Gain	00,12dB,26dB,36dB
Voltage	RG(4.5-18VDC)
Impedence	50 OHMs
Connector	TNCF
VSWR	2.0:1
Magnet	NM(No)
Finish	Weatherable Polymer
Color	W,O
Weight	15 oz max

These antennas were chosen for their ability to easily detect SV signals, but more importantly because the gain pattern for all signals between 0-75 degrees from zenith are the same. In order to establish a good basis for comparison of data captured from both receivers and to verify the data captured by the receivers are similar, initial measurements consisted of data captured in the same environment. Specifically, twenty minutes of data collected by both receivers on top of Reed Lab at the University of Florida were used for a base comparison of the rover and base station data and collection systems. In April 2007, GPS observations were collected at 11 locations. Of these GPS locations, 5 were collected in Hogtown natural forest and 6 from IMPAC, the managed forest. After our initial analysis we collected observations at 6 additional stations inside Hogtown natural forest in October 2007. All GPS data sets contain information from three different NMEA messages obtained at a rate of 1 HZ. Each data set provides information from each GPS point including a measurement of signal to noise levels of

each SV and positional information. In addition, zenith looking photographs using a fisheye lens where taken at each site for use as a control as explained in the introduction. Upon establishment of an understood variance in signal to noise in similar environments, comparison of data under canopy commenced using the same set up of each receiver as the initial comparison. For each GPS data collection point we have two sets of data, the base station data and the rover data under the forest. The rover antenna was mounted on a tripod at a height of 1.5 meters representing the height of a hiker, soldier, or surveyor. This setup height also avoids interference of most under growth on the forest floor.

At each point measurement data was collected for a total of twenty minutes. These measurements were then analyzed and compared with the base station data. Twenty minutes of measurements at each point allow for an analysis of the signal to noise ratio of each individual point and the amount of variance detected at each site; as well as, ALSM data of each site provides height of canopy and point cloud density.

5.3 Study Site

Each of the two forests used for the study are located in Gainesville, Florida. The first site is the Intensive Management Practice Assessment Center (IMPAC) located roughly 10 km north of downtown Gainesville. IMPAC is operated and managed by the Forest Biology Research Cooperative and consists of two different southern pines species: loblolly (Pinus taeda L.) and slash (Pinus elliottii var. elliottii) (Fernandez, 2007). In the managed forest each GPS point was positioned in a different plot resulting in either a different species, different amount of fertilizer, and of course slightly different forest parameters. However, measurements taken at the site show an average diameter at breast height of 20 cm and a tree average height of 18 to 20 meters. In addition, because this is a managed forest the trees were planted in equally spaced rows with trees planted roughly the same distance apart and to make the forest easily accessible there is

almost no under story whatsoever. In most cases the rows were planted about 4 meters apart with a spacing of about two meters between the trees inside each row. In some cases some trees did not survive so in these cases there is more space between them. Figure 5-2 is a zenith oriented photograph of the managed forest.

Figure 5-2. Example of a managed forest zenith oriented photo

The second forest in which data was collected was in Hogtown forest, a mixed coniferous and deciduous forest just north west of the University of Florida campus. An estimated measurement of tree distribution is 75 percent deciduous and 25 percent coniferous, but being a natural forest this varies from position to position. Hogtown forest consists of trees as tall as 35 meters and possesses the characteristics expected in a natural forest where there are multiple different layers of foliage, different and random spacing between trees, and significant undergrowth. The multiple layers of growth make the distribution of canopy foliage a function of tree height and canopy depth. Figure 5-3 is a zenith looking photo in Hogtown natural forest.

Figure 5-3. Example of a Hogtown forest zenith looking photograph.

5.4 Normalization

The ALSM system used provides one or more laser returns per square meter. In order to take into account as much information as possible about a research or mapping area, researchers almost always register several flight paths or data strips together. This process, as well as certain system processes, causes the distribution of laser point returns to be somewhat inconsistent. For our data sets the Hogtown forest has 5 flight paths while the natural forest has 7 flight paths covering the study area. Although this inconsistency does not negatively influence some applications, such as mapping, it definitely makes certain research, such as our conical analysis, have to account for this uneven distribution. We can account for this through the process of normalizing the planar point density.

A simple data normalization method is employed in this study. After combining several strips in the research area, the average point density in a two dimensional plane is computed. To unify the whole dataset with the proper point density, the number of points in each one meter

square grid is counted and then divided by the average 1x1 meter point density to produce the normalized data set.

5.5 Large Cone

To evaluate the attenuation of GPS signal by using ALSM data, a conical scope function is provided for simulating the signal passing through the path of propagation. The conical scope is set as the box to compute the point density above the GPS antenna. Two types of cones, a large one and a small one, are used for evaluating the signal transmission from all the satellites and individual satellites respectively. For the large cone, the angle θ above the horizon is set at the suggested value of 15 degrees, this is because the receiver obtains quality signals from these angles and there are less atmospheric effects at these angles. At the same time, the height of each cone will be set based on the highest tree within all the cones of our analysis. See figure 5-4 for a diagram of how our large cone scope function is setup.

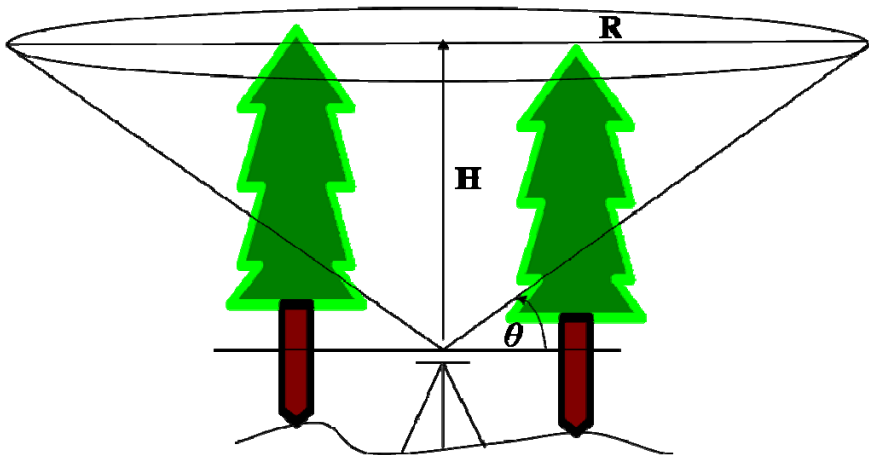

Figure 5-4. Large cone diagram

Once we get the cone height, the number of points inside each GPS cone can be counted and, thus, a unique point density can be computed for each GPS location. An example of the point returns inside a large cone taken at Hogtown forest in 2007 by GSE is illustrated in figure 5-5.

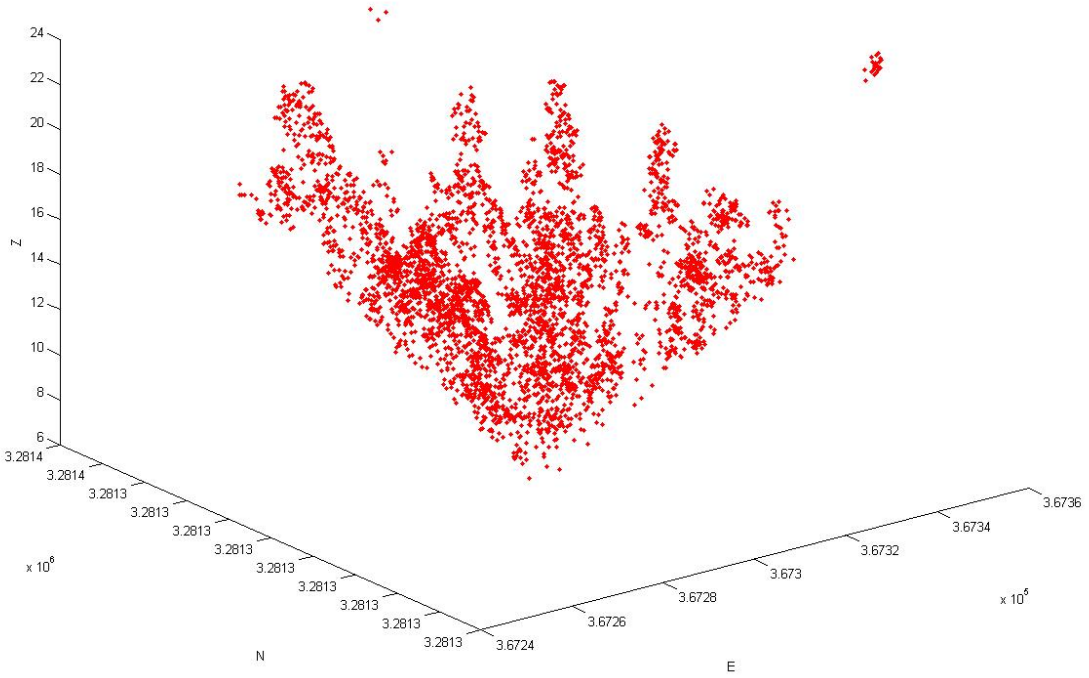

Figure 5-5. Large cone point returns from Hogtown forest point #1 generated using MATLAB

5.6 Small Conical Function

We next analyzed the signal transmission from individual satellites. To do this a small conical scope function was developed aimed in the direction of the satellite and was used to compute the density of foliage in the signal path. The direction of individual SVs including azimuth and zenith is easily acquired from the solution of GPS data from the GSV NMEA message or by using Trimble software (as used to generate the skyplots seen in figure 5-6). By using the conical scope functions and counting the point density, we can formulate the primarily relationship between GPS signal attenuation and canopy density as measured by ALSM.

GPS signals are transmitted along a strait path between the satellite and antenna if there is not any interference between the satellite and antenna. However, in the forest many factors

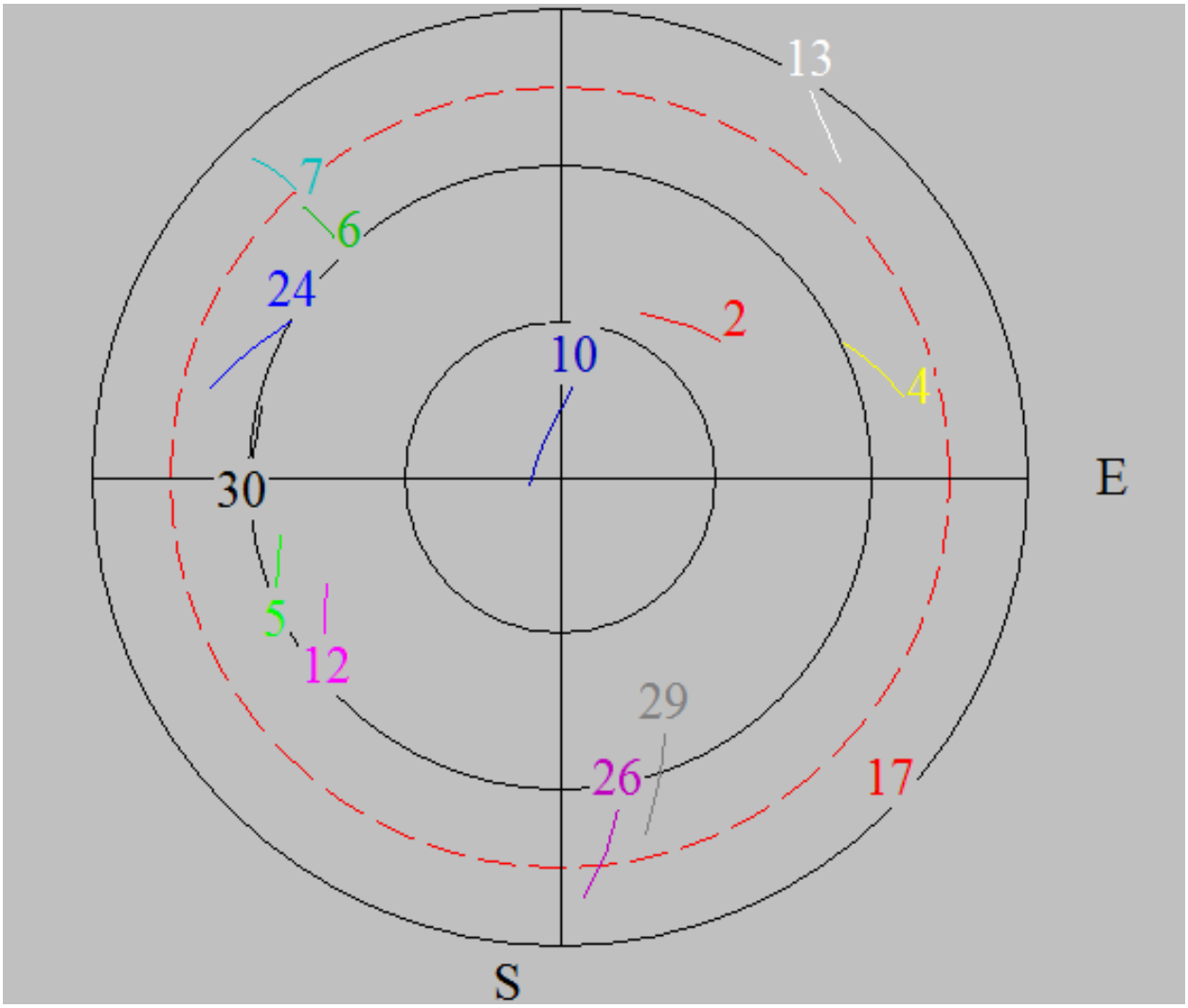

Figure 5-6. Pathfinder office skyplot of Managed forest point #1 generated using Pathfinder office software

interfere with the transmission of the signal such as the atmosphere, tree foliage, stems, and trunks; so the signal will on occasion be blocked and will most certainly be diffracted and attenuated. Figure 5-7 is an image that combines the information from the skyplots shown in figure 5-6 and zenith oriented photos. Figures like figure 5-7 provides a visualization that helps to better understand what environmental factors are affecting our SNR values. In order to evaluate the attenuation caused by foliage distribution, a conical function is used to take into account the foliage interference with the signal transmission along the transmitted path and a

propagation model is employed. The point of origin of the cone is the receiver antenna, the apex angle for each cone at 20 degrees, and the length of the cone is 200 meters. The length of 200

Figure 5-7. Visualization of Hogtown #3 developed by combining the information from skyplots and zenith oriented photographs.

meters was selected because no ALSM points used in this study were further from the receiver than that value, measured along the path of propagation. These cones are developed in order to capture the ALSM point returns inside each cone representing what is considered the interference in the signal path. In this particular case the angle θ above the horizon the SV must stay above is 15 degrees and any SVs that fall below this angle are removed from our analysis. This is because the receiver begins to lose quality signals at any angle closer to the horizon, there are more atmospheric effects, and the mask set for our GPS is 15 degrees. To set up each small cone the average zenith angle and azimuth to the SV during data collection are used for each

GPS point. With these parameters set, the 3D point density is calculated using a simple simulation using the ALSM dataset and the distribution of point returns caused by the vegetation in forest inside the cones. Figure 5-8 is a diagram of the developed cone function.

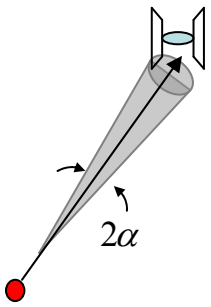

Figure 5-8. Small cone example diagram

Similar to figure 5-5, we can plot all the point returns that fall inside the small cone scope function using Matlab software. A visualization of these point returns is shown in figure 5-9.

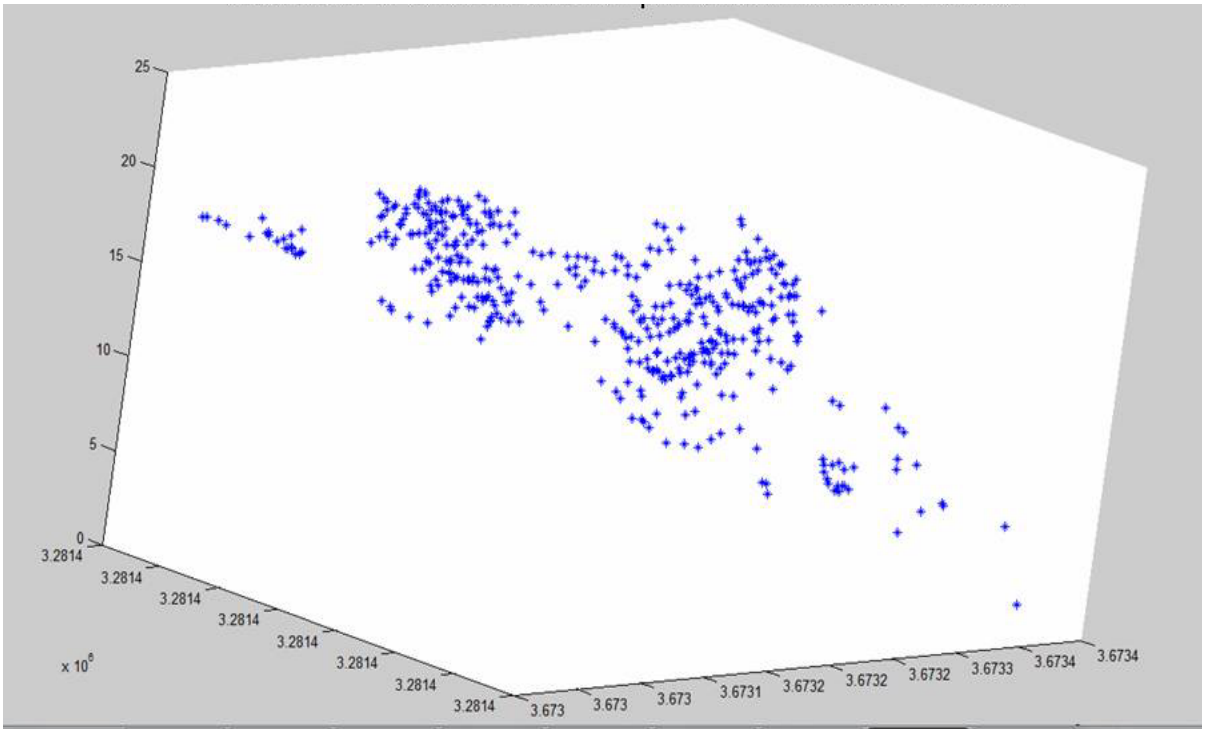

Figure 5-9. Example of ALSM point returns plotted that fall inside the small cone function

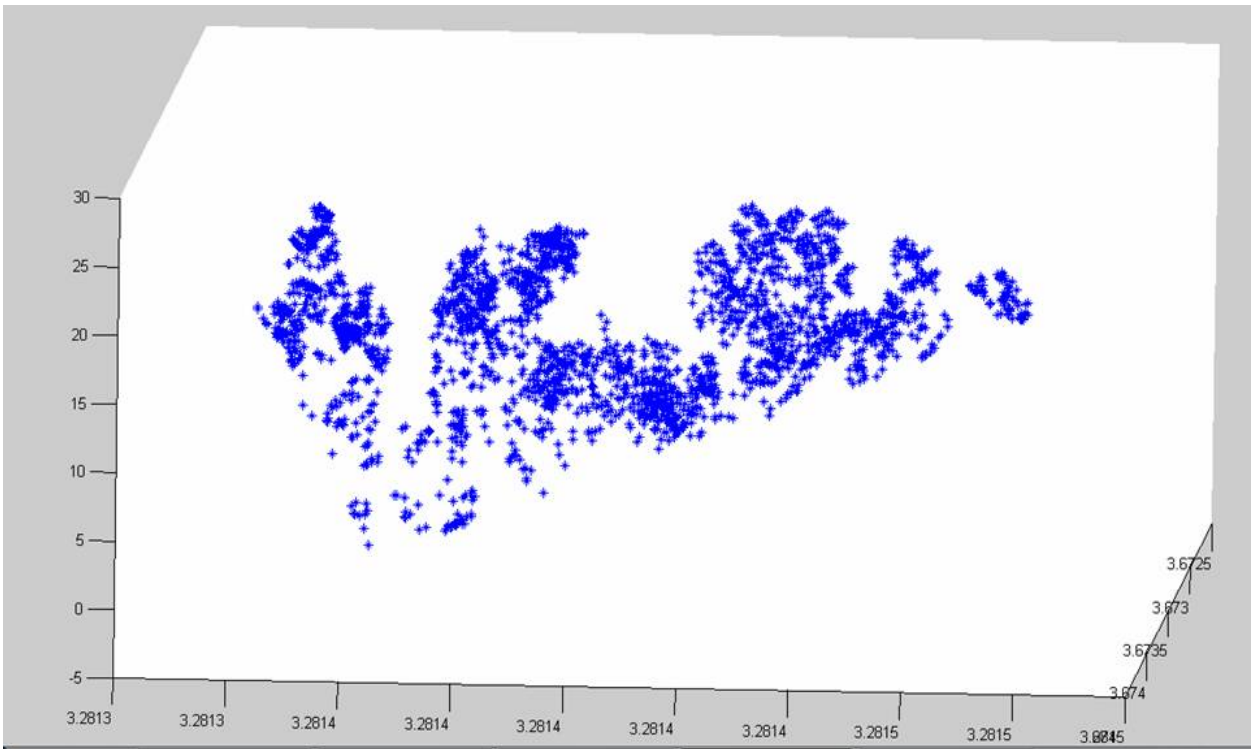

Figure 5-10. Multiple small cones plotted from a GPS station

We can assume that the higher the 3D point density in the cone the more signal blocked; however, to make the model more realistic a weighted function associated with the distance a point is from the antenna is considered. The points located farther from the antenna are assigned lower weight. The weighting formula is a second order polynomial and the weighted equation is $w = \frac{(d - d_{vanishing})^2}{d_{vanishing}^2}$. Where, d is the point distance far from antenna, and $d_{vanishing}$ is a distance threshold (Lee, 2007).

As shown in ESA, 1998 microwave signal attenuation in the forest is governed by the path length of the vegetation medium. An empirical signal lost model can be written as $L=\beta f^{\alpha} d$, where α and β are empirically determined values, f is the frequency of signal and d is the path length of vegetation medium. In this GPS experiment, the f parameter is fixed because the GPS receptions are L1 band. If we assume the vegetation parameter is the same in the forest, then the signal loss

is absolutely relative to transmitted path length. We can then compute what is viewed as the path length the signal is transmitted through the forest medium by measuring the distance between the farthest point and nearest point in our small cone.

CHAPTER 6
RESULTS AND DISCUSSION

6.1 Satellite Angles from Zenith

For the initial portion of the study it must first be verified that GPS signals, as measured using signal to noise ratios as reported using NMEA messages, can be measured and follow a logical pattern based upon the medium through which the signals are traveling. To do this each SV that was tracked during the April 2007 GPS data collection period is plotted using the signal to noise ratios; these signal to noise ratios were then grouped into three separate classes. First, the SV signal to noise levels from the SVs tracked by the base station are grouped together and plotted against the angle of the SV from zenith. Then, the same is done for the SVs as tracked under both IMPAC and Hogtown forest canopies using two different SNR readings. The SNR readings include SNR averages taking into account, or counting 0 readings (SNR (0)); as well as, SNR readings where zeros where not counted when the signal dropped completely (denoted as SNR on charts). This is because I expected to see a SNR drop simply due to the atmosphere as the angle from zenith increases, as well as, an increased drop as the angle increased under forested terrain. In addition, when the signal is completely blocked I expected to see an exponential drop in the SNR(0) levels. Figure 6-1 below is the result of this initial investigation.

The figure shows the SNR of the base station vs. angle from zenith of each SV; the SNR of each SV in each forest vs. the zenith angle; and the SNR (0) measurements for each SV. To add further information on signal loss, I plotted the SV SNR of each SV tracked in the forest against the base station SV across time. See figure 6-2 for the base station verses rover SNR plot. As you can see there is approximately a 10 percent loss in SNR for the SVs as tracked in the forest. At certain times the signal obtained inside the forest may come close to the same signal strength as obtained on the base station, but this is rare. You can also see certain periods of time where

no data is obtained by the receiver because the signal is completely blocked. Overall it seems evident that the signals from the base station have fewer variations than the forest environment.

These plots verify that the experimental set up is capable of measuring that both path length and forest foliage density through which the signal must travel effect signal degradation. While the plot for each variable follows a definite trend, there is a noticeable variance within the trend. This is expected because it is understood that the forest vegetation is not perfectly distributed and there is no measurement of the foliage around the receiver in this particular analysis.

The plot demonstrates multiple facets of the study. First, the plot shows that when we compare the SNR values in the forest to those of the base station, the measured SNR is clearly lower in the forest. This follows the expectation that as the signal propagates through forest canopy there is measurable signal degradation. Next we also see an exponential increase in the number of SNR(0) events recorded, which is expected when the SVs past behind tree trunks and heavy foliage, totaling blocking the signal. Finally, it is clear that in the SNR and SNR(0) as the SV gets closer to the horizon the signal degrades. This is important because it validates the concept of the Beers-Lambert Law as described earlier; as the SV gets closer to the horizon the amount of matter the signal must propagate through increases.

In figure 6-3 a plot shows the SNR readings of each SV and the overall PDOP during a particular GPS data collection period. As can be seen from the plot we can actually visually track the periods of time when SV signals completely drop out of our solution. It is important to note here that the method used in this particular receiver's NMEA message for reporting SNR is a method referred to as C-to-N-zero. This value is calculated in a 1Hz bandwidth and is determined from the Signal to Noise Count (SNC) from a 1 KHz bandwidth where SNC equals

the signal amplitude divided by the noise amplitude. This bandwidth is 1000 times smaller than more traditional measurements and results in a 30 dB change in the value. For example, if the C-to-N-zero value is 40 dB:1Hz the more traditional signal to noise reading would be 10 dB:1 kHz (Collins and Stewart, 1999). This helps to explain why in figure 6-3 the signal to noise values slowly decline to a point around the 30 dB:1Hz level and then drop completely out. The results of the SNR and SNR(0) vs. zenith angles confirm the expectation that the foliage will cause diffraction and signal attenuation as it moves through the medium. It is important to know for certain that the measured values in the forest compared to the base station values are both quantifiable and follows our expectations, and this analysis confirms that the setup is capable of achieving these results.

During the course of this portion of the study it seemed important to determine how often a tree trunk and/or significant foliage would obstruct the path of propagation. In the natural forest this is a difficult task; however, in the managed forest it is not nearly as challenging. In a thesis project by Fernandez (2007) a study was done and a detailed description of the spacing of trees inside the IMPAC plots was conducted. His findings show that there are 4 meters spacing between the rows of the trees and 2 meters between the trees planted in each row. Other parameters are given as well such a DBH (Diameter at Breast Height) and height of the trees at .2 meters and roughly 20 meters respectively. These parameters verify the data collected at the IMPAC site. Given this data, I plotted the spacing of the trees using ARCGIS in accordance with his findings. Then using simple math it was found that given the height of the trees at 20m, the distance in the horizontal direction will equal 20m divided by the tangent of the angle above the horizon. Given this data a map was generated showing the radius of interested trees inside the plot. See the map below in figure 6-4a. With this map we simply find the number of trees

inside each circle and then calculate the average number of trees that would be intersected at the designated angles from zenith. Since we know GPS SVs orbit the earth twice a day, we can assume that over the period of 20 minutes the SV travels 10 degrees in a two dimensional world. Given this information we can then take the 360 degree circle and take the average number of trees for a 10 degree portion of the circle. See the table below for findings.

Table 6-1. Tree obstruction prediction for the managed forest based on the angle from the horizon of the transmission source

Angle from the Horizon in Degrees	*# Trees Intersected*	*10 Degree Average*
75	10	.28
60	54	1.5
45	160	4.44
35	311	8.64
25	722	20.06
15	220	61.11

As you can see from the table, the closer to the horizon the SV is, the more likely the signal will be interrupted not only by foliage, but also from being completely blocked by tree trunks. This follows the logic found in Figure 6-1 demonstrating the SNR vs. Angle from Zenith comparisons for both the base station as well as under the forest.

Given this information, a comparison is needed between IMPAC and Hogtown forest. To do this I created a sketch centered on two collection points in Hogtown forest. Each sketch is a circle with a radius of 30 feet. Each tree with a DBH of 3" or more is marked on the sketch and plotted using a compass and measuring tape. Besides the erratic spacing of the trees in the natural forest, another significant contrast is the variety of species at the different points. While Hogtown #3 has a few pine trees, Hogtown #4 has none within a 30 foot radius. Given the information in the managed forest a 30 ft radius would be equivalent to approximately an angle from the horizon of 63 degrees. With this we can see from table 6-1 that roughly 50 trees with a DBH of .2 meters, or 7.2 inches, would be intersected inside a radius of 30 feet in the managed

forest. At Hogtown points #3 and #4 the number of trees with a DBH greater than 3" inside a 30 foot radius is 34 and 19 respectively. At first it may seem like this would suggest better signal reception inside Hogtown forest, however, this is not the case. One reason is that several of the trees inside Hogtown forest greatly exceeded the DBH of those in IMPAC. In addition to this, the tree species, namely deciduous in comparison to pine trees have significantly more foliage during the spring and summer months. Another factor is causing further signal degradation inside the natural forest is the undergrowth and layers of foliage that are not permitted to grow in the managed forest. See figure 6-4c for the Hogtown forest sketch. Figures 6-4b and 6-4d provide images of the two different forests. From these photos you can see how the managed forest is set up in rows of trees. undergrowth is not permitted to grow, and all the trees in a plot are of the same species. In contrast, you can see Hogtown forest has significant under growth, different diameters of trees, different tree species, and irregular spacing of trees.

6.2 Position Precision

One facet of this experiment I wanted to take a deeper look into was the position precision at each GPS location. To do this I used the standard deviation for the distance from the average position at each data point determined by taking the average of all position fixes at each point over the 20 minute data logging period. This was done for all 12 points collected in April of 2007. In addition to this, I also determined the maximum deviation from the average of each position. The results are shown in figures 6-5 and 6-6 with the addition of a sliding window standard deviation taken in increments of 1,2,5, and 10 minutes.

The results of these graphs may not seem important at this time, however this analysis is important in comparing the position precision to different factors such as the average signal to noise levels of all SVs tracked as well as the average PDOP and the effects of this information on

position precision as will be discussed in 6.3 and 6.4 of this chapter. However, there is some interesting information on the position precision analysis on its own.

The first item of interest is how much better the position precision from the base station is compared to the other GPS data stations. This is significant because besides the environmental conditions (tree foliage) the set up at each GPS point was the same at all 12 points. So, it

Table 6-2. Rollup of signal to noise variables and position STD

GPS Point	*Postion STD (m)*	*Ave. SNR*	*Average SNR (0)*	*SNR AVE of all Trackable SVs*	*Signal Loss*	*Signal Loss (0)*
Hogtown 1	5.65	45.69	28.50	23.32	6.8%	44.4%
Hogtown 2	2.08	45.92	37.97	20.71	9.8%	26.9%
Hogtown 3	2.41	45.47	33.73	18.40	11.6%	35.9%
Hogtown 4	4.58	44.95	36.88	20.12	11.6%	28.2%
Hogtown 5	1.46	45.40	35.61	24.92	9.0%	30.6%
Managed 1	4.67	43.43	24.25	22.23	9.5%	51.1%
Managed 2	7.77	43.91	28.50	26.13	9.5%	43.0%
Managed 3	1.39	45.44	30.27	22.70	6.4%	41.2%
Managed 4	1.22	45.88	31.05	23.29	6.7%	35.2%
Managed 5	1.69	45.70	34.36	28.11	7.2%	33.8%
Managed 6	0.97	46.82	37.28	30.50	7.0%	28.0%
Base Station	0.27	45.86	45.86	45.86		

appears clear that the addition of tree foliage impacts the level of GPS position precision. Next if you compare IMPAC point #2 to Hogtown point #1 you will see that the STD of position is better at Hogtown #1 for STD of 1 second and 1 minute, but after that, the IMPAC position gets better results. When you compare the max deviations of Hogtown #1, IMPAC #2 and Hogtown #4 we can start to make sense of these differences as attributed to outliers from the average position. With this in mind the question seems obvious: what is the cause of these outliers? Given the information in Chapter 2 dealing with GPS it seems obvious that the most likely cause of this is multi-path error. To see if this could be verified I collected a second set of data in October of 2007 where I set up a tripod and used two different antennas for the data collection at 4 different points. The first antenna is the same one I used for the data collection in April 2007 and the second antenna was a specially developed choke ring antenna designed to help eliminate multi-path errors. The result of this analysis is shown in table 6-3.

Table 6-3. Choke ring antenna verses non-choke ring antenna precision rollup.

	Easting	*Northing*	*Alt (m)*	*3d STD Position*	*2d STD Position*
Hog-Stake3	367299.82	3281348.16	33.92	1.60	0.79
Choke Ring	367299.75	3281348.42	34.23	1.46	1.25
HogDrive	367218.99	3281367.24	32.57	1.29	1.05
Choke Ring	367219.01	3281367.72	33.17	1.14	1.03
Hog2NS	367342.60	3281414.25	33.43	2.31	1.42
Choke Ring	367345.30	3281413.82	29.27	3.56	1.33
Hog2.2	367344.12	3281569.49	39.40	5.14	2.60
Choke Ring	367342.37	3281570.50	37.52	6.27	3.74

The results from this antenna analysis show that in 3 of the 4 cases the position precision is better with the choke ring antenna. However, in the one case where the position precision is worse the cause is a result of tracking fewer SVs during the logging period with the choke ring antenna. In fact in each case the choke ring antenna had a more difficult time obtaining and maintaining a lock on the SVs. This makes sense and is by design. The standard antenna is actually able to obtain a signal sometimes by detecting refracted signals and while it may cause a greater error in the precision of measurements, in certain cases it may be more beneficial to actually track a SV as opposed to losing the signal all together.

6.3 Dilution of Precision and Position Accuracy

As mentioned in the literary review, previous research has shown that PDOP may not be a good indicator of position accuracy. While many software programs will provide the user of GPS the ideal time to collected GPS data to ensure the best possible geometry, under forest canopy this may not be as important as one might expect. This makes sense based on what we already know; that signals closer to the horizon will be obstructed and limits the predicted geometry based on and unobstructed view of the GPS constellation.

With this in mind I wanted to attempt to reproduce the results that show that PDOP is not a good indicator of position precision. To do this, I used the precision values of the 11 forest GPS data points as discussed in 6.2 of this chapter and plotted this information against the average PDOP taken at each point. The resulting plot is shown in figure 6-7. As shown in figure 6-7

there does not appear to be any significant trend or correlation between PDOP and position precision. This follows previous research and can most likely be attributed to the effects of multi-path errors and the complexity of GPS measurements given the 20 minute logging interval.

6.4 Position Precision and Signal to Noise

In the same fashion as in 6.3 the relationship between position precision and signal to noise ratios are evaluated here. In contract to the PDOP results, in this analysis there is a relationship that does appear to follow a trend. In figures 6-8 and 6-9 position STD is plotted against SNR and SNR(0) respectfully. The results of these two plots are somewhat surprising. I did not expect to get a strong relationship between signal to noise and position precision for the same reasons as discussed earlier, namely multi-path error and the complex nature of the GPS solution. However, figures 6-8 and 6-9 do show an exponential correlation between the two. While the resulting R squared values are between .4 and .55 there is still a definite relationship.

6.5 Large Cone Results

An underlying question in this study is how well we can model signal attenuation simply by using the angle of the transmission source to the horizon. This leads to the follow on question of why, or when ALSM information is needed to model the three dimensional nature of forests for modeling signal attenuation. To look at this question we plotted the signal loss between the base station and the rover data against the zenith angle of each SV and calculated the residuals associated with them.

As discussed at the end of Chapter 5, simple experimental modeling of propagation attenuation has taken the form of $L=\beta f^{\alpha} d$ where L is attenuation in dB, β and α are empirically determined constants, f is frequency, and d is the path length through the medium (ESA, 1998). In our experiment this equation can be reduced further as we maintain the same frequency (L1) throughout the study. With this we find that the Beer's law model suggests the only factor that

effects signal attenuation is the path length. Assuming the forest canopy is evenly distributed and can be envisioned as a blanked over the receiver the factor that impacts path length is the angle of the SV from zenith.

The results indicate a significant variance between signal loss and zenith angle and while it does follow a definite trend we cannot simply model the forest canopy as a simple layer of equal vegetation density. This suggests the need for a model to represent the amount of vegetation in the particular path of propagation between the receiver and the EM transmission source.

Intuitively, the next step in this research was to utilize a technique of measuring the forest canopy density with the use of ALSM point returns. The first technique is the use of a large cone representing the entire hemisphere in which GPS signals could be obtained. In this case we set an elevation mask of 15 degrees as discussed earlier and took the average SNR (0) value for all SVs tracked during the 20 minute collection period. I then plotted the individual results for both the managed forest and Hogtown forest from the April 2007 collection and found that both follow an exponential fit (see figures 6-10 and 6-11). The results of this analysis show R squared values of .6 to .88 (when removing the one outlier). This level of correlation does show that a fairly good depiction of SNR(0) based upon ALSM data can be achieved. However, the results indicate that as the point density increases the SNR increases too. This is contrary to the expectations of this analysis; upon further thought it seems logical to take into account the SVs that were not obtained by the receiver in the forest but were obtained at the base station. This should account for areas in the forest with dense enough foliage to completely block SV signals for twenty minute duration figures 6-12 through 6-14 show these results.

While figure 6-12 shows one outlier, I removed this particular data point and re-plotted the data in figure 6-13 which then creates a very strong exponential correlation between the number

of normalized points and SNR(0) of all trackable SVs. Figure 6-13 shows the same strong correlation in Hogtown forest

Note that IMPAC forest and natural forest cannot be plotted in the same graph as a result of the significant difference between the total number of ALSM point returns in each area. This is primarily the result of the number of flights flown over each target area; the IMPAC site had many more flights than Hogtown forest. In order to unify these two datasets for this analysis we can find the number of laser pulses per square kilometers for each data set. Taking this information we can adjust the Hogtown point returns by multiplying it by the ratio of IMPAC pulses per kilometer to Hogtown pulses per kilometer where in this case we multiply the Hogtown forest points by a factor of 5.388. The result of this is shown in figure 6-15. As you can see this technique does appears to demonstrate that this scaling somewhat successfully unifies two different forest types.

The relevance of refining the technique of using a large cone is that it incorporates the density of foliage from all surrounding areas about which a signal could come. This in turn would allow us to generate a map depicting where to place or where not to place GPS receivers based upon our weighted density values in order to obtain quality signals. One benefit of a successful model using the large cone technique would be that we would not need to know the exact location or even the projected location of the SVs at a given time. In addition, the generation of a prediction map would be useful in the determination of locations where different forms of wireless communication could be set up to optimize signal reception and transmission.

6.6 Small Cone Results

While the large cone technique has its benefits, the establishment of small cones directed towards each individual SV should provide a more detailed understanding of how exactly the number of ALSM point returns inside the small cone effects the signal attenuation of each

individual SV transmission. This approach was used in comparing the data of the two different sets from the April 2007 collection; the first set being the six data points in the managed forest and the second set from the Hogtown natural forest. In this particular portion of the analysis SVs that fell below the 15 degree mask were removed from the data set as these points create a disparity in the data set that can be attributed to the fact that the 15 degree mask would cause the receiver to stop tracking the SV. The results from the managed forest are plotted in the figures 6-16 and 6-17.

We expect an exponential distribution when plotting the SNR against weighted cones; however, as you can see in the graphs a linear fit would work fairly well in this case as well. While an exponential trend line works best, a linear fit could work and may be attributed to the fact that in the managed forest the spacing of the trees are far enough apart to provide a single layer of foliage that is about the same density throughout. Upon looking at the zenith directed photos you can see this is the case, at least much more so than compared to the natural forest. In the managed forest the trees seem to only have branches at the top of the trees and there is almost no under growth. Figure 6-18 shows the relationship between the distance between the first and last points inside each cone for each of the SVs and the total number of normalized points inside each of the cones.

In figure 6-18 a clear exponential relationship is visible between the normalized number of points verses the distance of propagation through medium. The cause of this exponential curve can partly be attributed to the use of a cone for our scope function. The shape of a cone causes the area inside the cone to grow in such a way that the total area grows exponentially as we increase the length of the cone with all other parameters remaining the same. With an evenly distributed density of the forest canopy it is then logical for figure 6.18 to have the exponential

curve. If we assume the density of the foliage is relatively evenly distributed, then is stands to reason that the length through the medium is strongly influenced by the angle to the SV.

Our initial analysis shows that plotting the weighted point returns VS SNR(0) renders an good exponential fit following our expectations from having an exponential drop in SNR(0) based on angle from zenith or the distance the signal must propagate through the medium. One idea that can be taken away from these findings is that the creation of a moving cylinder or cone with a narrow scope that follows the path of the SV should provide an even more accurate technique of detecting signal behavior.

Next, the same small cone technique was used as described above accept the data collected inside the natural forest was used as shown in figures 6-19, 6-20, and 6-21. In the case of the natural forest the expected results are achieved. In this case you can now see a forest structure that has multiple layers of canopy. The result is that the scope functions more effectively model the environment. The distance between the first and last points inside the cone not only represents the distance of propagation, but also provides a better estimation of the density of foliage through the path of propagation. As seen in the figures of SNR loss and SNR(0) we do see the exponential loss of signal strength as the weighted point levels increase. Part of this can be explained when the distance vs. normalized number of points are compared (figures 6-18 and 6-21) from both the managed and natural forests. Here we see a higher exponential curve in the natural forest than that in the managed forest.

6.7 Prediction Map

Similar to the map described during the large cone discussion, we can do something very similar using the data given by the small cone weighted point densities. Given a transmission source of known location (azimuth, zenith, and distance) we can develop our prediction map. Given this information we can generate pixel values based upon a cone developed using the

azimuth and angle to the transmission source and converting the weighted point densities to SNR(0) expected values. This would allow for the generation of a map providing information on where you could obtain quality signals. A similar concept could be used in the development of an optimization analysis of site suitability for emplacing signal towers for a target area.

We took this approach and created maps that show the different parameters that we can generate using the small scope functions that can be obtained given the ALSM data in Hogtown forest. For figure 6-22 we assumed that we had a stationary broadcasting tower located due south of the center pixel of our map. We also set the source a distance of 500 meters south, and 350 meters high. Figure 6-22 is the resulting map with the dimensions of 100 meters by 100 meters where each 1x1 meter pixel is given a value based upon the scope of the small cone function aimed in the direction of the and the ALSM point returns for each X,Y location in the map.

The same process could be done assuming a geostationary satellite. In a case such as this we could assume a planar wave front, a stationary transmission source, and that the source distance is far enough away that the azimuth and angle to the satellite with respect to our small mapped area is negligible. We therefore could set the angle to the transmission source to the same angle and the azimuth to 180 degrees. Assumptions such as these could hold true for a geostationary SV but cannot be used for the example map where the direction and angle changes significantly from pixel to pixel or when mapping a very large area.

While figure 6-22 is a relatively small sized example, larger area maps can easily be made and have clear implications of usefulness. One example of the usefulness of a map such as these, while a larger area would be needed, is in many military situations Soldiers are outside the range of FM radio communications, and in these circumstances they may find themselves limited to

communication with satellite radio systems. If these Soldiers know they are going to operate in these conditions they could request a map such as the ones above with the input parameters of the satellite position for their area of operation. They could then use this map during the planning phase of the operation as well as during the actual execution of their operation to ensure communications are maintained. Another possible use for maps such as this is for the optimization of emplacing radio or cell phone towers. If you have a particular area where service needs improvement or if a company can purchase one site out of a few possible different locations, maps such as these could show the effectiveness of each site for particular areas.

There is a method to generate a GPS precision prediction map. To do this we are required to establish a certain time in which we are interested in GPS performance because we must know what the GPS constellation looks like so we can determine where each SV is located with respect to each point on the ground. Given this information we first determine the average predicted SNR for each SV using our small cone scope (similar to how we developed figure 6-22) and take the average of these values. The second step is to generate the GPS performance prediction map by using the equations derived in section 6.4. Figure 6-23 is an example of this two step process for generating a 50x50 meter GPS prediction map. In this particular case we assumed we were tracking 6 SVs positioned as shown in table 6-4. This information is taken directly from the SV positions during the Hogtown 2 data collection.

Table 6-4. Satillite positions for Figure 6-23.

Zenith (degrees)	Azimuth (degrees)
71	36
39	106
43	143
5	240
39	332
61	305

6.8 Point Return Analysis

ALSM is capable of providing three dimensional information of a target area. Each laser point return registered by the system provides an X, Y, and Z value. However, with each pulse we only get a limited number of returns depending on the system. In the case of the system used for this study, the system has a first and last return, or two stops. The University of Florida's new Gemini system has four stops. If the two stop system has a first and last return then it stands to reason that certain point returns inside the forest may not get registered. Consider a pulse where a portion of the pulse hits a leaf near the top of the canopy. In this case we will get a first return towards the top of the canopy. Now, if this pulse is capable of penetrating further down and hits several sections of the lower canopy, only the last return will be registered. In some cases this last return will be the ground, and in some others the last return may not reach all the way to the ground. A four stop system should help provide better information inside the canopy as a result of providing more depth with the middle two returns.

The data we used over both Hogtown and the IMPAC area taken in February 2006 by the two stop system is analyzed below. In this analysis each data collection point inside both forests are plotted in a 20x20m cube around the GPS point. The plot is setup to clearly show the height of the point returns through the canopy.

As can clearly be seen, in the managed forest there are clearly a disproportionate number of returns from the canopy top and from what we would most likely classify as ground points. From the ALSM figures there also appears to be vertical structuring of the mid-level points that suggest many of those points represent trees trunks which would degrade signal much more than "leaf" points. This makes sense for a number of reasons. First, the trees in the managed forest are coniferous and as such have needle like leaves. With these types of leaves the possibility that the pulse will be able to penetrate through the first layer of canopy is greatly increased. Another

reason for a heavy distribution of points along the top of the canopy and the ground is that there is no second layer of undergrowth permitted to grow. This would mean that the point returns between canopy height and the ground would be tree trucks, and from the images this makes visual sense. We know from 6.2 of this chapter that the trees are spaced 2 meters by 4 meters apart and in the diagrams above, the possible trees are spaced in accordance with these attributes.

In the figures plotting Hogtown forest we get a very different depiction of the forest structure. Here we have a more difficult time delineating what a tree trunk is and we have many more points located between the ground and the top of the tree canopy. The ALSM point return plots seem to show much more horizontal structure in the mid levels, which are likely to be "leaf" or "branch" hits. When we consider the structure of the natural forest, the reason for the distribution of point returns makes logical sense. Here we do not have evenly spaced trees, nor is there only one layer of canopy. So in the case of a natural forest, the likelihood of having a last return hit a second or third layer of tree canopy, or even just some undergrowth on the forest floor is much more likely.

In the case of the managed forest we see a fairly good ability of visually detecting tree crowns and tree trunks based on the height of the returns and the patterns. However, in the natural forest the structure is too complex to visually detect what point returns are tree trunks. As will be suggested in the conclusions section of this thesis, that future work on classifying each point return would allow for better weighting in the SNR prediction equations, and therefore, an increased ability to forecast signal strength given ALSM data.

Table 6-5. Laser point return distribution

	Hogtown Forest	Managed Forest
Top 6 Meters	14%	24%
Middle Returns	51%	18%
Bottom 4 Meters	35%	58%

6.9 Skyward Photography Analysis

Previous works have attempted to use skyward oriented photos of tree canopy in order to attempt to find a correlation between canopy closure and GPS precision accuracy. Below is an attempt to reproduce similar results and to compare these results to ALSM results. One of the first step in this process is converting the photos into black and white images and counting the number or percentage of the pixels that were black against the number of pixels that were white. Figure 6-27 are example images of the skyward photography that were converted to black and white using a threshold of 128. This threshold was set to ensure the black portion of the photo represents tree canopy while white is open sky. I used a Nikon D80 digital camera with a 10.5mm fisheye lens. For this analysis the camera and lens provides a field of view of approximately of 140 degrees left to right and 100 degrees from top to bottom. Once each of the zenith directed photos were converted to black and white, I used MATLAB to count the pixels representing both black and white and obtained the percent of the photo that was classified as tree canopy. When this was completed I then used this information against the SNR levels of each GPS point in each forest type as well as in combination. The results are plotted in figures 6-28 through 6-30. The overall results show that there is a very small correlation between canopy closure and SNR, and not much of any relationship between canopy closure and position precision, especially when used in combination with both forest environments.

In figure 6-28 the slope of the trend line is opposite of what we would expect. We expect that as there is more canopy closure that SNR(0) will decrease, however the tread line in this case does not follow this pattern. If we removed the point located at (70%, 28) the tread line would exhibit a very different pattern.

In figure 6-29 the trend line starts to follow our expectation. In the case of the trend line we do have the slope indicating that as canopy closure increases, SNR(0) decreases. One of the

most significant problems with both figure 6-28 and 6-29 is that there are only 5 or 6 points plotted and any outlier provides significant errors in the depiction of what is trying to be represented. In order to attempt to rectify this I plotted the data from both the managed forest and the natural forest in figure 6-30.

In figure 6-30 while the trend line R squared values indicates a small correlation, it is counter to our expectation. This is not too surprising as the photo analysis has no way of determining the extent of density of the forest foliage. Black in this case gets the same weight whether it is a tree trunk or a pine needle. In the case of EM (Electromagnetic) radiation the amount and density of matter in the path of the transmission source will make a significant difference in SNR levels obtained by the receiver.

Figure 6-31 is a plot of the relationship of position precision of the GPS measurements against the black and white photo analysis. The result of this plot shows there is little to no correlation between these two factors that is measurable using this type of analysis. There are many reasons that this result is not too surprising. The first factor is the simple technique used for the position determination using GPS. As discussed in the GPS chapter, GPS uses pseudo-ranging the determine position. These ranges are measured from SVs located in what can be perceived as point sources when viewed from the ground under the canopy. So taking the total canopy closure of the sky is not a true indicator of the foliage the signal must propagate through. More importantly, GPS has significant errors caused by different factors. In this particular case the most significant source of error is multi-path error and a simple error such as this can result in one position rather than another in forested environments in an almost random manor.

The results for the black and white analysis do not make much sense. It is expected to have signal attenuation caused by the forest, but not simply by if there is forest present, rather by

how much forest density is in the path of propagation. In the black and white analysis above, this seems to be a clear problem with this sort of analysis. One possible issue with the above analysis is that if the canopy density is significant enough to block the SV transmission entirely, then it should be taken into consideration. Therefore, I took the average SNR (0) values for each point, multiplied it by the total number of SVs tracked by the rover SV and then divided it by the number of SVs tracked by the base station. This in essence gives an average SNR(0) value considering all available SVs that should be detectable by the rover receiver. When these SNR(0) averages are plotted against canopy closure in both forests, a correlation that makes sense comes into fruition.

With this more successful approach and an increased need to gain a measure of not just canopy but how much canopy is in an area, I took the photo analysis a step further. I extracted the blue channel of the original zenith oriented photos; and given these converted images, the pixel values were set in such a way that the range was from 0-255. 255 being the highest blue pixel value and pixel values of 0 indicate no blue in the pixel. I then took the sum of all the pixel values inside the image resulting in a single value representing the amount of clear sky in the image. In addition to this the middle ranged values provide an indicator of the density of the tree foliage in these areas. Figures 6-33 and 6-34 are examples of the blue channel extracted photos with a color bar representing the level of blue in the pixels.

In the same fashion as the black and white analysis above, I plotted the pixel values against both the position standard deviation and the SNR (0) of all SVs in view. The results of these two plots are in figures 6-35 and 6-36.

Again in the case of using blue channel skyward photography, we do not get a good correlation between the position of the GPS measurements nor does the pattern make any sense when comparing the pixel values to the SNR(0).

Table 6-6. This table shows the rollup of the photo variables for each GPS data point

GPS Point	Black Pixels	White Pixels	Total # Pixels	% Canopy Closure	Blue Channel Pixel Sum	Postion STD (m)	SNR for all Trackable SVs
Hogtown 1	498511	202929	701440	0.71	55353425	5.65	23.32
Hogtown 2	616788	84652	701440	0.89	28495354	2.08	20.71
Hogtown 3	636067	65373	701440	0.91	25512227	2.41	18.40
Hogtown 4	640195	61245	701440	0.91	23265686	4.58	20.12
Hogtown 5	630282	71158	701440	0.90	26430616	1.46	24.92
Managed 1	438582	262858	701440	0.63	76738874	4.67	22.23
Managed 2	496044	205396	701440	0.71	63686664	7.77	26.13
Managed 3	522965	178475	701440	0.75	60871430	1.39	22.70
Managed 4	449426	252014	701440	0.64	76689223	1.22	23.29
Managed 5	424957	276483	701440	0.61	79877583	1.69	28.12
Managed 6	438733	262707	701440	0.63	74526797	0.97	30.50

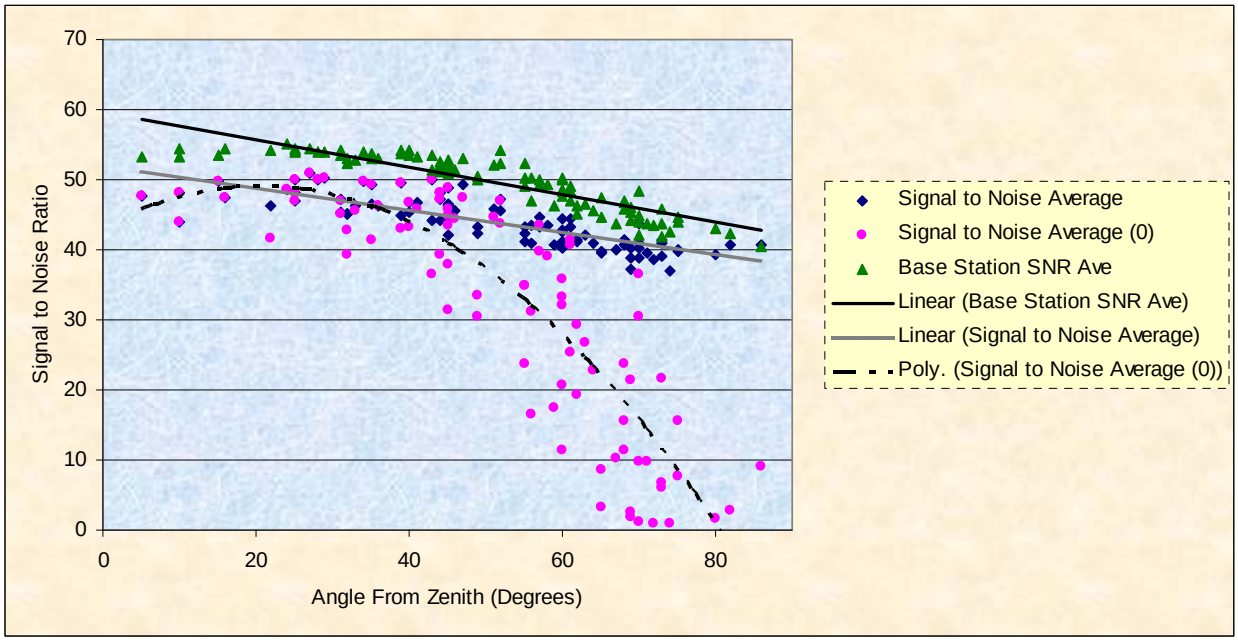

Figure 6-1. Signal to noise ratio VS angle from zenith plot

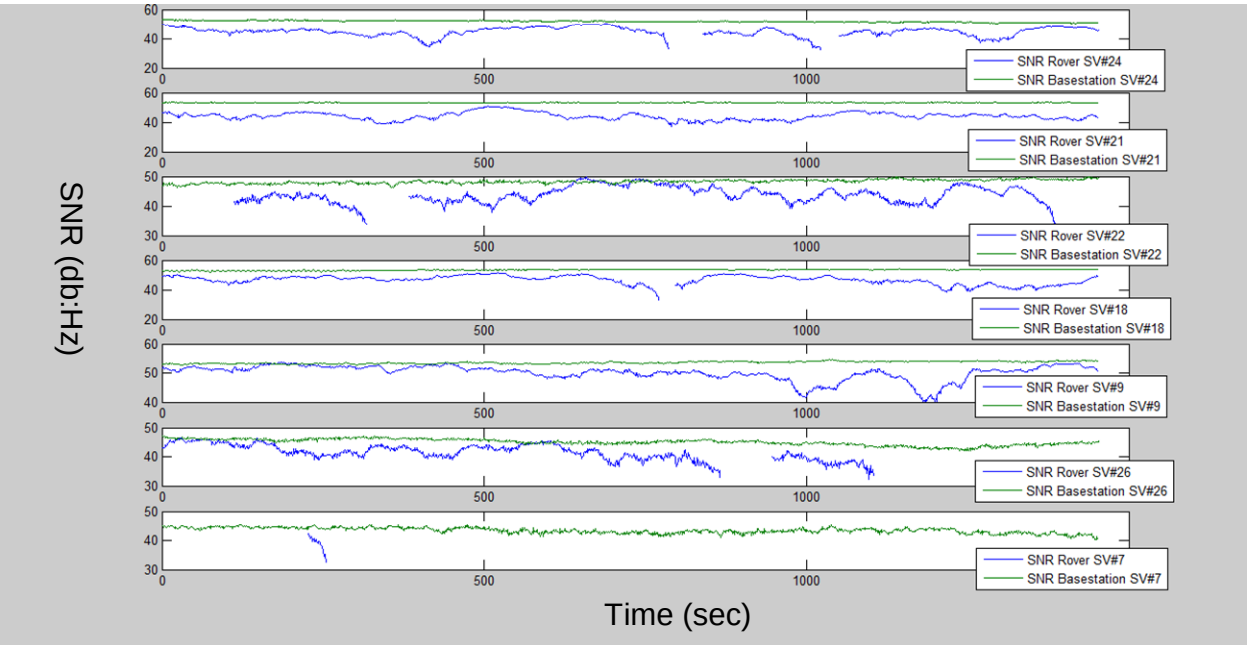

Figure 6-2. Base station VS rover SV SNR comparison

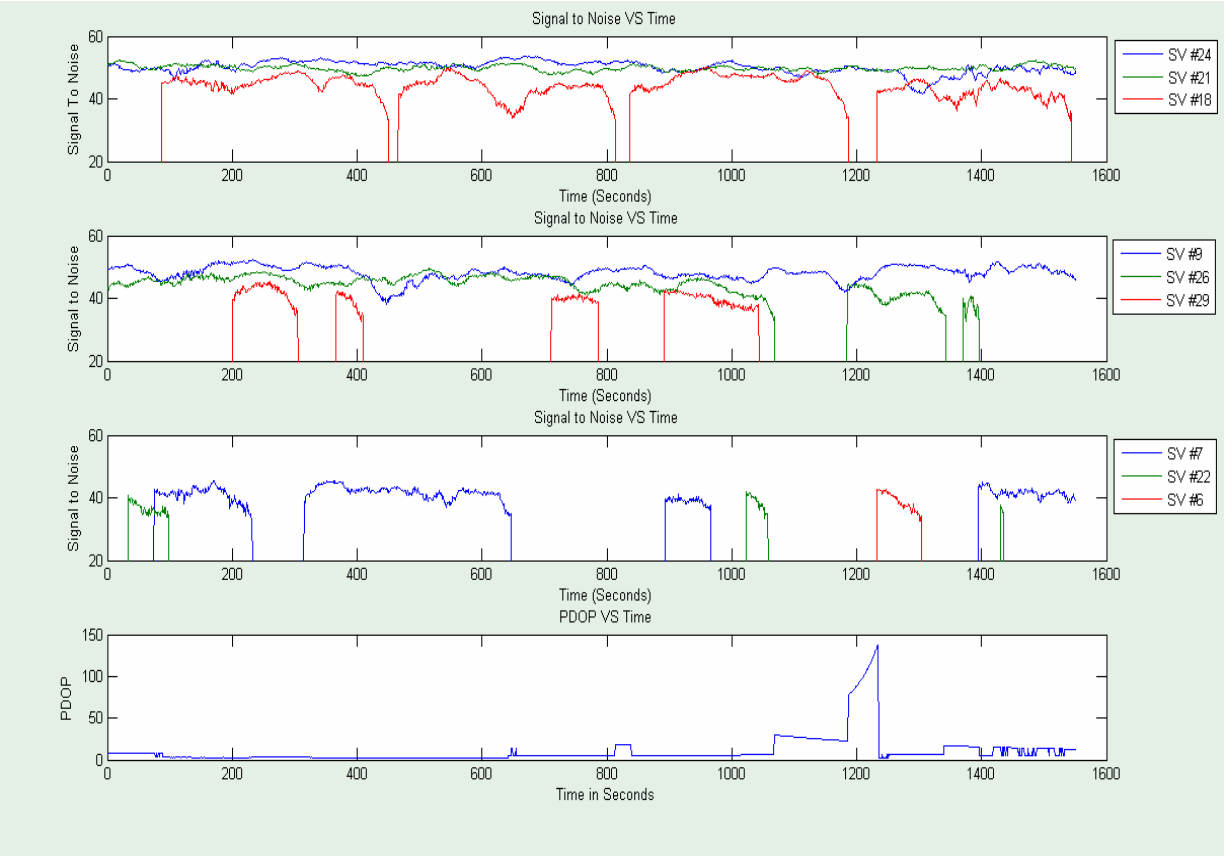

Figure 6-3. Signal readings of individual SVs tracked during data collection at Hogtown pt #1

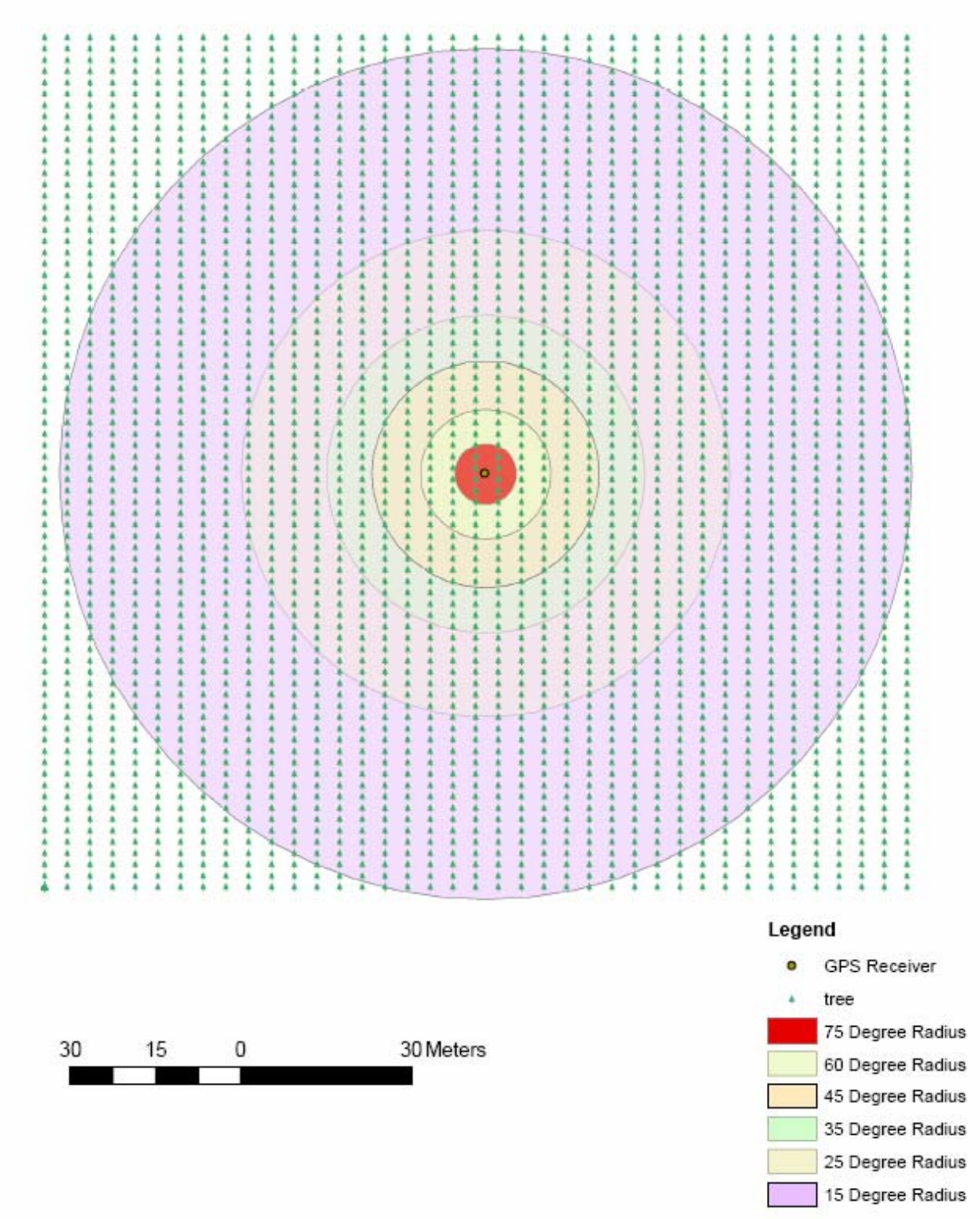

Figure 6-4a. Managed forest tree intersection diagram for different angles to SV from the horizon

Figure 6-4b. This photo is taken down a row of trees in IMPAC managed forest.

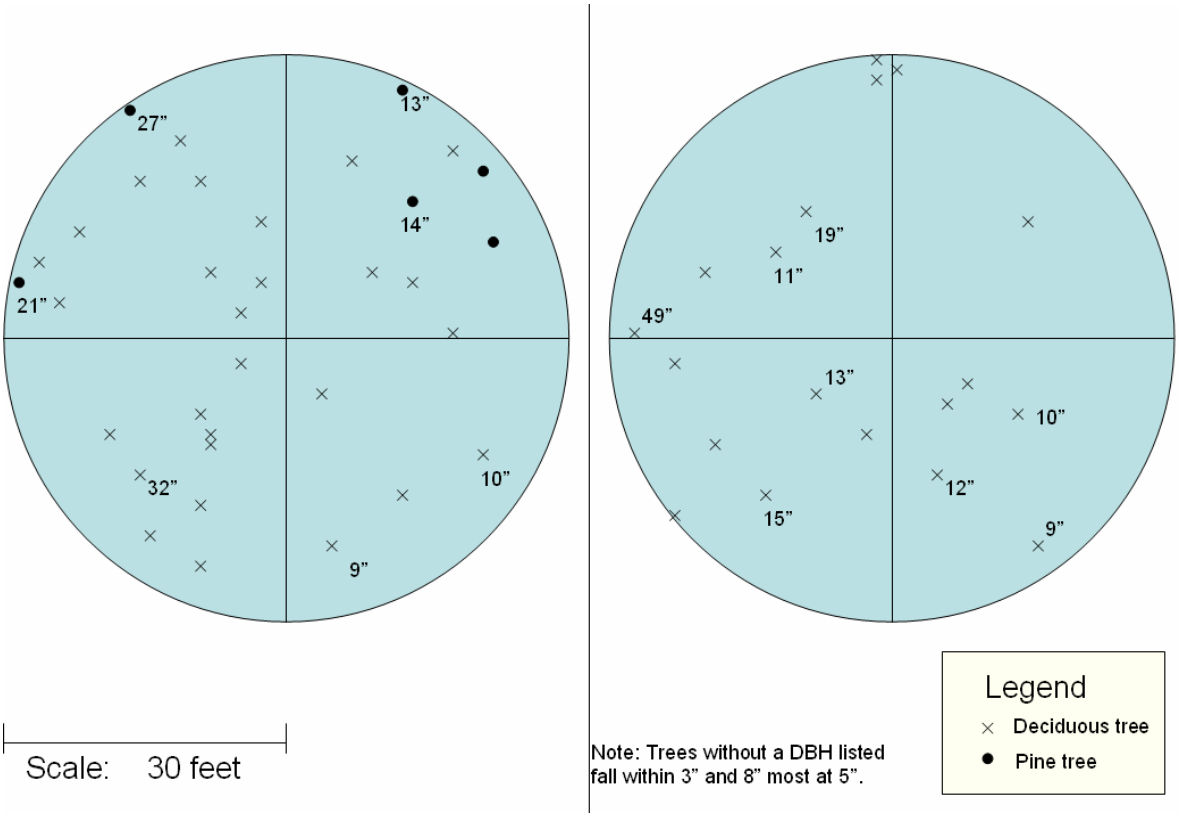

Figure 6-4c. Hogtown forest sketch of trees inside a 30 foot radius at Hogtown points #3 & #4. The left figure is Hogtown point 3 and the right figure is Hogtown point 4. Top is north.

Figure 6-4d. Photo taken during the set up of Hogtown forest #5.

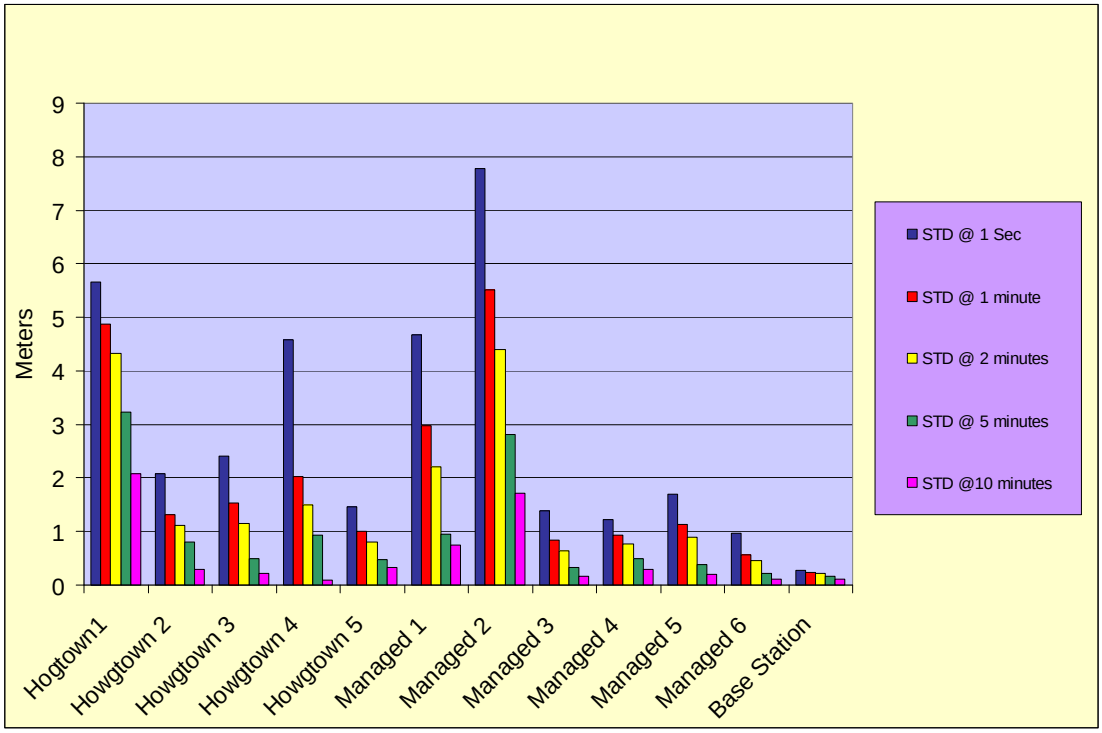

Figure 6-5. Position standard deviation

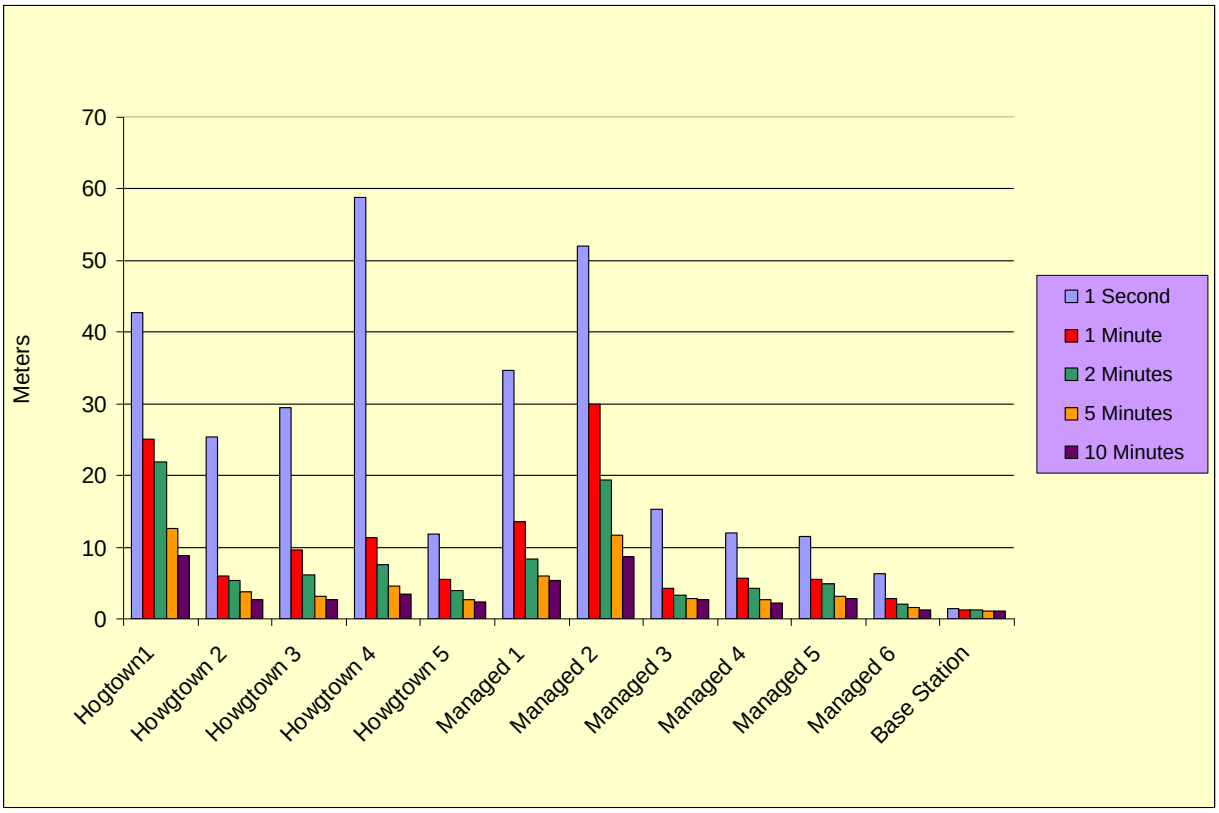

Figure 6-6. Maximum GPS position standard deviation

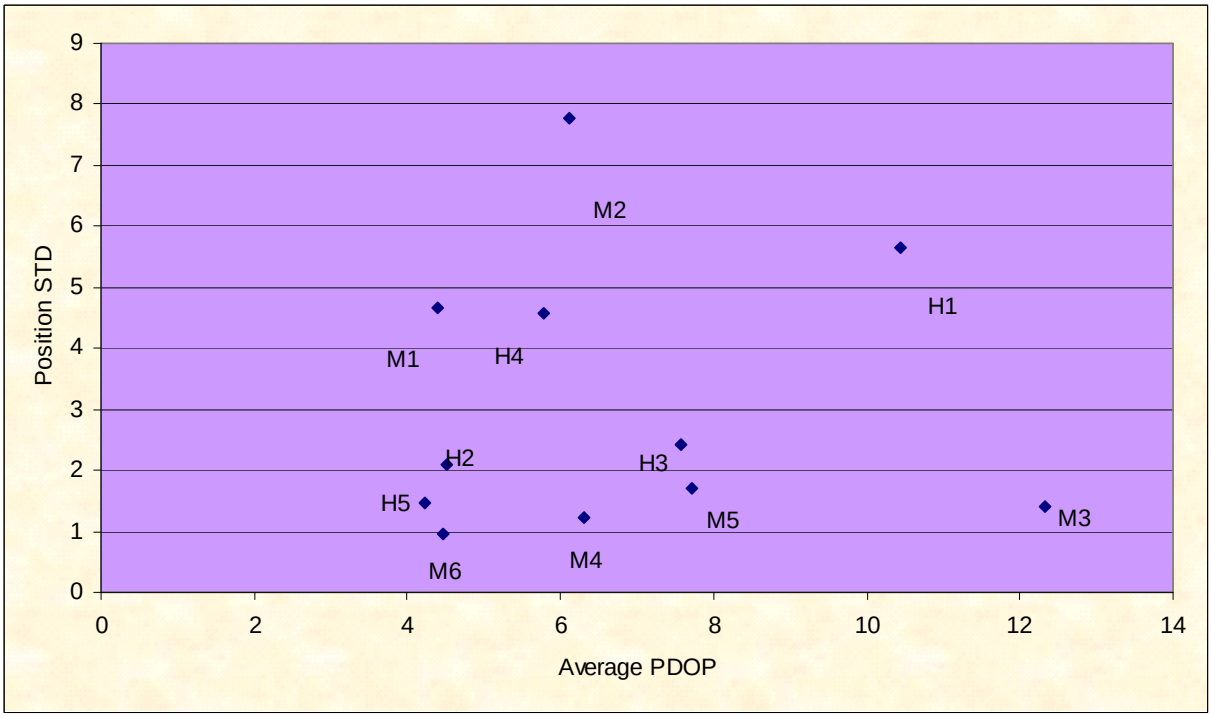

Figure 6-7. Dilution of precision VS position STD

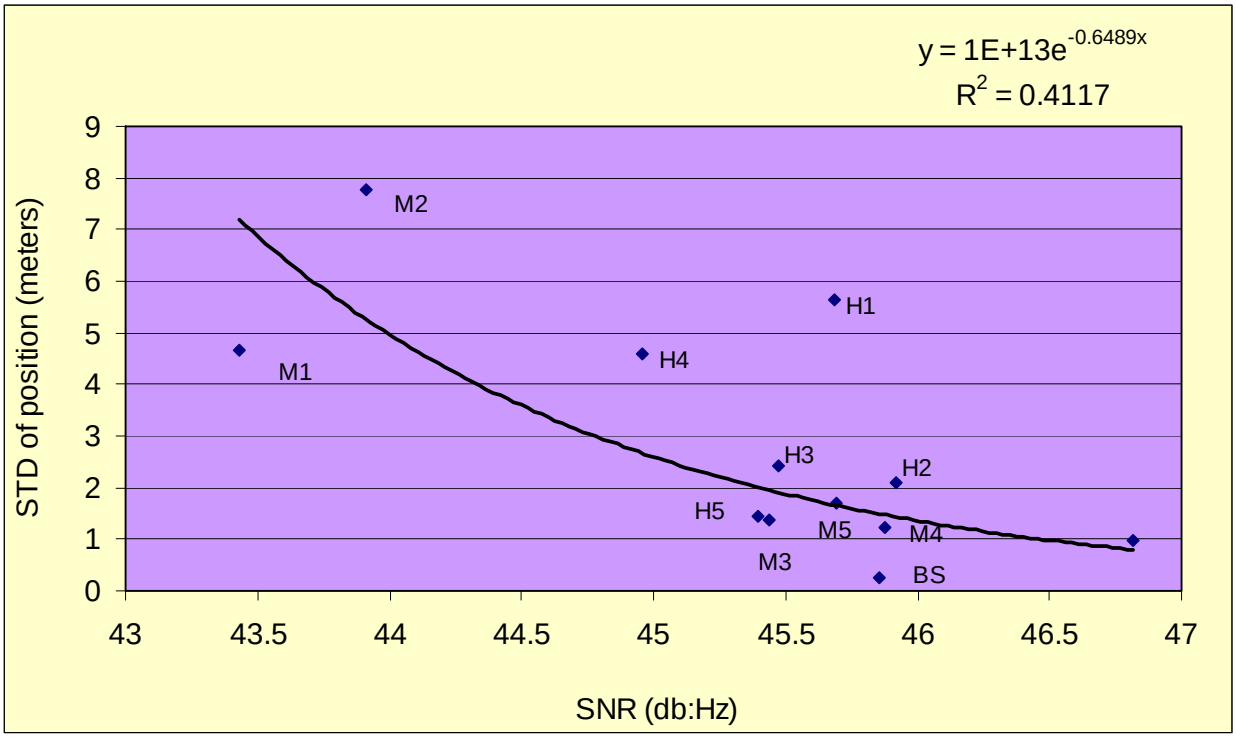

Figure 6-8. Position STD VS SNR

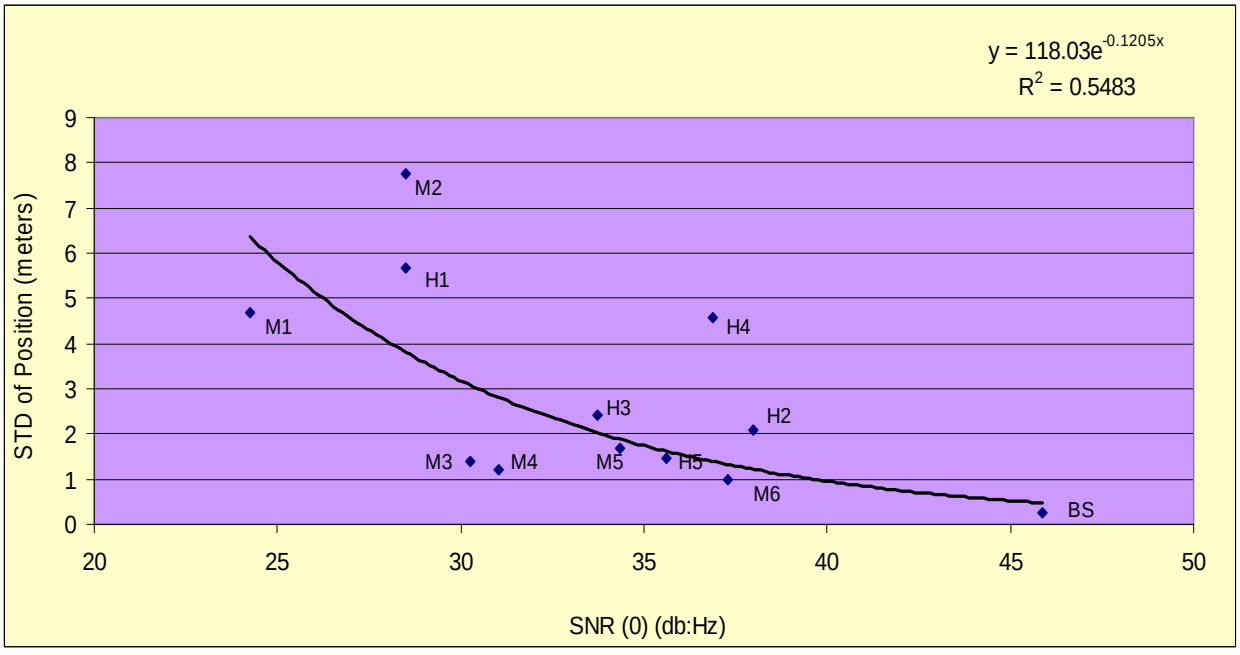

Figure 6-9. Position STD VS SNR(0)

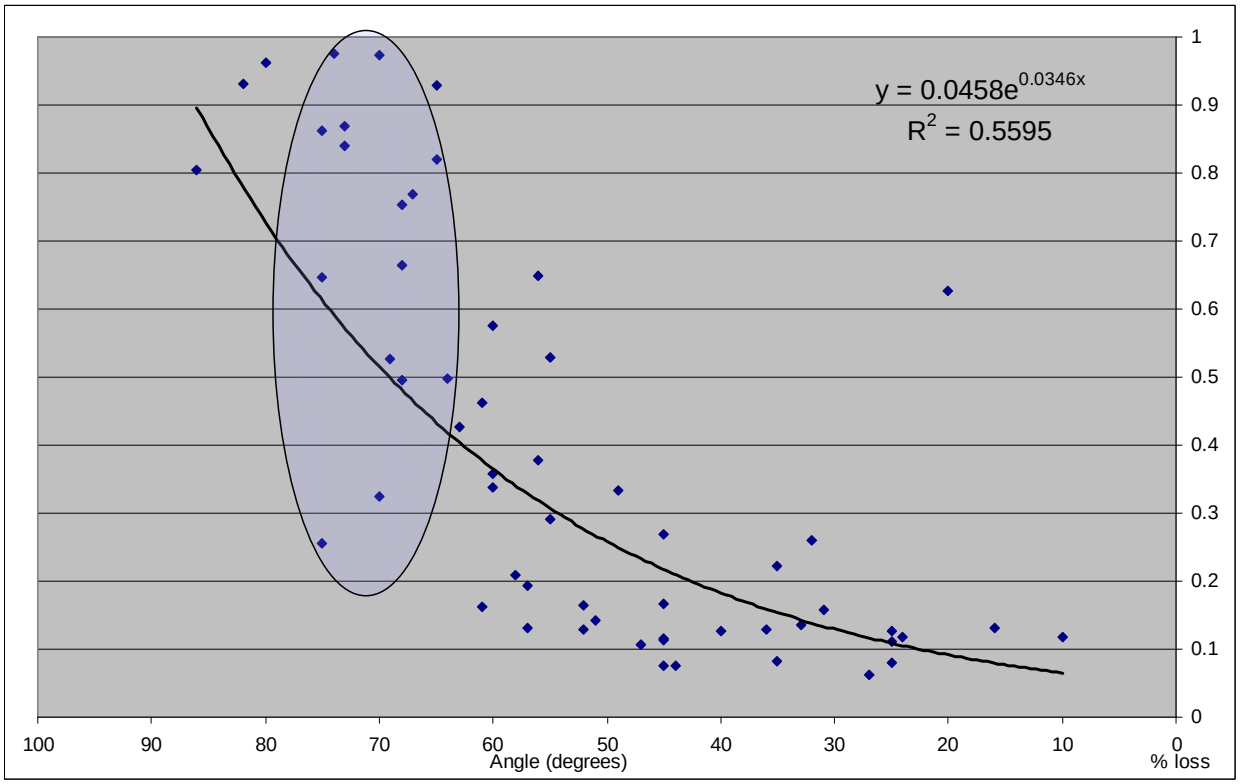

Figure 6-10. Signal attenuation plot for IMPAC forest.

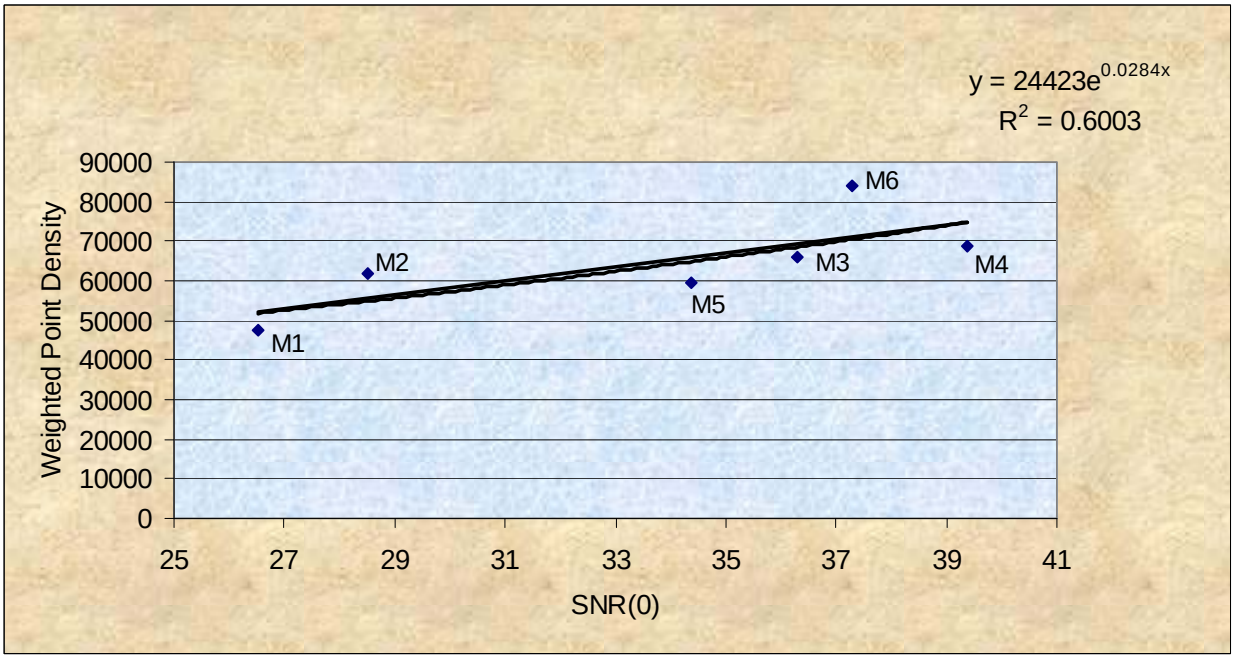

Figure 6-11. Managed forest SNR VS large cone ALSM weighted point density

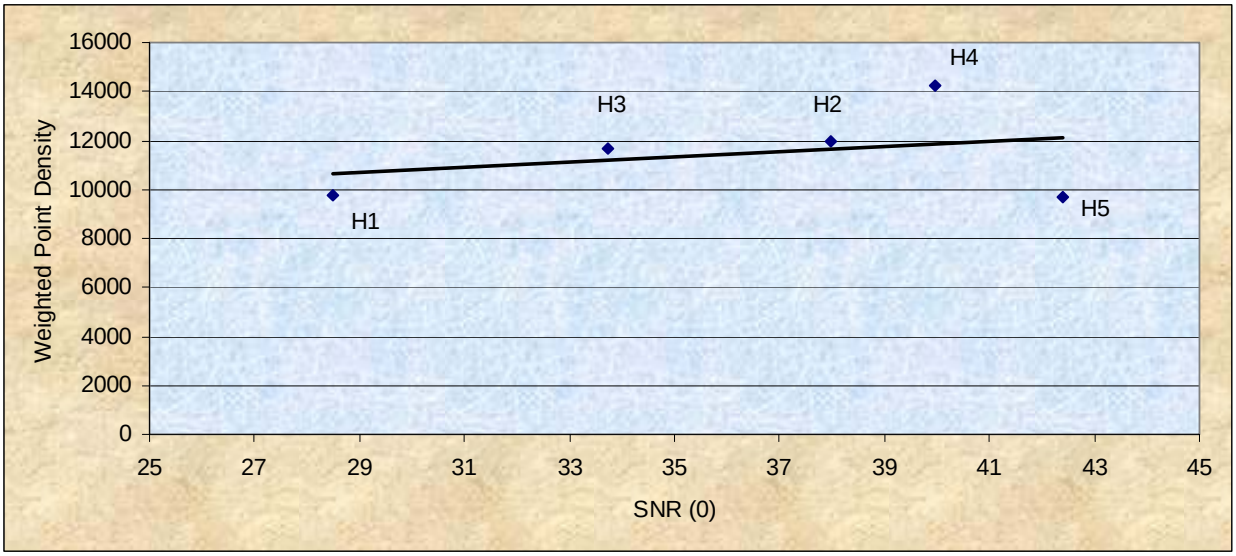

Figure 6-11b. Hogtown forest SNR VS large cone weighted point density

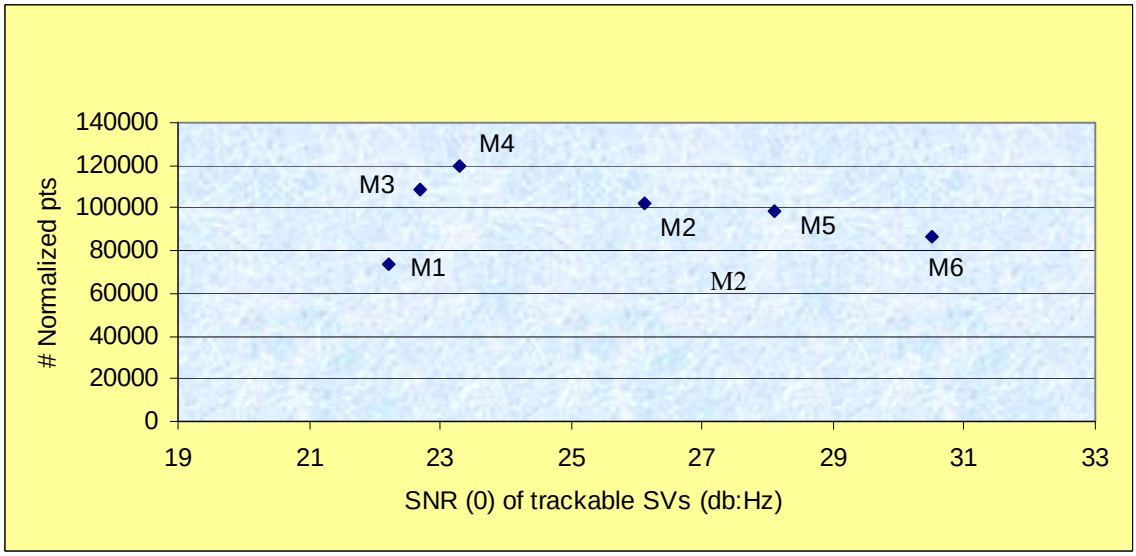

Figure 6-12. Large cone results taking total visible SV SNR(0) vs. # of normalized points for IMPAC site.

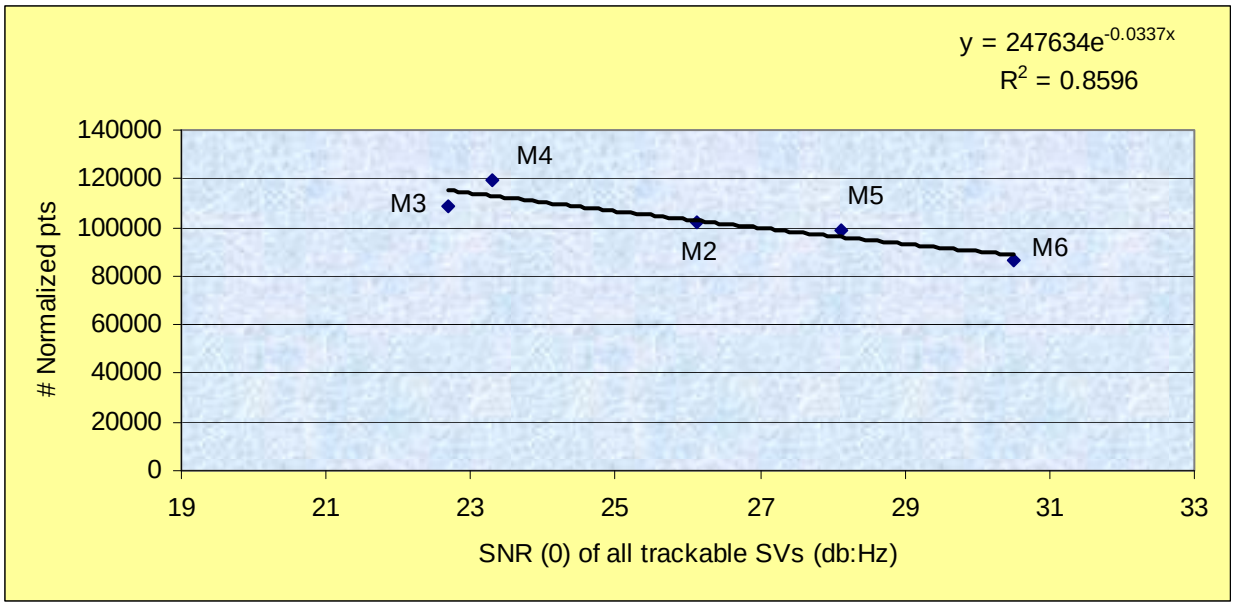

Figure 6-13. Large cone results from figure 6-12 with M1 removed as an outlier.

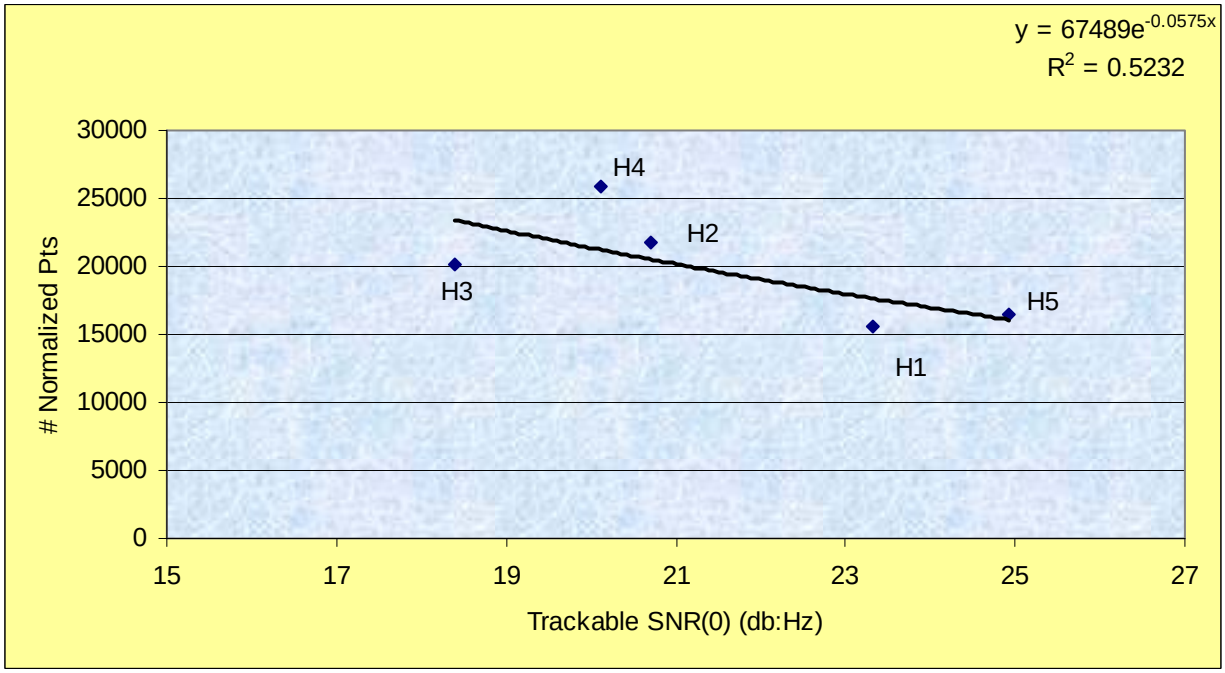

Figure 6-14. Hogtown forest large cone average SNR(0) of all obtainable SVs vs. # normalized points

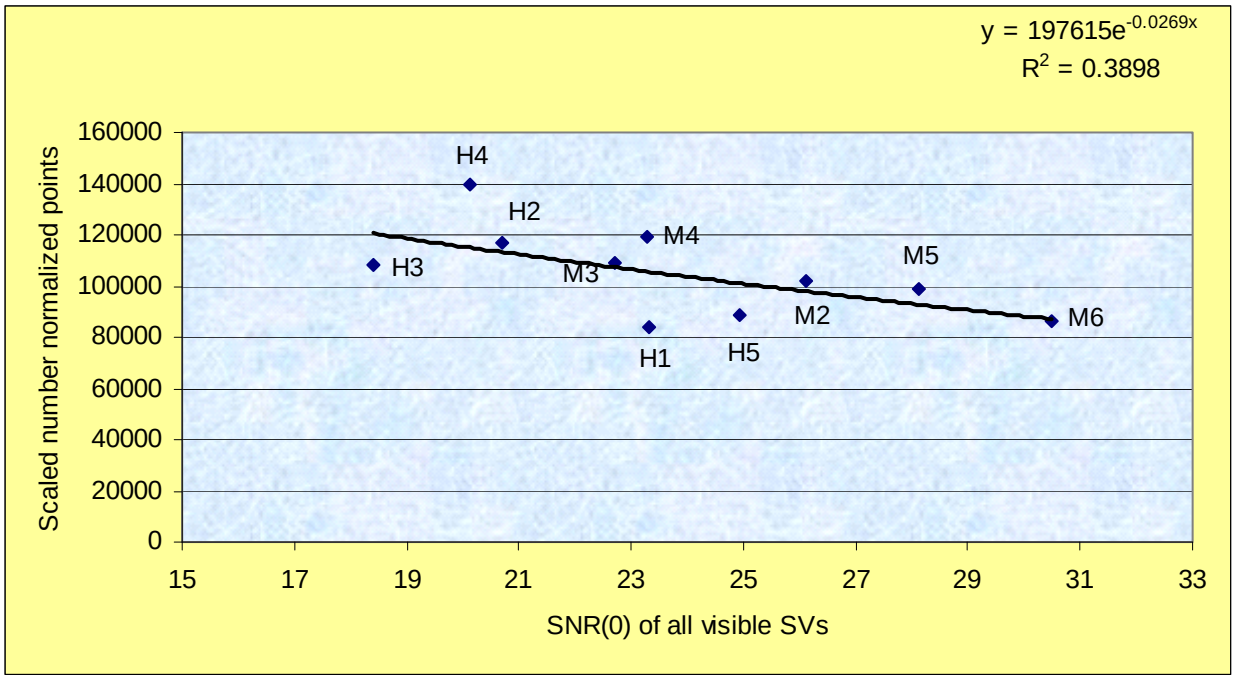

Figure 6-15. Scaled # normalized points vs. SNR of all visible SVs.

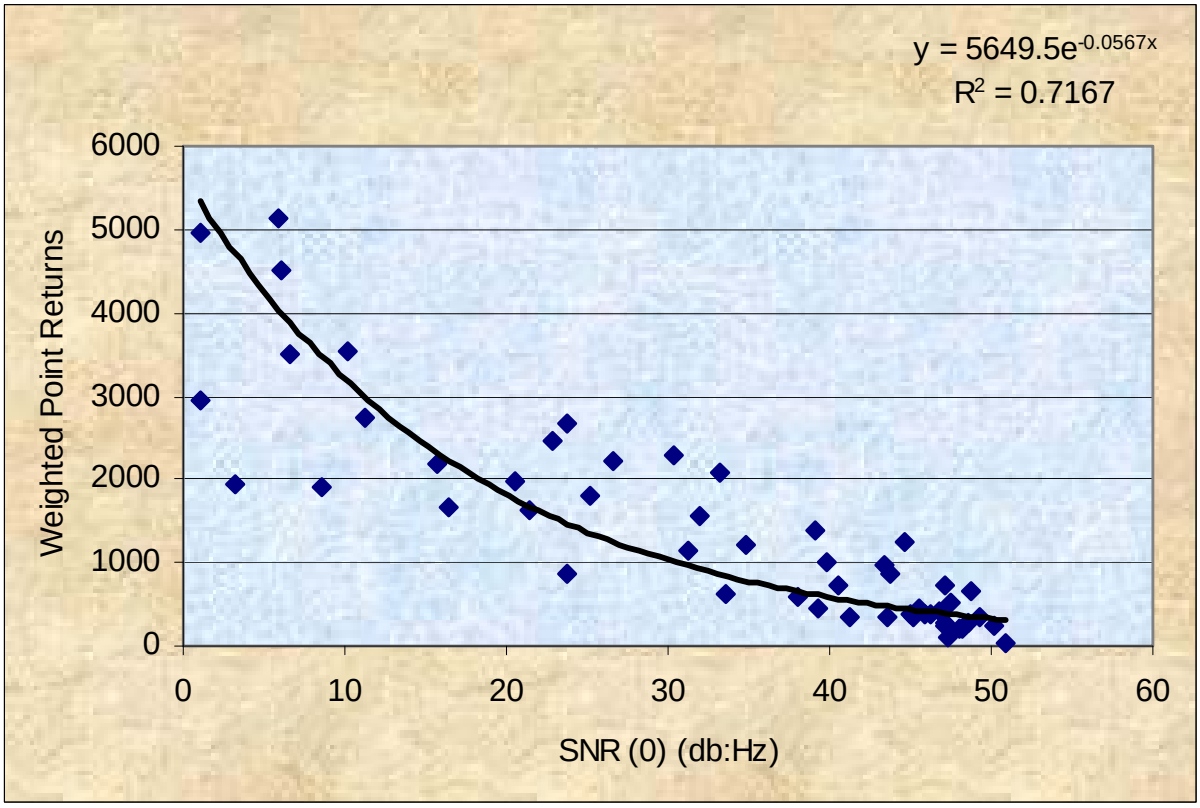

Figure 6-16. Small cone analysis at IMPAC of SNR (0) VS weighted point density

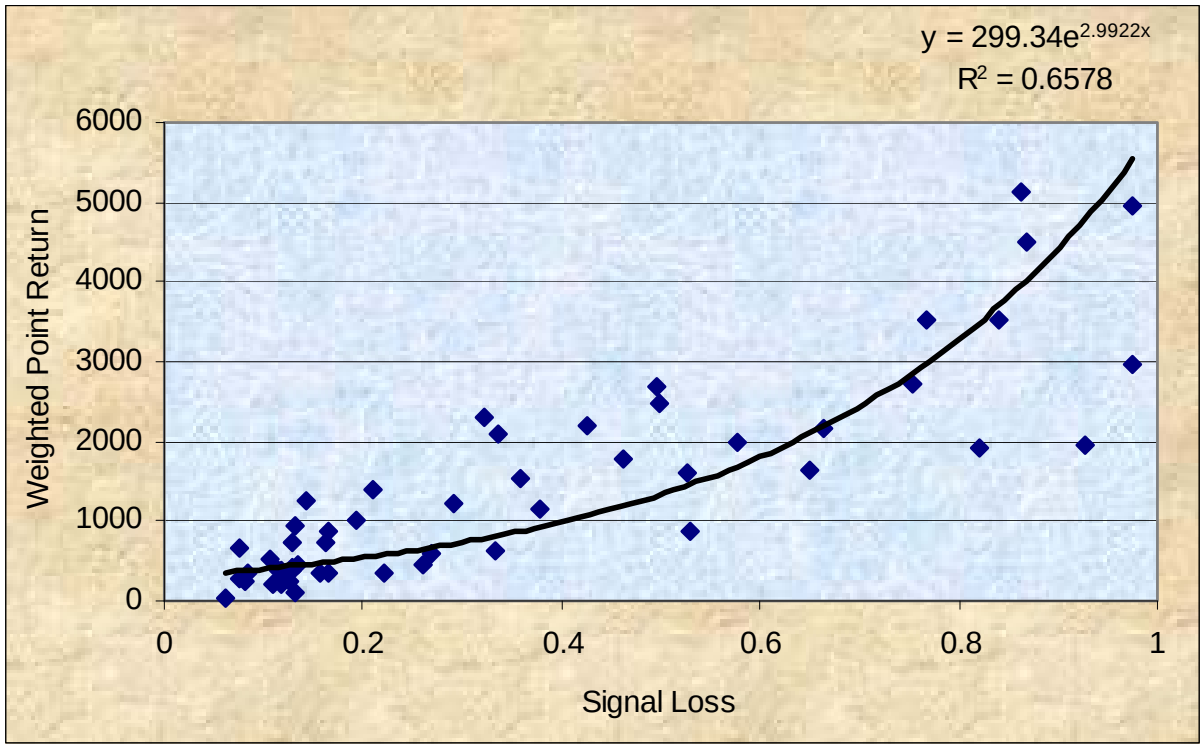

Figure 6-17. Small cone analysis at IMPAC of signal loss VS weighted point density

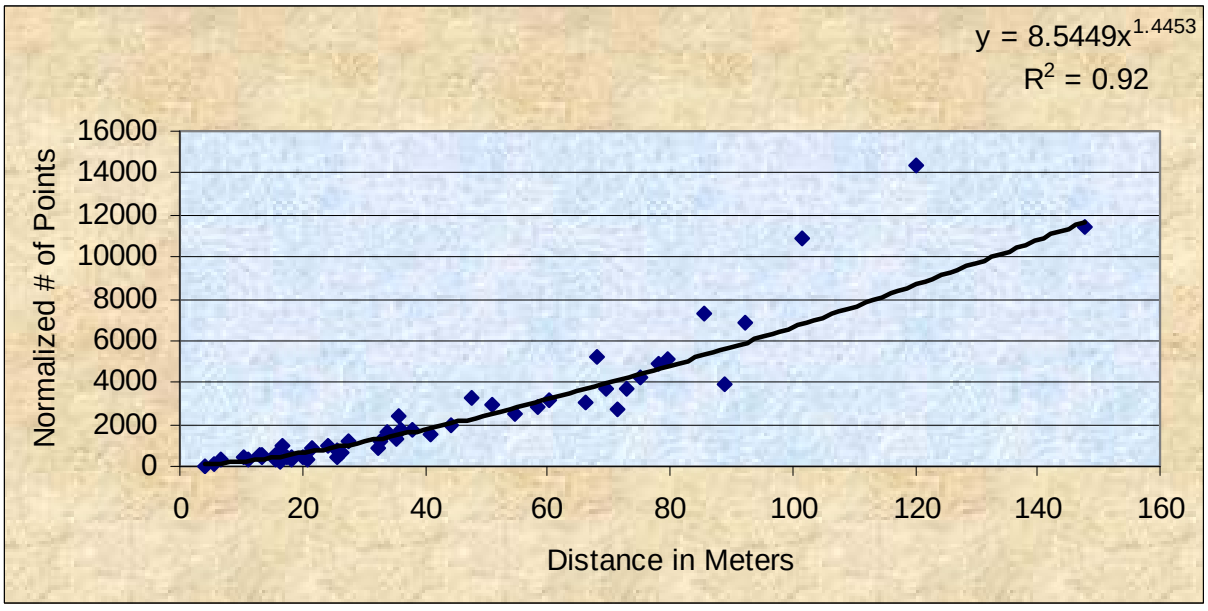

Figure 6-18. Small cone analysis in managed forest of distance of propagation through foliage VS total number of points

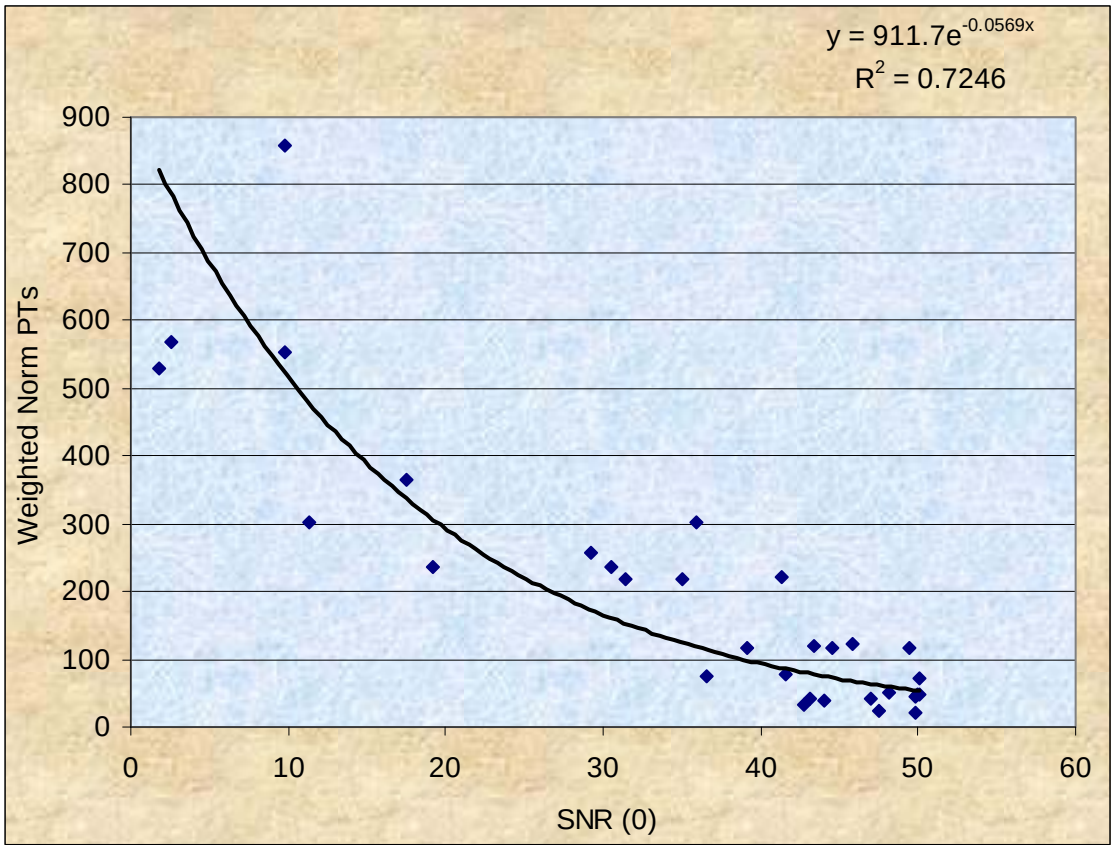

Figure 6-19. Small cone analysis in Hogtown forest of SNR (0) VS weighted point density

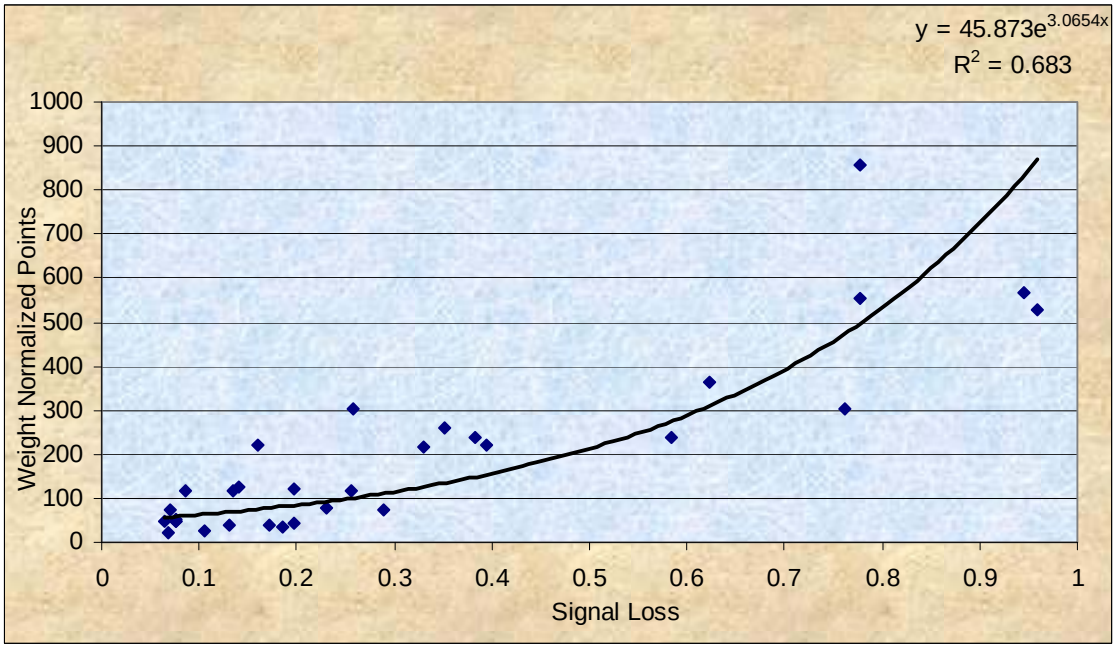

Figure 6-20. Small cone analysis in Hogtown forest of signal loss VS weighted point density

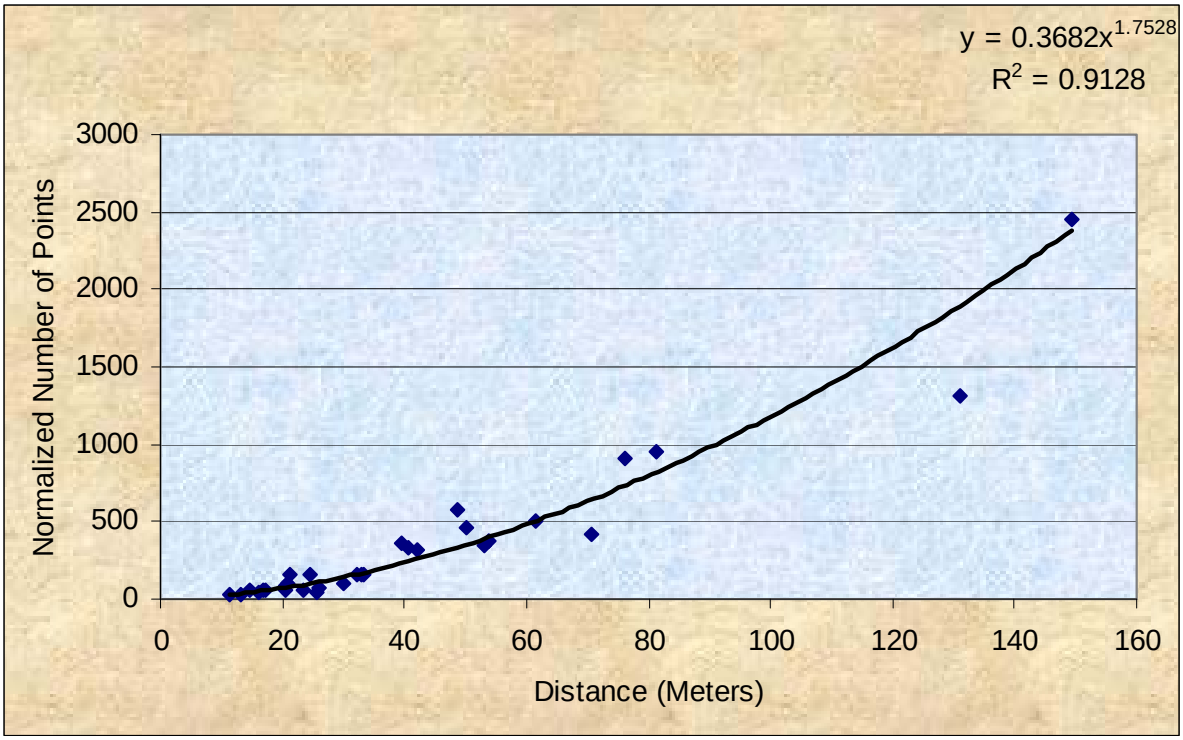

Figure 6-21. Small cone analysis in Hogtown forest of distance of propagation through foliage VS total number of points

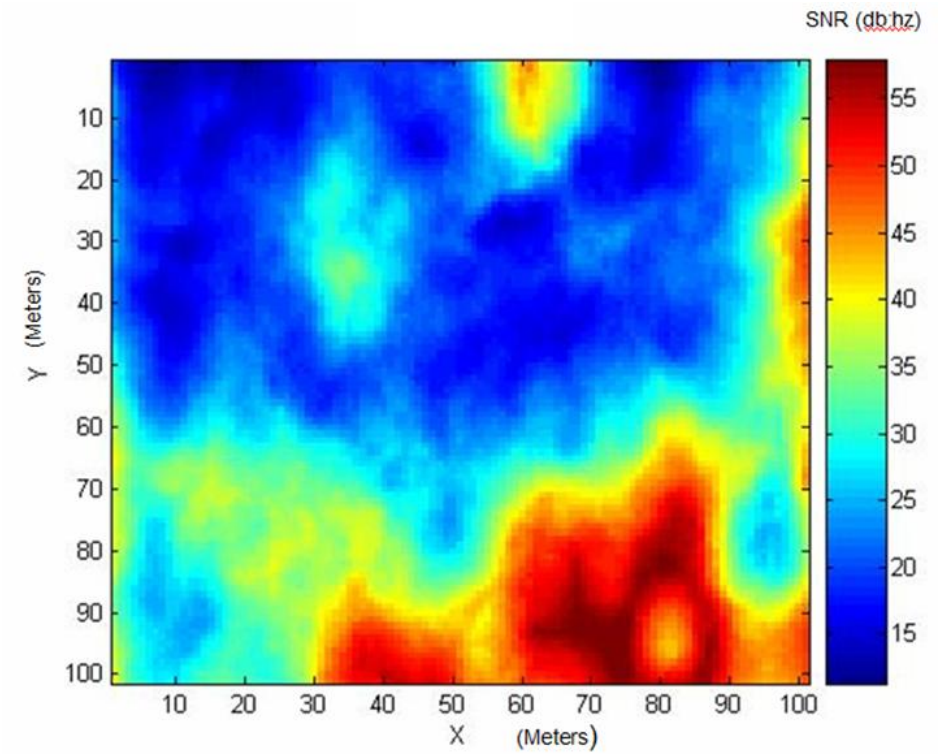

Figure 6-22. Prediction map of a 100x100 meter area

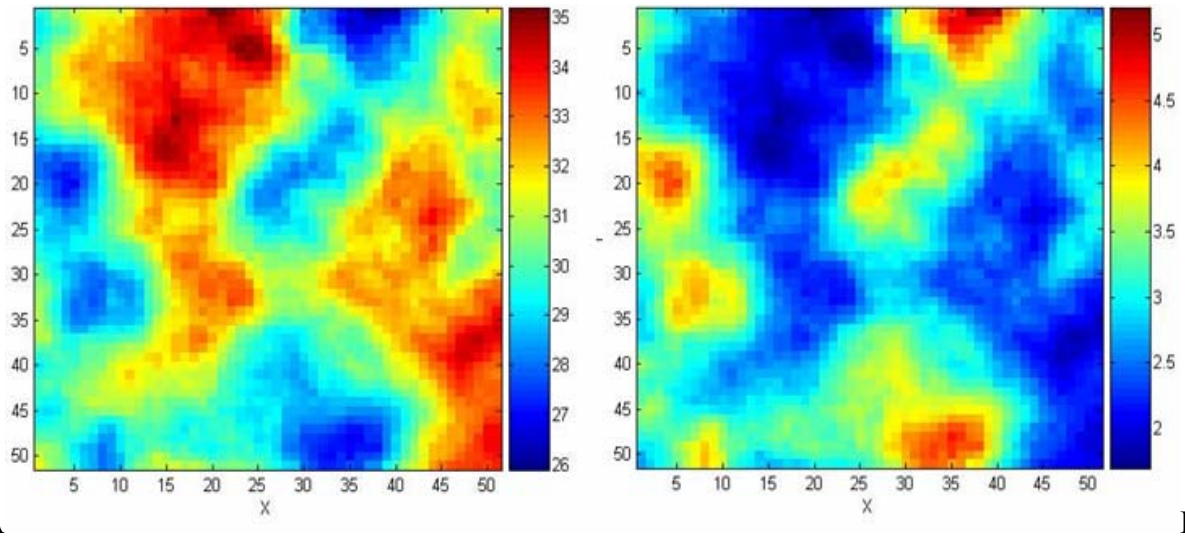

Figure 6-23. GPS prediction map (50x50 meter) A) The first step in the prediction process is generating an average SNR prediction for the SVs we assume will be tracked by the GPS receiver measured in db:Hz B) The GPS prediction map measured in meters.

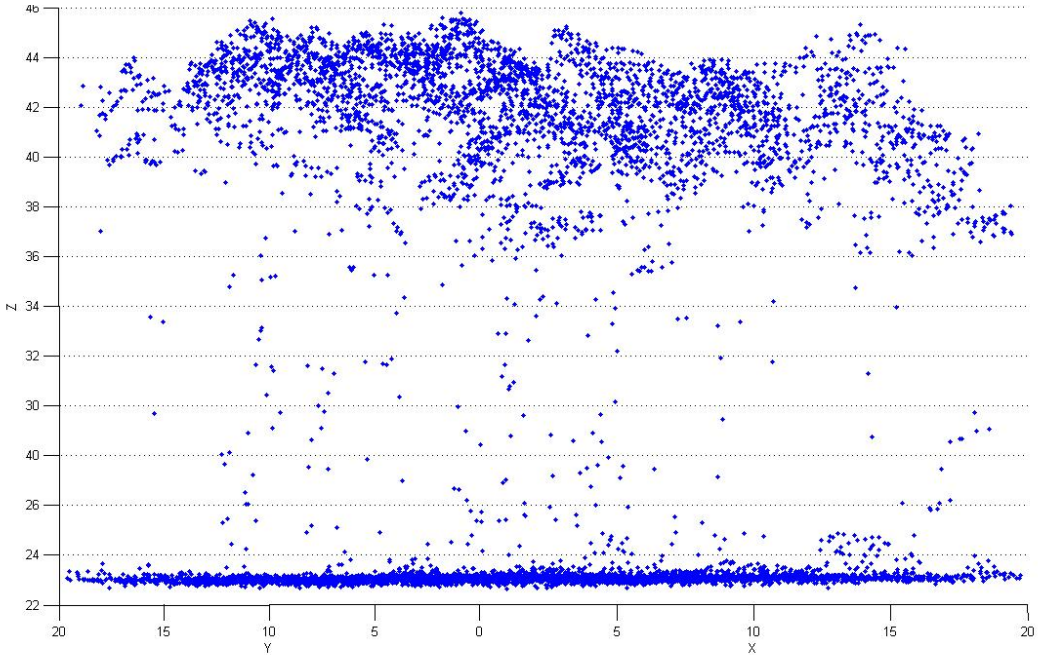

Figure 6-24a. Point returns of Managed Forest Point #1

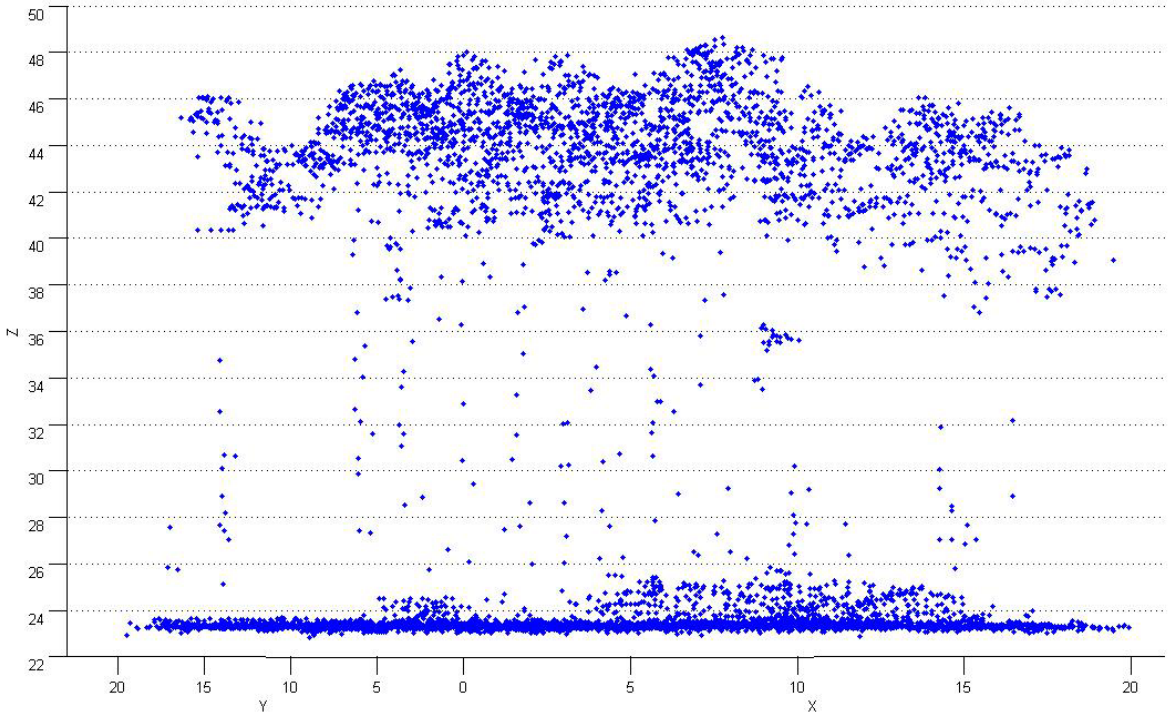

Figure 6-24b. Point returns of Managed Forest Point #4

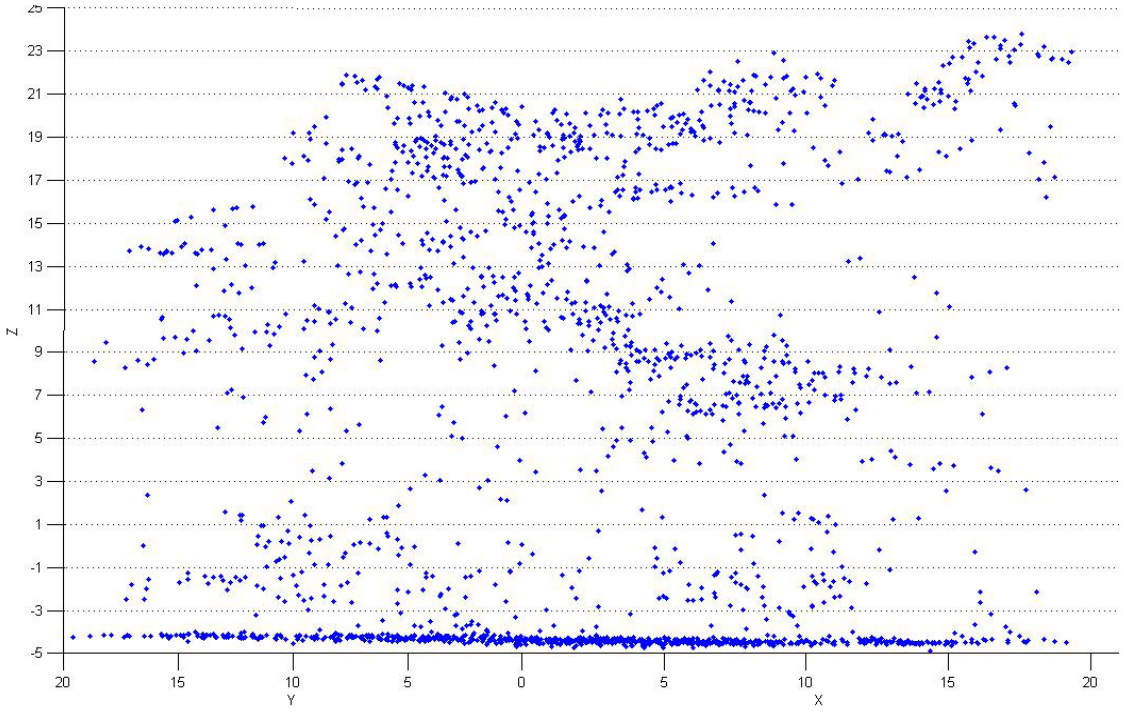

Figure 6-25. Point returns of Hogtown Forest Point #3

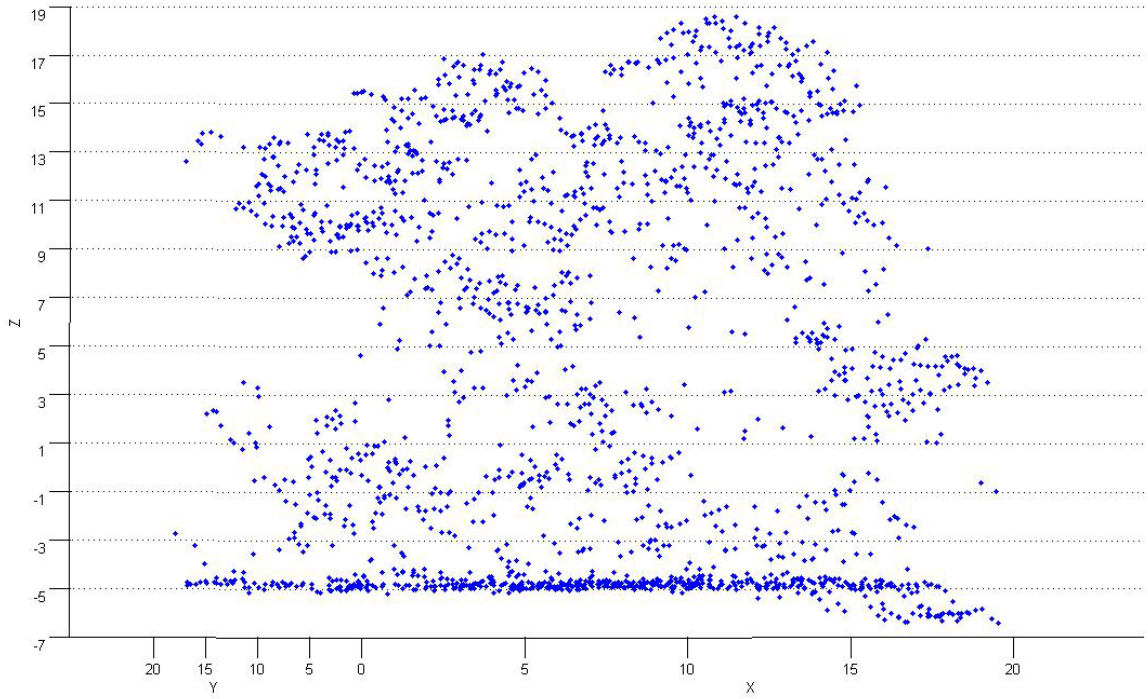

Figure 6-26. Point returns of Hogtown Forest Point #5

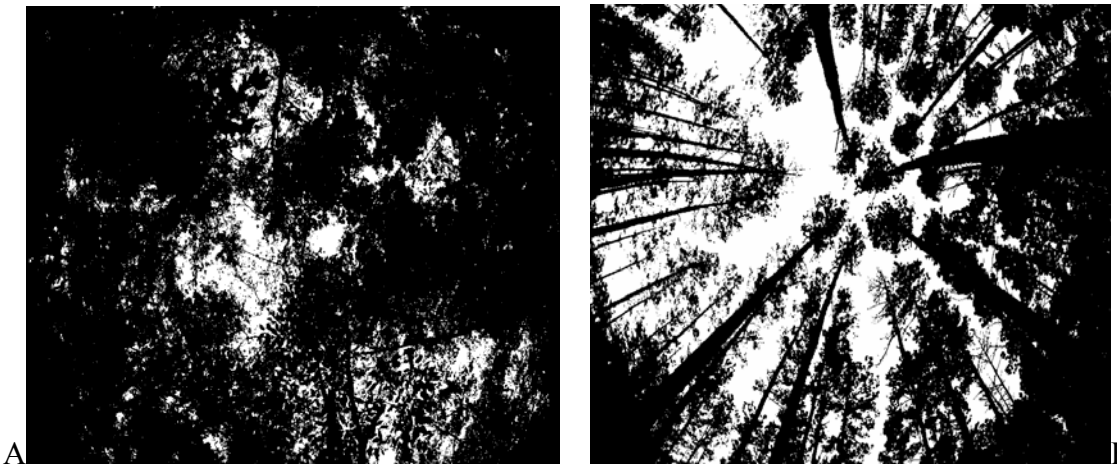

Figure 6-27. Black and white sample photos of both forest types. (A) Hogtown Point #2 black and white image. (B) IMPAC black and white converted image

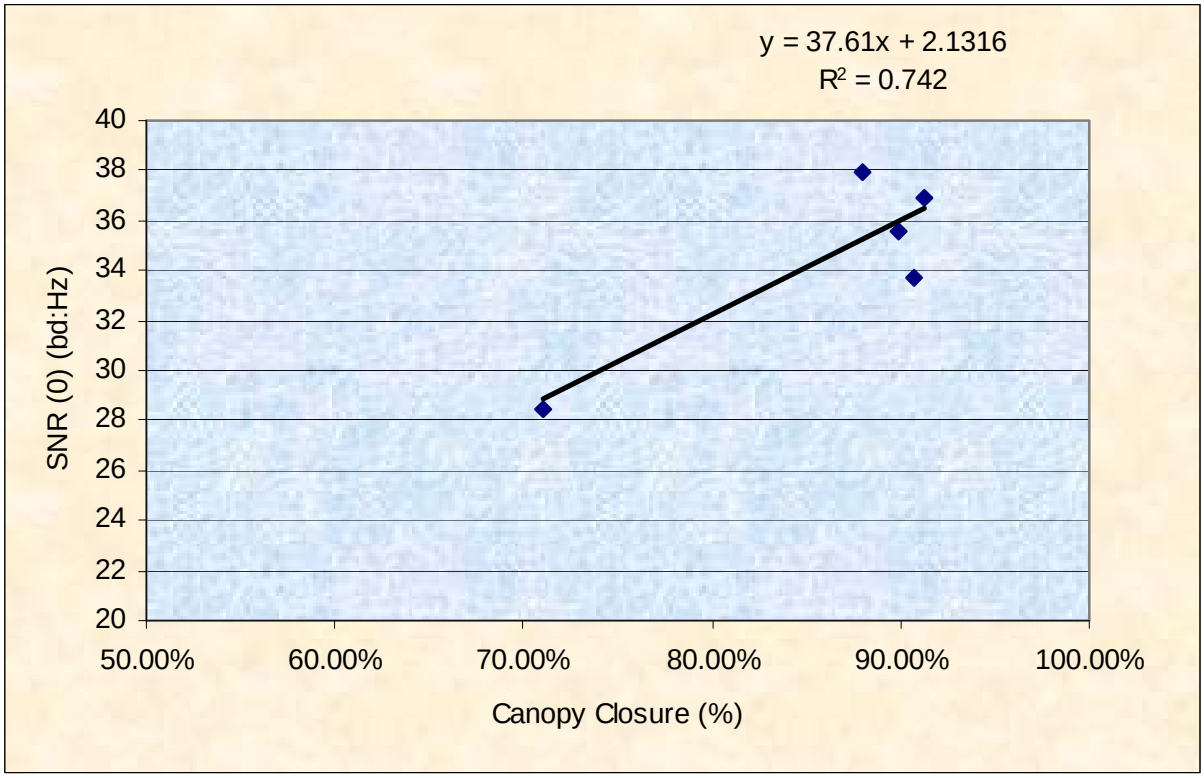

Figure 6-28. Black and white photo analysis of canopy closure VS SNR(0) in Hogtown forest

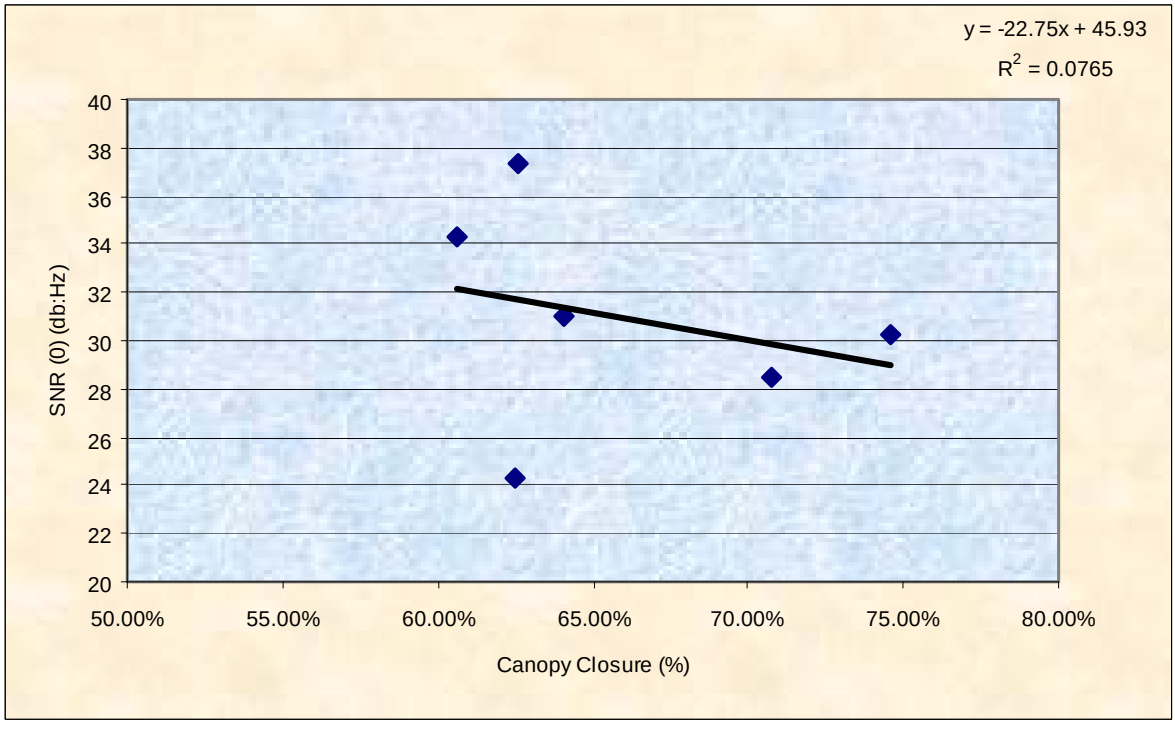

Figure 6-29. Black and white photo analysis of canopy closure VS SNR(0) in managed forest

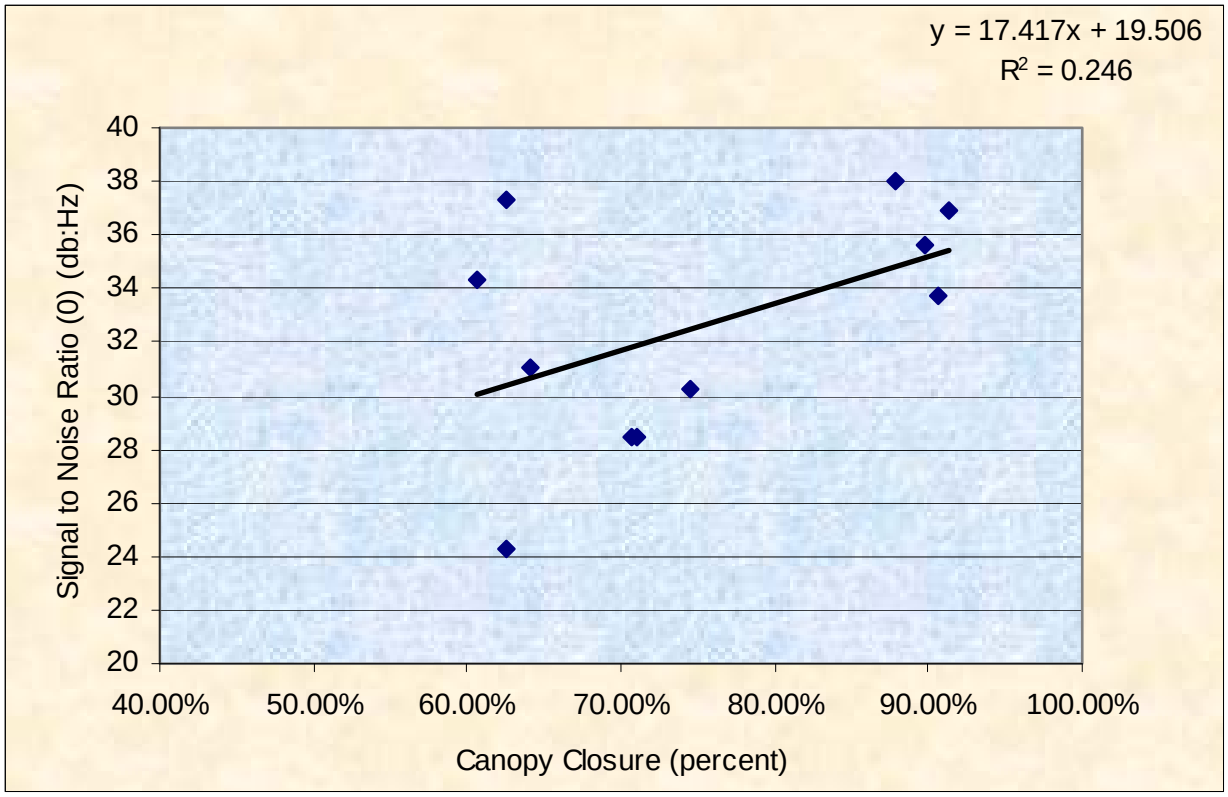

Figure 6-30. Black and white photo comparison of canopy closure and SNR(0) of both forests

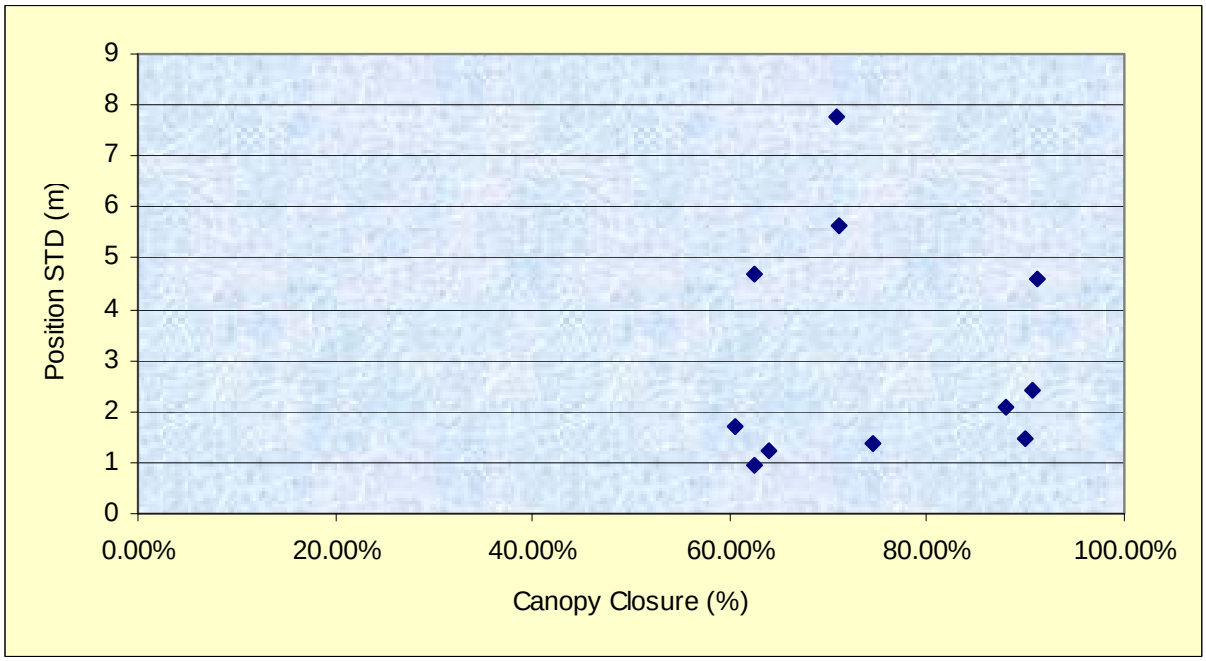

Figure 6-31. Black and white analysis of GPS position STD (meters) versus. canopy closure (%)

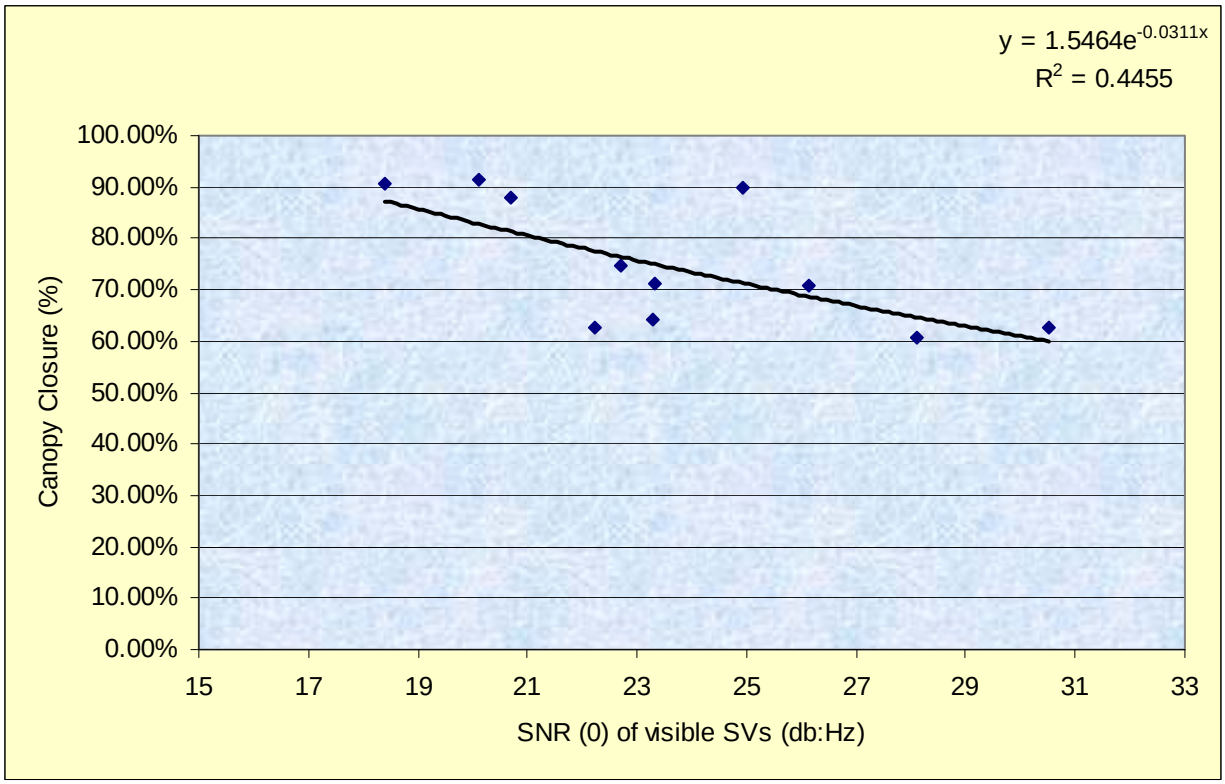

Figure 6-32. Plot of SNR(0) VS canopy closure considering all SVs in view

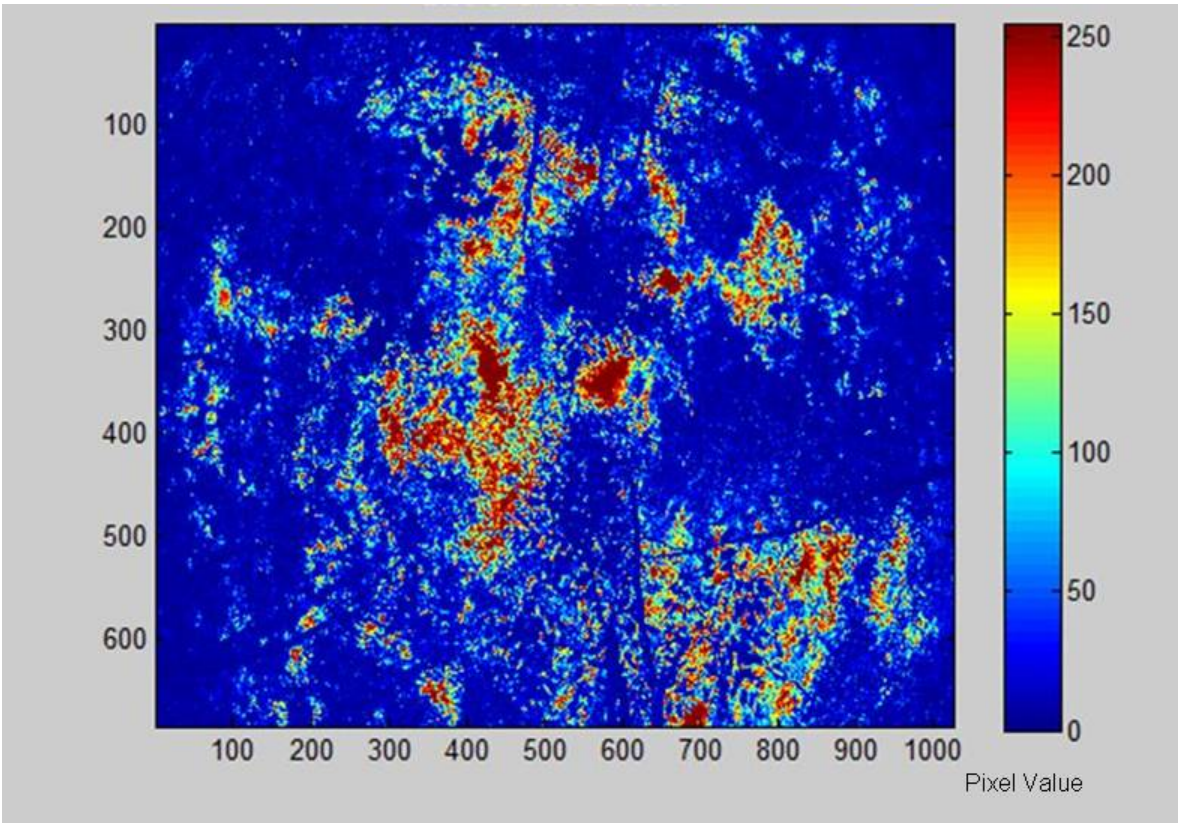

Figure 6-33. Blue channel photo extraction of Hogtown forest point #2

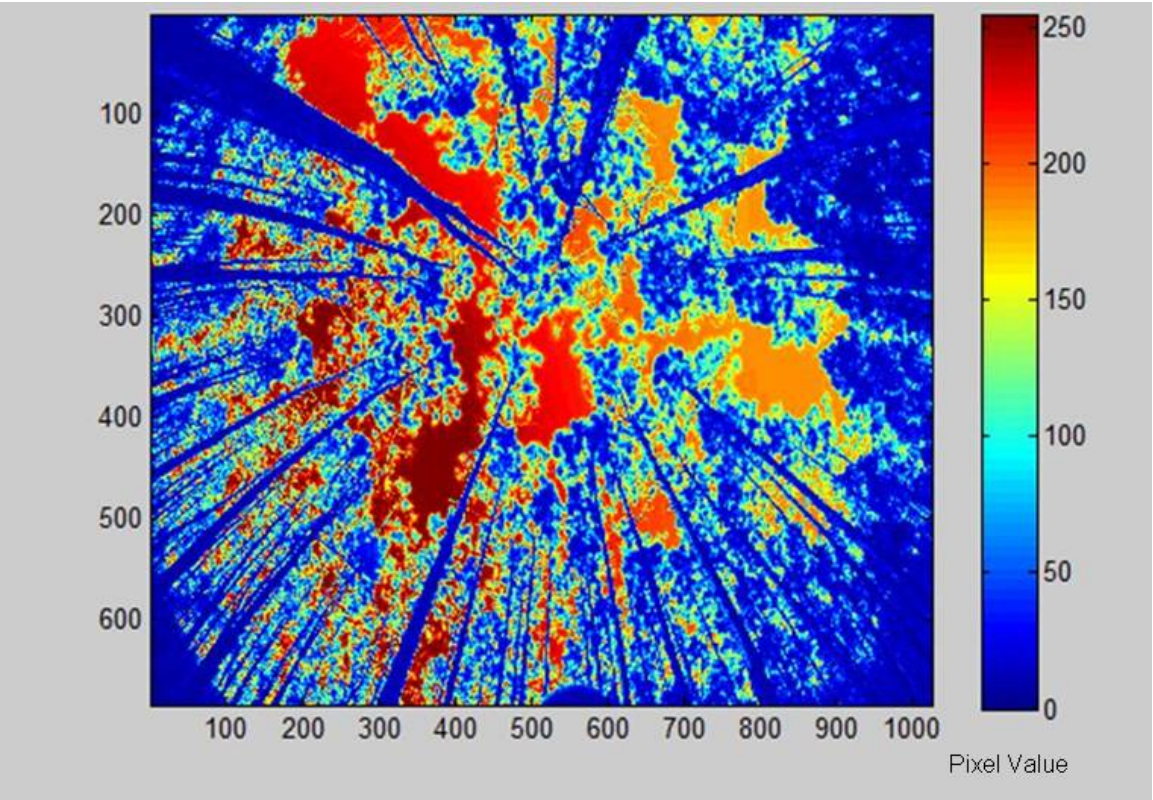

Figure 6-34. Blue channel photo extraction of managed forest Point #2

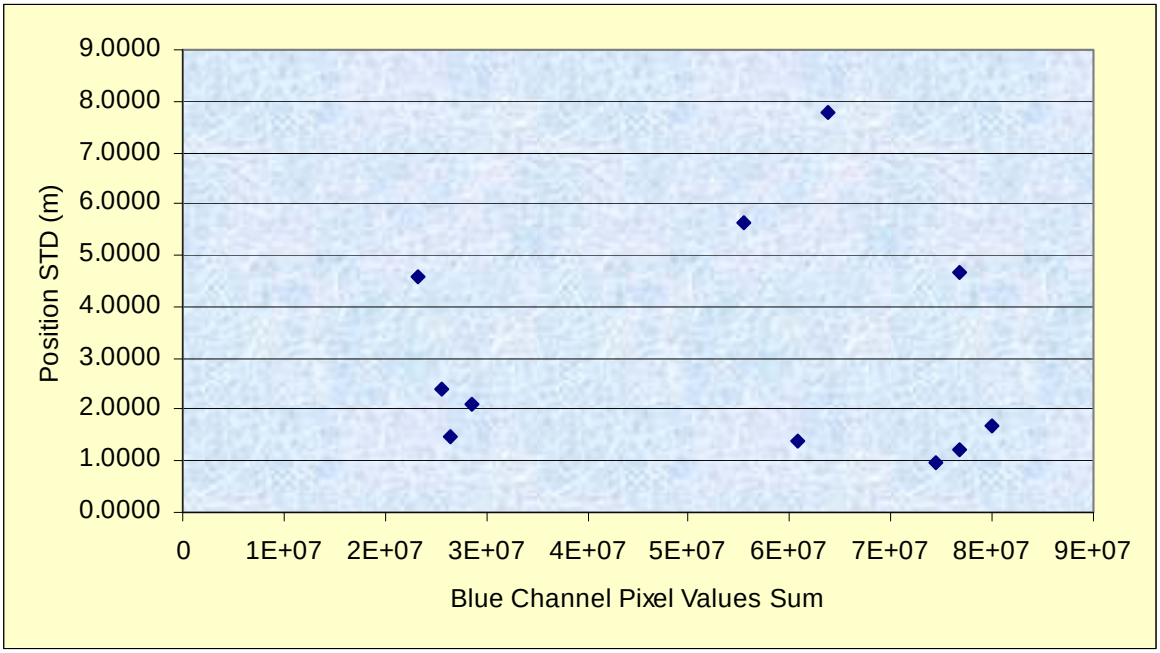

Figure 6-35. Blue channel pixel value sum VS GPS position STD

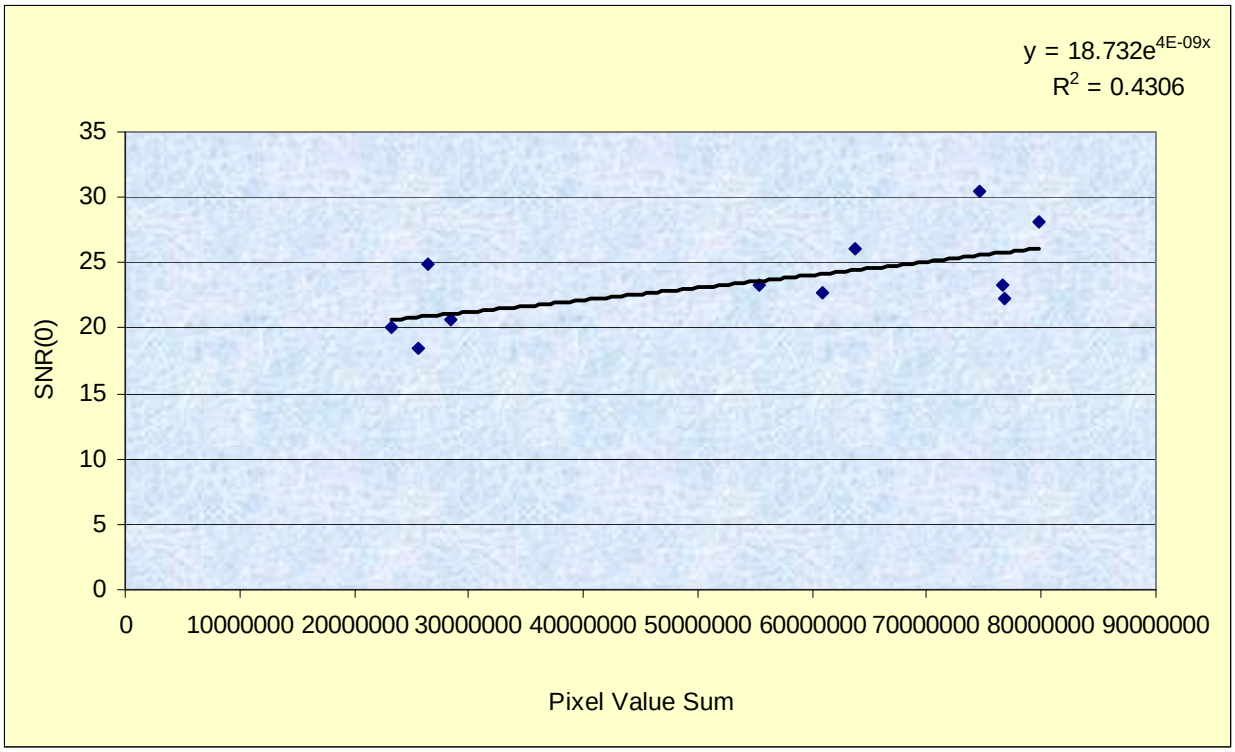

Figure 6-36. Blue channel pixel value VS SNR(0) of all visible SVs

CHAPTER 7
CONCLUSIONS AND RECOMMENDATIONS

7.1 Conclusions

This Thesis presents a method to predict GPS L-band signal degradation using ALSM data over a target area as well as the effects of this information on GPS performance. Initial analysis of this project was to determine if the experimental set up was capable of quantifying SNR readings and comparing them to the amount of matter between the source and receiver. Two different techniques were used for the ALSM analysis; the first technique used was simply using a large cone over the target area and the second was the use of a small cone aimed in the direction of the signal source. While the techniques only used L1 band signals this research does outline a method that could be used to study the effects on different frequencies as well.

Many different relationships were examined in this study and a brief summation of the findings is described below. The first relationship compares GPS precision to PDOP, where it was found that PDOP is not a good indicator of GPS position precision in forest canopy.

Next, The relationship between SNR and position precision does exhibit a correlation; and, while it is not an extremely strong correlation it does suggest that as SNR increases the GPS position precision will increase as well. As the study moved to analyze ALSM data, the results showed that by using ALSM data both in the scope of a large or small cone technique does provide decent results comparing the point density of ALSM point returns against SNR. Since the small cone technique provides better results and insights, prediction maps using this technique were developed allowing for the prediction of signal to noise ratios and GPS position precision. The prediction maps can provide users information on the effectiveness of wireless communications, GPS signal reception, satellite communication effectiveness for planning, and satellite communication effectiveness during tactical operations for the military. The ALSM

results not only show a marked improvement over previous techniques such as skyward photography, the results support and follow the predicted patterns of the Beers-Lambert Law.

7.2 Recommendations.

While the results in this Thesis provide new and improved methods for predicting signal behavior in the forest environment, the results also indicate that continued work is necessary to refine this technique. Some other research ideas that branch off of this project are outlined below. The first is the continued study of the effectiveness of differential carrier phase GPS performance as measured by ALSM data. The level of precision that can be achieved with this form of GPS measurement may in fact be able to show a measurable effect caused by forest foliage diffracting off the forest canopy structure. The question with this is whether or not a lock can be maintained under such environments to achieve an effective carrier phase fix.

While we get a very strong correlation in the distance vs. normalized number of points with R squared values in excess of .9, we still only get R squared values in the realm of .77 to .68 when using the weighted points against signal loss and SNR (0) without removing outliers. This indicates to us that we need to look more closely at a couple different aspects. First, as indicated before, the small cone may not be the best scope to use in the case study. I propose developing a moving cylinder or cone with a narrow diameter or angle that follows the path of the SV on its orbit. This should more accurately model the proper path of propagation of the SV transmission. A second source of the disparity in values may be attributed to the vegetation being modeled. In this study I simply assign a value based upon the fact there is a point return, and at this time there is no way to know for sure if a point return is a tree trunk, leaf, or a tree branch. Clearly, the density of a branch or tree trunk is more significant than that of a pine needle or an oak leaf; therefore, a technique to classify the different point returns from ALSM data and identify each

return to the different parameters of the forest environment will provide needed information to obtain a better model for this study.

Finally, this same study can be performed using a four stop return ALSM system which would provide better data than just a first and last return system. With the first and last return ALSM system we get a heavy volume of points from the top portion of the tree canopy and towards the ground, but with a four stop system we would gain more point returns from between the top of the canopy and the ground. This would help model the forest structure better and allow for better analysis.

APPENDIX A
ZENITH ORIENTED PHOTOS

Figure A-1. Managed Forest 1

Figure A-2. Managed Forest 2

Figure A-3. Managed Forest 3

Figure A-4. Managed Forest 4

Figure A-5. Managed Forest 5

Figure A-6. Managed Forest 6

Figure A-7. Hogtown Forest 1

Figure A-8. Hogtown Forest 2

Figure A-9. Hogtown Forest 3

Figure A-10. Hogtown Forest 4

Figure A-11. Hogtown Forest 5

Figure A-12. Hogtown Forest 6

APPENDIX B
FIELD TECHNIQUES

The purpose of this appendix is to describe the techniques used throughout this study to collect data and process data for this research. With the initial findings from this research, many different aspects of this study could be further researched and an understanding of what techniques worked well can be time saving to future studies. A significant portion of the techniques described in this appendix has already been discussed in previous chapters but this appendix does go into greater detail.

Table B. Reporting parameters for NMEA messages

GGA Message	**GSA Message**	GSN Message
UTC Time	Mode (manual or automatic)	# SVs
Latitude	Fix type: no fix, 2D, or 3D	1st SV #
Direction of Latitude	SVs used in solution	Signal to Noise (STN) of 1st SV
Longitude	PDOP	2nd SV #
Direction of Longitude	HDOP	STN of 2nd SV
Position Type	VDOP	3rd SV
Number of SVs	Checksum	3rd STN
HDOP		4th SV
Geoidal Height		4th STN
Altitude		….
Geoidal separation		….
Age of differential corrections		M SV#
Base station Id		M STN
Checksum		Check Sum

All the equipment used for our research was obtained through the Geosensing division of the Civil Engineering department at UF. Data collection devices include two identical GPS receivers, two antennas, cables, and computers for data capture. At the base station, I used the already installed antenna that is mounted to the roof of Reed Lab, a building located next to Weil Hall on the University of Florida campus. In order to establish a good basis for comparison of data captured from both receivers and to verify the data captured by the receivers are similar, initial measurements consisted of data captured in the same environment. Data collection

included three NMEA messages collected at a rate of 1 Hz. In addition to these NMEA messages the GSV NMEA message is also an important message to consider in future research as it will report the azimuth and zenith angle to all the detected SVs (See table B-1 for a listing of the parameters reported by the different NMEA messages).

Upon completion of the data collection effort, the text files with the captured NMEA messages were converted into single line data strings with three NMEA messages on a single line representing a particular second of data capture information. To do this I simply did a "find replace" command inside Microsoft notepad and removed the character returns for two of the three NMEA messages collected each second. This information was combined with the base station data to provide a relative data comparison to an open field of view. To calculate and sort the data further I manually sorted the remaining items inside Microsoft Excel.

The antennas used for both the base station and the rover are model AT 1671-1 see figure 5-1 and table 5-1 for more information on this antenna. As discussed previously, these antennas were chosen for their ability to easily detect SV signals, but more importantly because the gain pattern for all signals between 0-75 degrees from zenith are the same. It is important to consider the antennas you will use for your data collection so you account for any gain pattern. I recommend a test as I conducted where you collected data with both the base station and rover on the roof to ensure each set up records similar SNR values in the same environment.

Figure B. Data logging set up in Hogtown forest

LIST OF REFERENCES

Andrade, A., 2001. *The Global Navigation Satellite System: Navigating Into the New Millennium*, Ashgate Publishing Co., Burlington, VT.

Andrews, A., M. Grewal, L. Weill, 2007. *Global Positioning Systems, Inertial Navigation, and Integration*, John Wiley and Sons Inc., New York.

Axelrad, P., and C.P. Behre, 1998. Satellite Attitude Determination Based on GPS Signal-to-Noise Ratio, *Proceedings of the IEEE*, (87): 133-144.

Bortolot, Z.J, and R.H. Wynne, 2005. Estimating Forest Biomass Using Small Footprint LiDAR Data: An Individual Tree-based Approach that Incorporates Training Data, *ISPRS Journal of Photogrammetry and Remote Sensing*, 59(6): 342-360.

Carter, W.E., R.L. Shrestha, and K.C. Slatton, 2007. Geodetic Laser Scanning, *Physics Today*, (December): 41-47.

Collins, P. and Stewart, P., 1999. GPS SNR Observations, Geodetic Research Laboratory.

Dana, Peter H. 2008. University of Colorado at Boulder, Department of Geography, Retrieved February, 2008 from http://www.colorado.edu/geography/gcraft/notes/gps/gif/

Fernandez, J.C., 2007. Scientific *Applications of the Mobile Terrestrial Laser Scanner*, Masters Thesis, University of Florida, Gainesville, Florida.

Forestry Commission, 2006. The Research Agency of the Forest Commission, Retrieved December, 2007 from http://www.forestresearch.gov.uk/lidar

Harding, D.J., M.A. Leffsky, G.G Parker, and J.B. Blair, 2001. Laser Altimeter Canopy Heights Profiles Methods and Validation for Closed-Canopy, Broadleaf Forests, *Remote Sensing of Environment*, (76): 283-297.

Holden N.M., A.A. Martin, P.M.O. Owende, and S.M. Ward, 2001. A Method for Relating GPS Performance to Forest Canopy, *International Journal of Forest Engineer*ing, 12(2).

Hurn, Jeff, 1993. *Differential GPS Explained*, Trimble Navigation Ltd., Sunnyvale, CA.

Land Mobile Satellite Propagation Model for Non-Urban Areas, Final Report, European Space Agency (ESA), Document Reference: 4300/7290/6/1, 1998.

Larson, Kristine 2006. University of Colorado at Boulder, Department of Aerospace Engineering Sciences, Retrieved October, 2006 from http://spot.colorado.edu/~kristine/Home.html.

Lee, H., K. Kampa, and K.C. Slatton, 2005. Segmentation of ALSM Point Data and the Prediction of Subcanopy Sunlight Distribution, *Geoscience and Remote Sensing Symposium, IGARSS 2005. Proceedings. 2005 IEEE International,* (1):25-29.

Lee, H., K.C. Slatton, and H. Jhee, 2005. Detecting Forest Trails Occluded by Dense Canopies Using ALSM Data, *Geoscience and Remote Sensing Symposium, 2005. IGARSS 2005. Proceedings. 2005 IEEE International*, (5): 25-29.

Lee, H., K.C. Slatton, B.E. Roth, and W.P. Cropper, 2007. Prediction of Forest Canopy Light Interception Using Three-Dimensional Airborne LiDAR Data, *International Journal of Remote Sensing*, (Accepted).

Logsdon, Tom, 1995. *Understanding the NAVSTAR: GPS, GIS, and IVHS*; Von Nostrang Reinhold Publishing, New York.

Luzum, B.J., K.C. Slatton, R.L. Shrestha, 2004. Identification and Analysis of Airborne Laser Swath Mapping Data in a novel Feature Space, *Geoscience and Remote Sensing Letters*, (1):268-271

Markel, Mathew, 2002. *Interference Mitigation for GPS Based Attitude Determination*. PhD Thesis, University of Florida, Gainesville, Florida.

National Center for Airborne Laser Mapping (NCALM), 2007. Retrieved October, 2006 from http://www.ncalm.ufl.edu/.

NAVSTAR GPS Operations, 2006. US Naval Observatory. Retrieved October, 2006 from http://tycho.usno.navy.mil/gpsinfo.html.

OPTECH homepage, 2007. Retrived December, 2007 from http://www.optech.ca/.

Oxendine, Christopher, 2007. West Point Instructor, EV 380 - Surveying.

Rogers, R. M., 2003. *Applied Mathematics in Intergraded Navigation Systems,* American Institute of Aeronautics and Astronautics, Inc., Reston, Va.

Sigrist P., P. Coppin, and M. Hermy, 1999. Impacts of Forest Canopy on Quality and Accuracy of GPS Measurements, *International Journal of Remote Sensing*, 20 (18): 3595-3610.

Singhania, A., 2007. *Lidar Aided Camera Calibration in Hybrid Imaging Mapping Systems*, Masters Thesis, University of Florida, Gainesville, Florida.

Trimble, Mapping and GIS, 2006. Retrieved October, 2006 from http://www.trimble.com/mgis.shtml.

Wells, D., N. Beck, D. Delikaraoglou, A. Kleusberg, E. Krakiwsky, G. Lachapelle, R. Langley, M. Nakiboglu, K. Schwarz, J. Tranquilla, and P. Vanicek 1986. *Guide to GPS Positioning*, Canadian GPS Associates, Fredericton, New Brunswick.

BIOGRAPHICAL SKETCH

William Charles Wright was born in Birmingham, Alabama, to David Bruce Wright and Elizabeth Ann Wright. His family is also composed of a sister: Joyce Raymer and two brothers Michael and Robert. From a very young age Will developed an interest in earth sciences and space technology. Upon his successful acceptance to the United States Military Academy at West Point, he employed this interest while obtaining his Bachelors of Science degree with a Major in Mapping, Charting, and Geodesy in 1999. He then served the United States Army as a Cavalry Officer and deployed around the world to both peacekeeping and hostile environments. Some of his deployments include Bosnia Herzegovina, Egypt, Kuwait, and Iraq. Upon completion of his Troop Command, Captain Wright was selected by the Army to attend graduate school in order to obtain a master's degree in science and return to the Military Academy to teach in the Geospatial Information Science program. Upon the completion of his first year of graduate school, William led a group of students on a month long data collection and Geographic Information Systems data update effort at the Cold Regions Test Center in Delta Junction, Alaska. William's academic interests include customization of Geographic Information Systems, Global Positioning collection systems, and Airborne Laser Swath mapping technologies.